

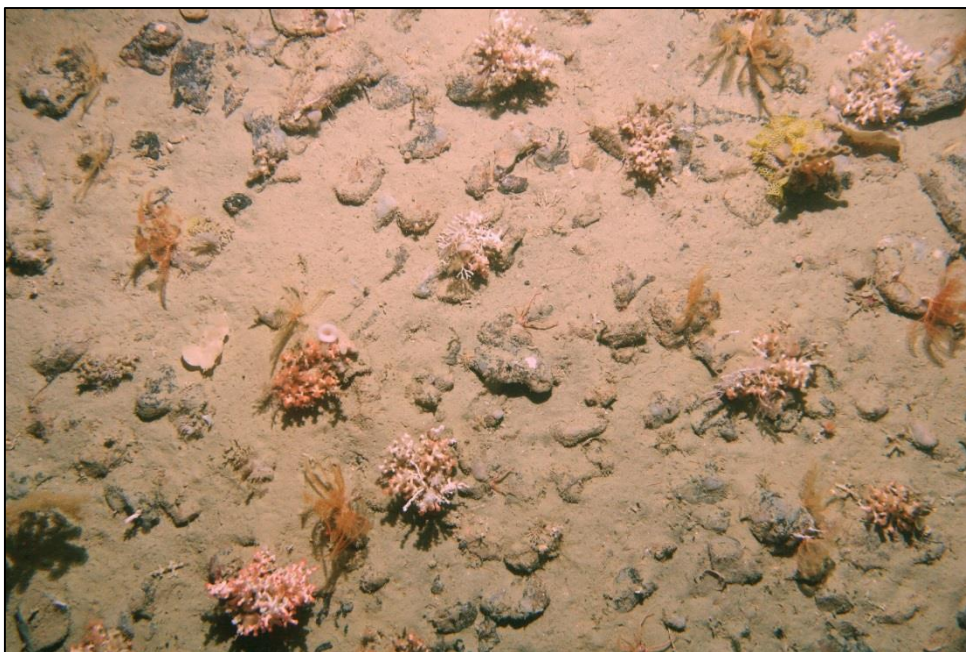
## Appendix 16

Benthic epifauna communities of the central Chatham Rise crest (Rowden et al. 2014a)

## Benthic epifauna communities of the central Chatham Rise crest

Prepared for Chatham Rock Phosphate Ltd

March 2014



**Authors/Contributors:**

Ashley Rowden  
Daniel Leduc  
Leigh Torres  
David Bowden  
Alan Hart  
Caroline Chin  
Nikki Davey  
Scott Nodder  
Arne Pallentin  
Kevin Mackay  
Lisa Northcote  
James Sturman

**For any information regarding this report please contact:**

Dr Ashley A Rowden  
Principal Scientist  
Benthic Ecology  
+64-4-386 0334  
a.rowden@niwa.co.nz

National Institute of Water & Atmospheric Research Ltd  
Gate 10, Silverdale Road  
Hillcrest, Hamilton 3216  
PO Box 11115, Hillcrest  
Hamilton 3251  
New Zealand

Phone +64-7-856 7026  
Fax +64-7-856 0151

NIWA Client Report No: WLG2014-9  
Report date: March 2014  
NIWA Project: CRP14301

---

© All rights reserved. This publication may not be reproduced or copied in any form without the permission of the copyright owner(s). Such permission is only to be given in accordance with the terms of the client's contract with NIWA. This copyright extends to all forms of copying and any storage of material in any kind of information retrieval system.

Whilst NIWA has used all reasonable endeavours to ensure that the information contained in this document is accurate, NIWA does not give any express or implied warranty as to the completeness of the information contained herein, or that it will be suitable for any purpose(s) other than those specifically contemplated during the Project or agreed by NIWA and the Client.

# Contents

|  |           |
|--|-----------|
| <b>Executive summary</b> .....   | <b>7</b>  |
| <b>1 Introduction</b> .....  | <b>9</b>  |
| 1.1 Proposed phosphorite nodule mining on the Chatham Rise .....                     | 9         |
| 1.2 Benthic communities on the Chatham Rise .....                                    | 11        |
| 1.3 Objectives .....   | 14        |
| <b>2 Methods</b> .....   | <b>14</b> |
| 2.1 Survey design and planning .....   | 14        |
| 2.2 The surveys .....  | 19        |
| 2.3 Multibeam echo-sounder data acquisition .....                                    | 22        |
| 2.4 Biological sampling methods.....   | 24        |
| 2.5 Laboratory sample treatment.....   | 27        |
| 2.6 Habitat characterisation.....  | 30        |
| 2.7 Benthic community analysis .....   | 33        |
| 2.8 Habitat suitability modelling.....   | 37        |
| <b>3 Results</b> .....   | <b>39</b> |
| 3.1 Habitat characterisation.....  | 39        |
| 3.2 Benthic community analysis .....   | 40        |
| 3.3 Habitat suitability modelling.....   | 53        |
| <b>4 Discussion</b> .....  | <b>67</b> |
| 4.1 Epifauna community structure and distribution in the study area .....            | 67        |
| 4.2 Comparison with epifauna communities identified by Rowden et al.<br>(2013) ..... | 70        |
| 4.3 Comparison with epifauna communities elsewhere on the Chatham Rise .....         | 71        |
| <b>5 Conclusions and Recommendations</b> .....                                       | <b>74</b> |
| <b>6 Acknowledgements</b> .....  | <b>75</b> |
| <b>7 References</b> .....  | <b>75</b> |
| <b>Appendix A Epifauna taxa identified from seafloor images</b> .....                | <b>82</b> |
| <b>Appendix B Displaying predicted habitat suitability</b> .....                     | <b>85</b> |
| <b>Appendix C Gridded layers for environmental variables</b> .....                   | <b>87</b> |



|                   |  |            |
|-------------------|--|------------|
| <b>Appendix D</b> | <b>Maps of survey areas showing distribution of epifauna communities (image-level) on ROV/DTIS transects .....</b> | <b>98</b>  |
| <b>Appendix E</b> | <b>Fitted functions for BRT models of epifauna community (image-level) habitat suitability .....</b>               | <b>106</b> |
| <b>Appendix F</b> | <b>Bottom trawl footprint .....</b>  | <b>111</b> |

## Tables

|            |   |    |
|------------|---|----|
| Table 2-1: | Results of SIMPER analysis showing the taxa responsible for the difference in community structure between selected transects from the CRP Environmental Survey and the Chatham Rise Benthos (OS/20/20) Survey, and derived correction factor. | 34 |
| Table 3-1: | Results of the SIMPER analysis showing taxa accounting for >90% of the within group similarity for epifauna communities (image-level) identified by SIMPROF.  | 42 |
| Table 3-2: | Mean dissimilarity (%) between epifauna community groups (image-level) identified by SIMPROF.   | 44 |
| Table 3-3: | Results of the DistLM analysis showing correlations between predictor variables and epifauna community structure (image-level).   | 46 |
| Table 3-4: | Results of SIMPER analysis showing taxa accounting for >90% of within group similarity for the epifauna communities (transect-level) identified by SIMPROF.   | 48 |
| Table 3-5: | Mean dissimilarity (%) between epifauna community groups (transect-level) identified by SIMPROF.  | 48 |
| Table 3-6: | Results of DistLM analyses showing correlations between predictor variables and epifauna community structure (transect data).   | 52 |
| Table 3-7: | Results of DistLM analyses showing correlations between predictor variables and multivariate dispersion (mean deviation from centroid) among transects.   | 53 |
| Table 3-8: | Model <i>parameters and performance metrics of epifauna community (image-level) and Goniocorella dumosa</i> boosted regression tree models.   | 55 |

## Figures

|             |   |    |
|-------------|---|----|
| Figure 1-1: | Map showing the Chatham Rise and the location of Chatham Rock Phosphate's Mineral Mining License and Mineral Mining Permit areas (numbered).  | 10 |
| Figure 2-1: | Map showing the location of the CRP Environment Survey areas within the mineral mining licence area (red boxes are mining target areas; the licence area is outlined in green; blue area is a digital terrain model based on multibeam bathymetric data; contours are for water depth in metres). | 16 |
| Figure 2-2: | Map showing survey regions of the Chatham Rise Benthos (OS20/20) Survey.  | 18 |
| Figure 2-3: | Map showing the distribution of survey areas within each region of the Chatham Rise Benthos (OS20/20) Survey.   | 20 |

---

|              |   |    |
|--------------|---|----|
| Figure 2-4:  | Map showing the location of the ROV transects (orange lines) and box-core stations (red squares with station numbers) within the survey areas (red boxes are mining target areas) of the CRP Environment Survey.      | 21 |
| Figure 2-5:  | Map showing the location of the DTIS transects (blue lines) and box-core stations (red crosses) within the survey areas (small shaded boxes) and CREST region (red box) of the Chatham Rise Benthos (OS20/20) Survey. | 23 |
| Figure 2-6:  | Remotely operated vehicle (ROV) <i>Zeus II</i> used to take images of the seafloor and obtain multi-beam echo sounder data.   | 24 |
| Figure 2-7:  | NIWA's Deep Towed Imaging System used to take images of the seafloor during OS20/20 surveys.  | 26 |
| Figure 3-1:  | Dendrogram showing groups of samples identified as epifauna communities (image-level) by SIMPROF (after initial k-means classification).  | 40 |
| Figure 3-2:  | Seafloor images representative of the epifauna communities (image-level) identified by SIMPROF (Communities <i>f, g, j, m, n, o, p, q</i> ).  | 43 |
| Figure 3-3:  | Distribution of within-transect heterogeneity in epifauna community structure across the study area.  | 45 |
| Figure 3-4:  | Dendrogram showing groups of samples identified as epifauna communities (transect-level) by SIMPROF.  | 47 |
| Figure 3-5:  | Seafloor images representative of the epifauna communities (transect-level) identified by SIMPROF (Communities <i>a, b, d, j, l</i> ).  | 49 |
| Figure 3-6:  | Distribution of the relative abundance of the stony coral <i>Goniocorella dumosa</i> in the study area.   | 50 |
| Figure 3-7:  | Distribution of epifauna communities (transect-level) in the study area.  | 51 |
| Figure 3-8:  | Predicted habitat suitability for epifauna Community <i>f</i> (image-level) in the study area.  | 58 |
| Figure 3-9:  | Predicted habitat suitability for epifauna Community <i>g</i> (image-level) in the study area.  | 59 |
| Figure 3-10: | Predicted habitat suitability for epifauna Community <i>j</i> (image-level) in the study area.  | 60 |
| Figure 3-11: | Predicted habitat suitability for epifauna Community <i>m</i> (image-level) in the study area.  | 61 |
| Figure 3-12: | Predicted habitat suitability for epifauna Community <i>n</i> (image-level) in the study area.  | 62 |
| Figure 3-13: | Predicted habitat suitability for epifauna Community <i>o</i> (image-level) in the study area.  | 63 |
| Figure 3-14: | Predicted habitat suitability for epifauna Community <i>p</i> (image-level) in the study area.  | 64 |
| Figure 3-15: | Predicted habitat suitability for epifauna Community <i>q</i> (image-level) in the study area.  | 65 |
| Figure 3-16: | Predicted habitat suitability for the stony coral <i>Goniocorella dumosa</i> (image-level) in the study area.   | 66 |

Reviewed by

Approved for release by

Handwritten signature of Alison MacDiarmid in black ink.Handwritten signature of Julie Hall in black ink.

Dr Alison MacDiarmid

Dr Julie Hall

---

## Executive summary

The mineral prospecting licence area 50270 of Chatham Rock Phosphate Limited (CRP) covers an area of 4726 km<sup>2</sup> on the Chatham Rise. CRP has a mineral mining permit for part of this area, and in support of the 'marine consent' to undertake mining, information regarding the benthic communities in the permit and license area is required. This information will be used to assess the implications of the proposed mining activities on benthic communities, and to design measures to mitigate, and monitor, potential environmental effects.

The objectives of the present project were to: determine the benthic epifauna community structure within the mining permit area and elsewhere on the crest of the central Chatham Rise, and the environmental drivers of any patterns observed; use these data to produce predictive models of the distribution of benthic epifauna communities within the mining permit area and elsewhere on the crest of the central Chatham Rise; and compare the structure and distribution of benthic epifauna communities in the mining permit area and elsewhere on the crest of the central Chatham Rise with benthic epifauna communities previously sampled elsewhere in the New Zealand region.

Seafloor images were obtained from ROV and towed camera transects undertaken during a CRP Environmental Survey in 2012, and two OS20/20 surveys in 2007 and 2013 (the Chatham Rise-Challenger Plateau Survey and the Chatham Rise Benthos, respectively). Seafloor images were used to obtain data on benthic epifauna from each survey, and the datasets merged. The seafloor habitat was characterised using the same images, as well as topographic metrics from multi-beam echo sounder data collected during the surveys and from archived data. Habitat characterisation was also achieved by using available data layers for regional scale environmental variables, and deriving substratum data layers from archived data and recent sampling.

Multivariate statistics analyses identified 13 epifauna communities at the image-level scale, their distributions, and the characterising taxa of the 8 main communities. The potential extent of suitable habitat for each of these main communities in the study area was then predicted by modelling. The environmental variables that explain the overall community structure and the distribution of the individual communities were also identified by both these analyses. The structure and predicted distribution of suitable habitat for the communities was explained by combinations of many predictor variables, although some variables were of particular importance.

Overall, the structure of the epifauna communities is mostly relatable to the presence of mud/sand and phosphorite nodules. Habitat suitability models indicate that as well as local variables that characterise the substrate, regional-scale variables can also be important for predicting the distribution of the identified communities. Two of the epifauna communities are dominated by the stony coral *Goniocorella dumosa*, and show a patchy distribution in the study area that was associated with presence of phosphorite nodules that are concentrated in the mining permit and license area. However, habitat suitability models predict that these two epifauna communities could be more widespread within the study area. These predictions are largely driven by high values of sea surface temperature gradient, that are indicative of a front between overlying water-masses in the northwestern part of study area and which extends into the mining permit area.

Comparison of the benthic communities identified by the study, and communities described from previous sampling on the Chatham Rise, indicates that some epifauna communities within the mining permit and license area have not been found elsewhere on the Rise to date. These apparently unique communities include the two communities dominated by high abundances of *Goniocorella dumosa*. These communities can be classed as coral thickets which are sensitive environments under Environmental Protection Authority regulations, and the stony coral on which they are based is a protected species in New Zealand waters.

Confidence in using the habitat suitability models to design mitigation measures (i.e., identify no-mining or reserve areas) will depend upon the field validation of the models. This can be achieved by conducting additional targeted sampling using a towed camera, particularly in the areas identified to be suitable habitat for *Goniocorella dumosa* dominated communities, and which overlap with the bottom trawl footprint.

# 1 Introduction

## 1.1 Proposed phosphorite nodule mining on the Chatham Rise

Phosphorite deposits are potentially the most important economic marine mineral resource around New Zealand, and the main deposits are on the Chatham Rise (Glasby & Wright 1990). The distribution and characteristics of these deposits has been well studied since 1975 (e.g., Pasho 1976, Cullen 1980, Kudrass & Cullen 1982, Kudrass & von Rad 1984a, von Rad & Kudrass 1987), and the results of these studies have been reviewed by Glasby & Wright (1990).

Phosphorite deposits are formed by the phosphatisation of limestone, which was followed by the fragmentation of this chalk hardground on the Chatham Rise, in a process that began in the mid-Miocene. Phosphorite occurs as “nodules” (2 to > 150 mm diameter, maximum frequency 10 - 40 mm diameter) in a matrix of glauconitic sand, and can extend beneath the seafloor sediment surface to 0.7 m. Nodules are found in water depths of about 400 m along approximately 400 km of the crest of the Chatham Rise. Nodule distribution is very patchy at a number of spatial scales as a result of biological and physical processes that took place during and after phosphatisation (e.g., upwelling, bioturbation, iceberg scouring). The region with the highest concentration of nodules is between longitudes 179° and 180° East. Here combined nodule weight averages 66 kg/m<sup>2</sup>, which represents a total of about 100 million tonnes (Glasby & Wright 1990). Nodules contain minerals that can be used as a component of agricultural fertilizer, which is why there has been a long interest in mining these deposits.

A Mineral Mining Permit (MMP) and Mineral Prospecting Licence (MPL) have been issued to Chatham Rock Phosphate Limited (MMP 55549 within MPL 50270). The combined area of the Chatham Rise covered by this permit and license is 4726 km<sup>2</sup> (of which the MMP is 821 km<sup>2</sup>) – hereafter collectively referred to as the ‘mining permit area’. Chatham Rock Phosphate also holds two Mineral Prospecting Permits (MPP) to the west and east of the aforementioned mining permit area (MPP 55971 and 55967, which have areas of 1502 km<sup>2</sup> and 4985 km<sup>2</sup>, respectively) (Figure 1-1). The Mineral Prospecting Licence and Permits provides mining companies with the right to undertake sampling and other activities that allow them to evaluate the economic worth of phosphorite deposits within their licence and permit areas, and to gather information that will inform any future mining operations (e.g., practical operation of mining tools), before they submit an application for a Mineral Mining Permit to New Zealand Petroleum and Minerals. A Mineral Mining Permit grants a resource company the right to mine the seabed for commercial purpose, dependent upon a number of conditions. Before commercial mining can commence, mining companies need to seek a ‘marine consent’, pursuant to the Exclusive Economic Zone and Continental Shelf (Environmental Effects) Act 2012. Chatham Rock Phosphate Limited (CRP) is seeking such a consent, and in support of their application they are producing an Environmental Impact Assessment (EIA). The EIA includes information that has been used to design spatial planning measures that aim to mitigate, and monitor, the environment effects of the proposed mining activities. Knowledge of the structure and distribution of benthic communities on the Chatham Rise is essential information for the EIA.

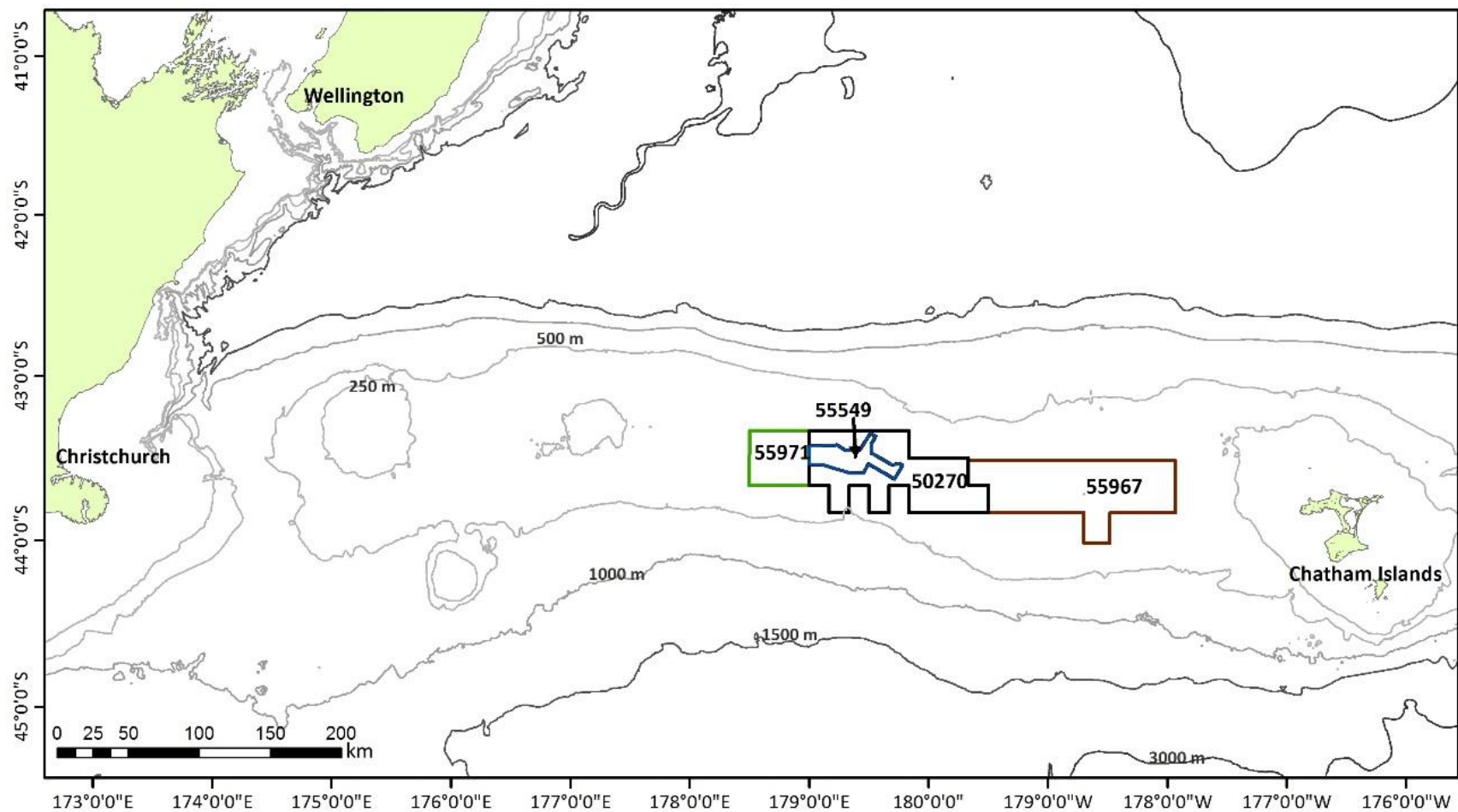


**Figure 1-1: Map showing the Chatham Rise and the location of Chatham Rock Phosphate's Mineral Mining License and Mineral Mining Permit areas (numbered).**



## 1.2 Benthic communities on the Chatham Rise

The Chatham Rise is a prominent submarine feature that extends 100 km from Banks Peninsula eastwards for 1400 km. Five areas with depths less than 200 m occur across the rise: Mernoo, Veryan, Reserve and Wharekauri Banks and the Chatham Islands. West of the Chatham Islands, the Rise is generally flat topped at 200-400 m, whilst east, north and south of the feature the water depths increase to over 2000 m (MacKay et al. 2005). Surface sediments on the Rise are predominantly fine-grained sands and muds with occasional outcrops of coarser material. Below 150 m water depth the calcareous organic fraction of the surface sediment is composed mostly of foraminiferan tests, whereas molluscan fragments are more common above 150 m water depth and may dominate the surface sediments at shallower depth (e.g., the biogenic sediments of the Mernoo and Veryan Banks) (Norris 1964).

Of the prominent banks on the Chatham Rise shallower than 300 m, only the benthic fauna of the Mernoo Bank has been partially described, and only then for molluscs occurring at three shallow (77-104 m) essentially shelf stations (Dell 1951). Descriptions of the slope/bathyal fauna began with a brief report by Hurley (1961) who examined six stations from depths of 403-604 m from sandy mud on the Chatham Rise. Hurley (1961) described a "*Serolis bromleyana* [*Brucerolis hurleyi*]-*Spatangus multispinus* community" and considered this community to be "sufficiently distinct from any sublittoral communities previously described to warrant distinctive recognition." Probert and co-workers began (from 1989) to examine in a systematic way the composition and distribution of benthic fauna across the rise, which became incorporated into a wider study led by Nodder (from 1997) to understand the influence of the Subtropical Front (STF), an oceanographic feature that overlies and characterises the Chatham Rise ecosystem (Sutton 2001).

Studies of the mega- (visible animals usually larger than 1-5 cm) and macrofauna (animals retained on sieve mesh >300  $\mu\text{m}$ ) have used different sampling gears to sample the two main components of the benthic community. Anchor-box dredges, box-corers and multi-corers to sample the fauna mainly residing within the sediment (infauna) (Probert and McKnight 1993, Probert et al. 1996, Probert et al. 2009), and small trawls, benthic sleds and towed cameras to sample the fauna of the seafloor surface (epifauna) (see references below). There have also been studies of the supra- or hyper-benthos (animals of the benthic boundary layer ~1 m above the seafloor surface) (Lörz 2010, Knox et al. 2012), and those that have focussed on the meiofauna (animals retained on sieve mesh >45  $\mu\text{m}$  but <300  $\mu\text{m}$ ) of the Chatham Rise (e.g., Grove et al. 2006, Leduc et al. 2012). Only the mega- and macro-epifauna are considered further here.

### 1.2.1 Epifauna communities

McKnight & Probert (1997) described the epifaunal component of the Chatham Rise macrobenthos from samples taken with a small Agassiz trawl at generally the same stations as previous dredged for infauna (Probert & McKnight 1993, Probert et al. 1996), augmented with samples taken in 1993 from a further 16 stations on the central sampling transect. Using multivariate analyses, McKnight & Probert (1997) identified three benthic "community groups"; the shallowest community was characterised mainly by crustaceans and two deeper water communities characterised mainly by echinoderms. Group A was found on mainly sandy sediments on the crest and shallower flanks of the rise at 237-602 m; Group B at 462-1693 m was associated with muddy sediments; Group C on muddy sediments at 799-

2039 m. McKnight & Probert (1997) considered community “A” to be similar to the *Serolis bromleyana* [*Brucerolis hurleyi*]-*Spatangus multispinus* community described by Hurley (1961), and commented that whilst some species of this community and of communities “B” and “C” were found elsewhere in New Zealand (and some globally) at bathyal depths, the extent of their respective distributions was poorly known. It was also noted that the bathymetric range of assemblages on the north and south flanks of the Chatham Rise appeared to be asymmetric, presumably because of temperature differences caused by the vertical displacement of the Antarctic Intermediate water on the north flank (McKnight & Probert 1997).

In 2007 an Ocean Survey 20/20 (OS20/20) survey was conducted on the Challenger Plateau and Chatham Rise, which included sampling of the epifauna using a benthic sled, trawl, and taking of video and still images using a towed camera (Bowden 2011). Floerl et al. (2012), using multivariate analysis, identified 9 main “biological groups” (represented by >2 sites) of which 8 were observed on the Chatham Rise, and three of them only on the rise. The distribution of these groups showed a marked across-rise pattern, that these authors presumed to be driven by depth, slope and productivity (Floerl et al. 2012).

### 1.2.2 Environmental drivers

As is noted above, environmental factors such as substrate type and depth were first related to the patterns of benthic community structure and distribution on the Chatham Rise. It was also speculated early on that patterns were most likely related to food availability as controlled by oceanographic processes. A multidisciplinary study to understand benthic-pelagic coupling processes associated with the STF on the Chatham Rise (that confirmed some of the benthic patterns observed by Probert and co-workers), clearly established that the spatial pattern in the make-up of benthic communities across the rise that reflects variability in the transportation of organic matter to the seabed (Nodder et al. 2003). This variability was related to both the position of STF, where surface waters have seasonally high levels of plankton biomass, and the influence of currents that advect particles of sinking organic matter that result from the death of planktonic organisms (Nodder et al. 2003). A spring deposition event of phytodetritus on the southern flank of the rise recorded in a subsequent study by (Nodder et al. 2007) was coincident with a region of current convergence, and with elevated benthic biomass and sediment community respiration rates. A study by Berkenbusch et al. (2011), that included data for meiofauna, reiterated the importance of phytodetritus flux in structuring benthic assemblages in the Chatham Rise/Subtropical Front region.

While it is evident that significant sampling of benthic communities has taken place on the Chatham Rise, and a broad understanding of community structure and distribution has been developed in the context of the main environmental drivers of these patterns – studies to date have been restricted to relatively few sites, particularly on the crest of the rise, and there has been very little information generated to date for the MPL area 50270 of Chatham Rock Phosphate Limited (CRP) (Beaumont & Baird 2011).

### 1.2.3 Benthic communities of the mining permit area

Dawson (1984) summarised the taxon-focused studies which were published in the 1960s and 1970s, as well as geologically-focused sampling (grabs and photo/video images) undertaken by NZ-German collaborative studies (in 1978 and 1981 using the RV *Valdivia* and RV *Sonne*, respectively), when qualitatively describing the benthic fauna and assessing

possible effects of phosphorite nodule mining on the rise. The wide expanse of sediments that make up much of the surface of the rise where mining is proposed were deemed to be characterised by large echinoids (*Paramaretia* and *Spatangus*), asteroids (*Zoroaster*, *Astropecten*, *Plutonaster*, *Mediaster*), conical sponges (*Hyalascus*), crabs (*Carcinoplax victoriensis*, *Trichopeltarion fantasticum*), galatheids (*Munida*), gastropods (*Cymatona* and *Fusitriton*), and smaller burrowing polychaetes, bivalves, isopods, amphipods, cumaceans (Dawson 1984). Polychaetes were the dominant group in terms of frequency of occurrence (by station). In places where there was hard substratum suitable for colonisation by sessile fauna, Dawson (1984) noted that a “quite extensive epifauna” of corals (such as *Goniocoralla dumosa*), bryozoans, cnidarians, bivalves and brachiopods developed. Dawson considered the “*Goniocoralla* clumps” as “epifaunal oases” which “undoubtedly attract small fish as feeding areas and may well be more the centre of energy dispersal than the smoother parts of the Rise”.

Dawson’s (1984) summary was in part based on the observations recorded by Kudrass & von Rad (1984b) from underwater imagery taken during the RV *Sonne* survey. Analysis of this imagery led these authors to note a series of correlations between the distribution of phosphorite nodules and macrobenthic fauna. In particular they noted that “colonies of branching corals (e.g., *Goniocoralla dumosa*) and gorgonian corals form patches of dense growth, especially in areas where large phosphorite nodules cover the seafloor in Area 4 [eastern part of their study area]”. They also remarked that “those corals are much less frequent in Areas 1 and 2 [western part of their study area] where phosphorite nodules are smaller.”. Other positive correlations with nodules were noted for small burrowing crabs, molluscs, brachiopods, asteroids, and cidarid echinoids. Other types of echinoid were observed to show a negative correlation with visible phosphorite nodules (Kudrass & von Rad 1984b).

Between the survey described in this report and the surveys by RV *Valdivia* and RV *Sonne*, no samples have been taken that can be used to provide a better appreciation of the benthic communities of the permit area than that summarised by Dawson (1984), and detailed in part by Kudrass & von Rad (1984b). However, data from the 2007 OS20/20 survey of the Challenger Plateau and Chatham Rise has been used to make predictions of the distribution of benthic communities across the slope areas off central New Zealand (Compton et al. 2012), that includes the permit area. Model predictions are a useful way to provide an indication of the structure of benthic communities in unsampled areas, and are particularly useful for spatial management planning (Guisam & Thuiller 2005). At the large spatial scale of the 2007 OS20/20 survey models, there was little in the way of predicted change in assemblage composition across the permit area (Compton et al. 2012). This result is not surprising, given the spatial scale at which the models were operating and the fact that the models did not include any data from within the mining permit area.

Thus it is important to obtain information on the structure and distribution of the benthic communities within the permit area, and for these data to be used to generate predictive maps that can inform the management of the environmental effects of the proposed mining of phosphorite nodules on the Chatham Rise. It is also important to place information on the benthic communities within the mining permit area in the context of what is known about communities elsewhere on the rise.

A previous study provided such information for the permit area (Rowden et al. 2013). The present study provides additional information over a wider area, which was made possible by

data gathered during an Ocean Survey (OS) 20/20 survey of the Chatham Rise in 2013. Data for benthic epifauna (but not infauna) were merged with similar data gathered by the Environmental Survey carried out by CRP in 2012, and an earlier OS20/20 survey of the Chatham Rise (and Challenger Plateau) conducted in 2007.

## 1.3 Objectives

The project reported here had three objectives:

1. Determine the benthic epifauna community structure within the mining permit area and elsewhere on the crest of the central Chatham Rise, and the environmental drivers of any patterns observed.
2. Use these data to produce predictive models of the distribution of benthic epifauna communities within the mining permit area and elsewhere on the crest of the central Chatham Rise.
3. Compare the structure and distribution of benthic epifauna communities in the mining permit area and elsewhere on the crest of the central Chatham Rise with benthic epifauna communities previously sampled elsewhere in the New Zealand region.

## 2 Methods

### 2.1 Survey design and planning

#### 2.1.1 Rationale for CRP Environmental Survey design

The main aim of the CRP Environmental Survey was to characterise the benthic habitats and communities within the mining permit area, and to provide CRP with additional geotechnical information about their permit area.

CRP designated eight areas for geotechnical investigation within the mining permit area, with the expectation that these areas will be the first sites of any future mining. These mining target areas span the shallower, central part of north-western region of the permit area. Each area occupies approximately 15 km<sup>2</sup>.

As the potential site of future mining, it is important that the benthic communities of these targets areas are known so the direct physical impact of mining activities can be assessed. It is also important to know what benthic communities exist in other parts of the permit area, and outside of the permit area, in order to be able to assess the indirect impacts of future mining activities (e.g., from the dispersal of suspended sediment). In addition, wider sampling gives a more robust understanding of the regional biodiversity in order to assess the particular biotic characteristics within the permit area.

Knowledge of the character and distribution of benthic communities will also provide information that can be used to plan future management strategies. For example, to identify areas with benthic communities similar to those areas that will be directly impacted, which could be 'set aside' as 'reserve' areas to provide potential sources of colonising fauna to aid recovery of the disturbed areas.

### 2.1.2 Planning for CRP Environmental Survey

All available information about the benthic habitats and communities of the licence area, and its vicinity (Beaumont & Baird 2011), were compiled and where possible converted into data layers for use in a geographic information system (GIS). Subsidiary data that could be useful for planning purposes were also converted to layers. Data layers included: bathymetry (including multi-beam echo-sounder and side scan data from an exploratory survey conducted by CRP), sediment composition, benthic invertebrates (phylum level), phosphorite nodule density, seismic facies, commercial fishing tows, research survey fish catch rates (hoki, hake, ling), sample data from RV *Valdavia* and RV *Sonne* (including video transects), and sample data held in NIWA databases (for different gear types and target sample type, and specifically for an OS20/20 survey of the Chatham Rise that was undertaken in 2007).

Relatively few data were available for benthic invertebrates in the licence area, and in the absence of time to analyse all data in great detail or with sophisticated methods, 'expert knowledge' was used to review the data layers. This review aimed to determine the likely distribution of different benthic habitats, and thus the scale at which faunal communities are likely to vary among, and within, the mining target areas, and the broader licence area.

The multi-beam echo-sounder (MBES) data gathered by the earlier exploratory survey were deemed the most useful data for this purpose because it illustrated the scale at which seabed depth and topography varied across the region of the licence area that is likely to be the focus of the proposed mining. Depth and topography are important habitat characteristics known to be correlated with the distribution and composition of benthic communities (e.g., Kostylev 2001).

Based on the initial bathymetric data, the eight mining target areas appeared to represent a range of different habitats, although areas 1 and 2 appeared to be similar to one another. A further six areas (covering a similar areal extent to the mining target areas) were selected to represent areas of both similar and dissimilar habitat within the region of the licence area where the target areas are located. Two further areas (areas 9 and 13) were selected that represent 'far-field' sites at the western and eastern extremes of the licence area. The western far-field area (area 9) was located outside of the area of MPL 50270 (in the licence area of another mining company at the time, but now part of a license held by CRP) in order to be some distance from its neighbouring target area (Figure 2-1).

The video and still images taken by a remotely operated vehicle (ROV) were used to determine the structure (composition and relative abundance) of mega-and macro-epifauna communities, and the *lebensspuren* (life traces) of infauna communities, while direct samples of the seafloor taken by a box-corer were used to determine the structure of infauna communities. Together these sampling methods provide good information about the seabed habitat and benthic communities.

The depth and topography within the designated areas are used to assess the orientation of the proposed ROV transects and the number of box-core stations that would be required to adequately capture the habitat heterogeneity within each area. Within the 16 survey areas, the locations of 3 ROV transects and 2 box-core stations per transect were planned prior to the survey.

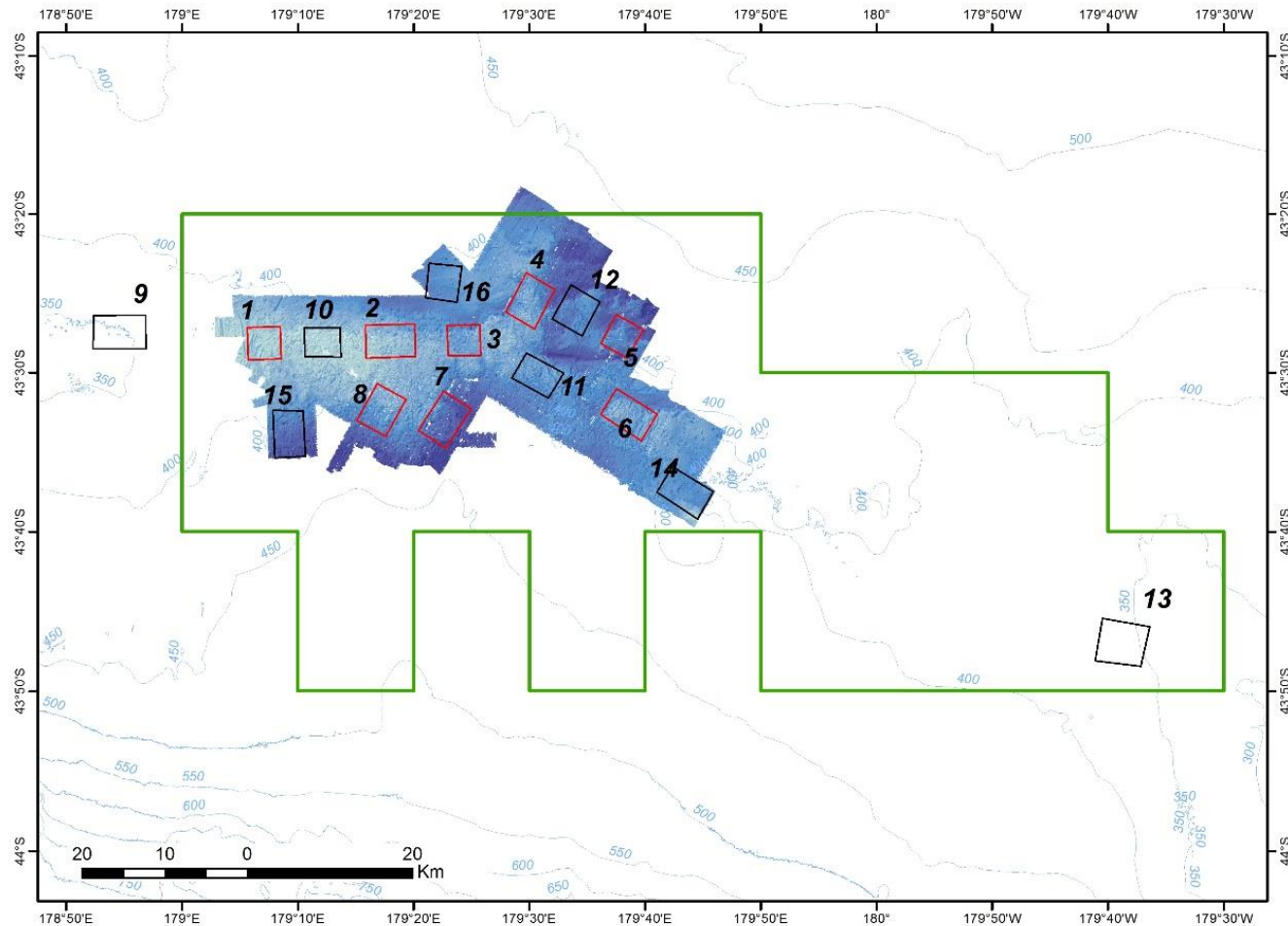


**Figure 2-1: Map showing the location of the CRP Environment Survey areas within the mineral mining licence area (red boxes are mining target areas; the licence area is outlined in green; blue area is a digital terrain model based on multibeam bathymetric data; contours are for water depth in metres).**



### 2.1.3 Rationale for Chatham Rise Benthos (OS20/20) Survey design

In May 2013, the Ministry of Primary Industries (MPI) submitted a successful proposal for use of Ocean Survey 20/20 (OS 20/20) ship time to study seabed habitats and fauna on Chatham Rise. The proposal was to collect and analyse high definition swath map data, benthic imagery and benthic samples from data-poor and previously sampled locations on the Chatham Rise to: (1) enable further testing of the utility of the Benthic Optimised Marine Environment Classification (BOMECE) (Leathwick et al. 2012) and biotic habitat classes (Hewitt et al. 2011) for spatial management purposes; (2) improve understanding of links between fishing intensity (seabed disturbance) and benthic biodiversity (sensitivity, functional groupings); and (3) improve the ability to determine the validity of biodiversity offsetting as a conservation tool in deep-water marine habitats (200-800 m). At the time of the OS20/20 bid, MPI recognised that these objectives were broad and had not been subject to robust consideration of their scientific feasibility.

Final agreement to proceed with the project was made contingent on discussion between MPI and NIWA scientists to assess which of the three proposed objectives (above), if any, were realistic, given available resources. Two research objectives were agreed upon in the subsequent contract between MPI and NIWA (Project MPI13304 –Chatham Rise Benthos):

1. Determine whether there are quantifiable effects of variations in seabed trawling intensity on benthic communities.
2. Conduct seabed mapping and photographic surveys in previously unsampled areas on the central crest of the rise.

The first of these objectives was to focus on an investigation of fishing intensity effects on benthic habitats and fauna in hoki fishing depths (ca. 500–700 m) and within a single BOMECE class. The second was to be more exploratory and more closely aligned with MPI's broader interests. Collecting data from previously unsampled areas on Chatham Rise, particularly within the Central Chatham Rise benthic Protection Area (BPA), would contribute to understanding of biodiversity distributions and thus feed into both the refinement of existing marine environment classifications, and managers' ability to make informed judgements on conservation, biodiversity, and ecosystem integrity questions in the future.

### 2.1.4 Planning for Chatham Rise Benthos (OS20/20) Survey

Recent summaries of trawling history across Chatham Rise (Baird et al. 2011; Black et al. 2013) show highest trawling intensity, primarily from the hoki fishery, at 500–700 m depth in Mernoo Gap and on the southern and northern central flanks of Chatham Rise. Taking the area south of Mernoo Gap (MERNOO) and the central-southern flank of the rise (SOUTH) as the two study regions for the first objective of the OS20/20 Survey, the aim was to sample within each region at a minimum of five survey areas selected to span a gradient of cumulative trawling intensities (Figure 2-2).

To satisfy the second objective of the OS20/20 survey, the aim was to sample 8 survey areas distributed across the Central Chatham Rise BPA, or the CREST region (Figure 2-2). Sampling within the CREST region would enable comparisons with samples collected during the CRP Environmental Survey.



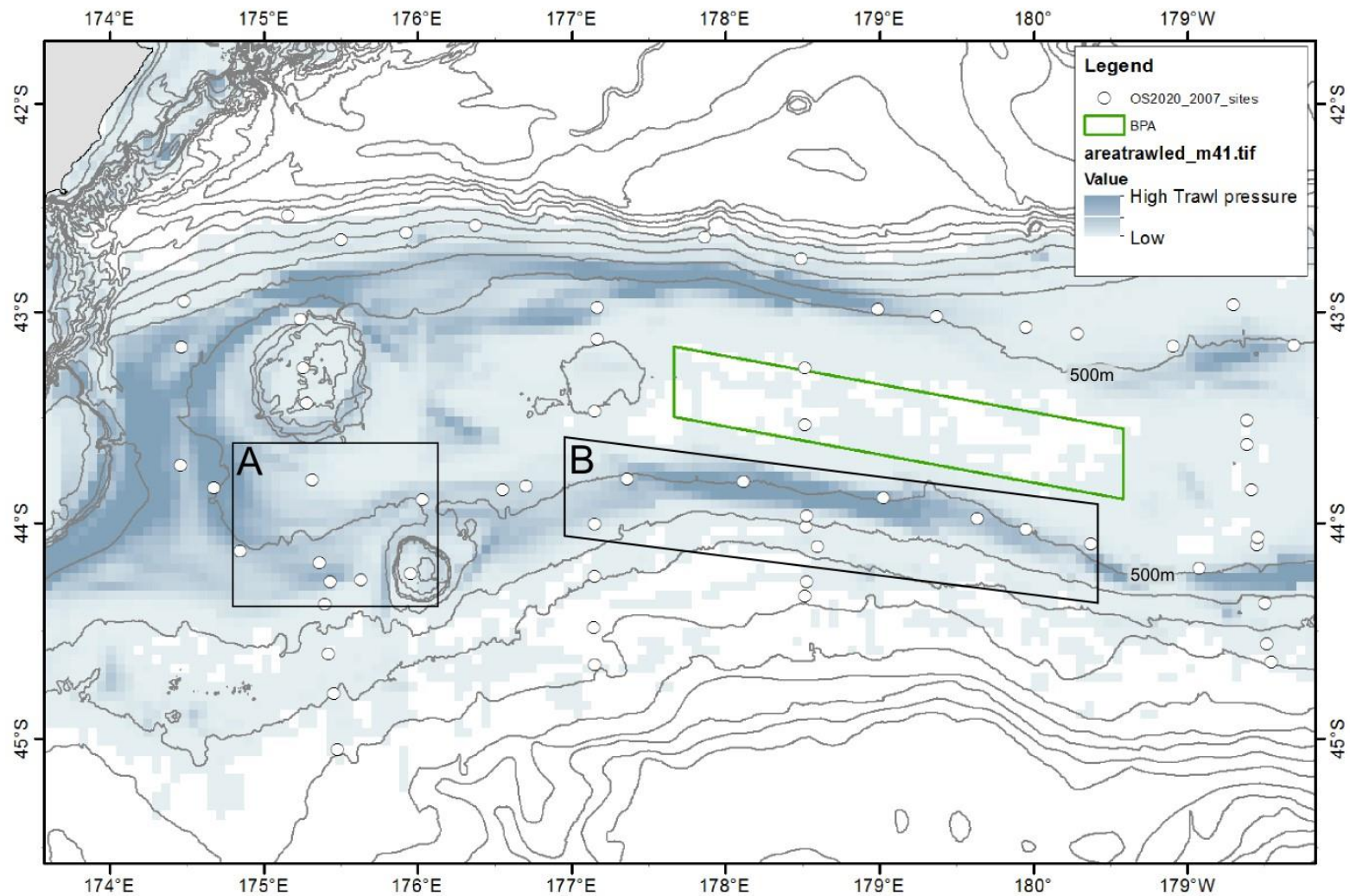


**Figure 2-2: Map showing survey regions of the Chatham Rise Benthos (OS20/20) Survey.** A= MERNOO region; B= SOUTH region; green outline = BPA/CREST region; white dots = Chatham-Challenger (OS20/20) Survey stations; blue shading = relative intensity of trawling.

Within each survey area (Figure 2-3), towed camera transects were to be made using NIWA's Deep Towed Imaging System (DTIS) to determine the structure (composition and relative abundance) of mega-and macro-epifauna communities, the lebensspuren (life traces) of infauna communities, and the substratum habitat characteristics. Three arbitrarily positioned DTIS transects were planned within each survey area. Two survey areas (L and Q) in the CREST region were also to be sampled using the box-corer to determine the structure of macro-infauna communities. Multicorer deployments were planned for survey areas in the MERNOO and SOUTH regions (not reported upon here).

CREST survey areas L, M, N, O and P were within CRP's mining permit area. Two survey areas (L and Q) had originally been included in the survey plan for CRP Environmental Survey (as areas 13 and 9) but were not sampled during the 2012 voyage because of time limitations (see below). It was intended from the outset that DTIS transects collected during the 2007 OS20/20 Chatham Rise voyage (TAN0705, see Figure 2-2) would also be analysed to provide complementary data.

### **2.1.5 Rationale for the Chatham-Challenger (OS20/20) Survey design**

The rationale for the design of the Chatham-Challenger (OS20/20) Survey carried out in 2007 is detailed in Nodder (2007).

### **2.1.6 Planning for the Chatham-Challenger (OS20/20) Survey**

The planning procedure for the Chatham-Challenger (OS20/20) Survey carried out in 2007 is detailed in Nodder (2007).

## **2.2 The surveys**

### **2.2.1 CRP Environmental Survey**

The CRP Environmental Survey was conducted from the RV *Dorado Discovery*, operated by Odyssey Marine Explorations. The survey was undertaken at the CRP licence area between 17<sup>th</sup> and 31<sup>st</sup> March 2012.

The highest priority was placed on sampling the mining target areas (1-8). Areas 1 and 2 were likely to be similar habitats and thus area 2 was the lowest mining target area priority. Area 7 was in deeper water and had less potential mining interest and was to be sampled after area 8. Priority order for mining target areas was therefore: 1, 3, 4, 5, 6, 8, 7, 2. Of the other sample areas (9-16), the areas within the main focus region that represent habitats different from the mining target areas were to be sampled next (14, 15, 16). Thereafter, areas that had habitats that were likely to be similar to one of the mining target areas were to be sampled (11, 12, 10), before finally sampling areas outside of the focus area (13, 9). Priority order for remaining sample areas was 14, 15, 16, 11, 12, 10, 13, 9.

Weather conditions and gear performance issues during the CRP survey meant that survey areas 10, 13 and 9 were not sampled (which include the two 'far-field' sites). The remaining areas were all sampled with 3 ROV transects, and most areas were sampled with 2 box-core stations per transect (i.e., 6 stations). Exceptions were areas 3, 16 (5 stations), and area 12 (4 stations) (Figure 2-4).

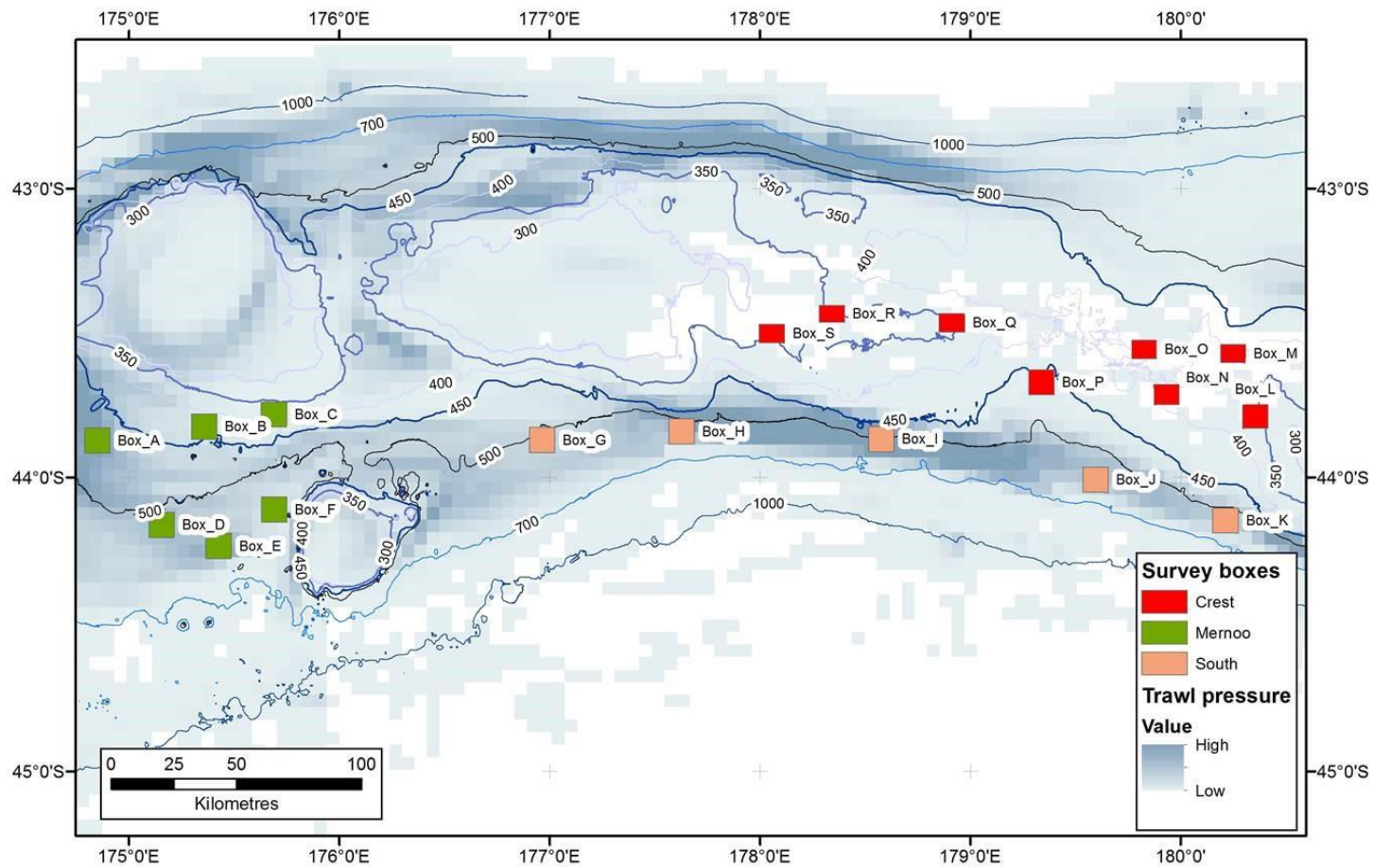
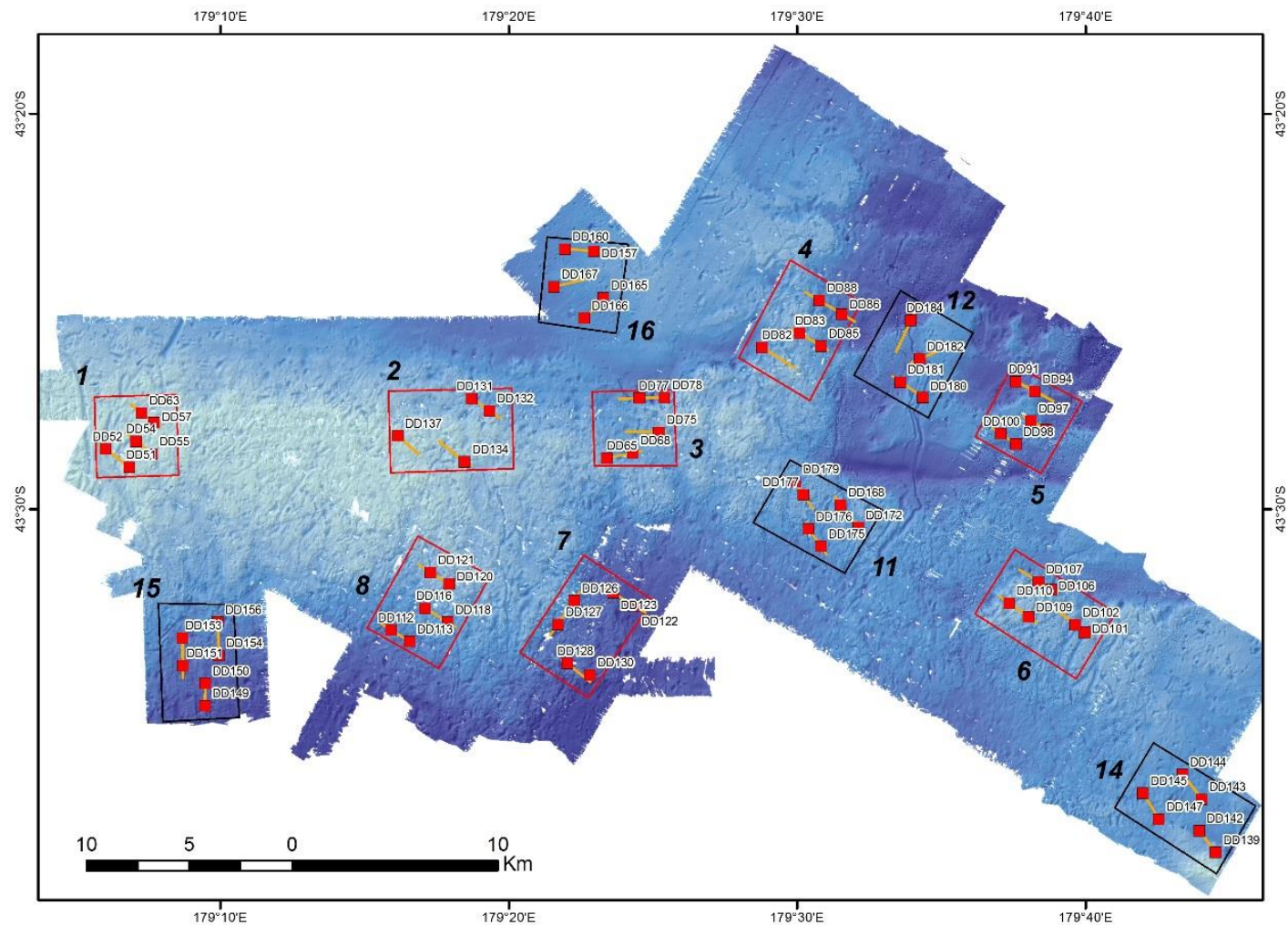


Figure 2-3: Map showing the distribution of survey areas within each region of the Chatham Rise Benthos (OS20/20) Survey.





**Figure 2-4: Map showing the location of the ROV transects (orange lines) and box-core stations (red squares with station numbers) within the survey areas (red boxes are mining target areas) of the CRP Environment Survey.**

## 2.2.2 The Chatham Rise Benthos (OS20/20) Survey

The Chatham Rise Benthos (OS20/20) Survey was undertaken from the RV *Tangaroa*, operated by NIWA, between 4th and 23rd June 2013. Sampling took place across three broad regions on Chatham Rise: a region south of Mernoo Bank (MERNOO); a region on the southern flank of the rise between approximately 176°30' E and 179°30'W (SOUTH), and within the boundaries of the Central Chatham Rise Benthic Protection Area (BPA) (CREST) (Figure 2-2).

In total, 19 survey areas were sampled during the voyage: 6 in the MERNOO region; 5 in the SOUTH region, and 8 in the CREST region (Figure 2.5). Success rate with all gear was high, with the following exceptions for the CREST region. DTIS: Adverse sea state during sampling at survey area O resulted in lower quality imagery. Box corer: Of nine deployments, only one sample (station 126) was too washed out to use for macrofauna analysis. This sample was in an area of high phosphorite nodule concentration and these had prevented the box-corer spade from closing completely.

## 2.2.3 The Chatham-Challenger (OS20/20) Survey

The Chatham-Challenger (OS20/20) Survey was undertaken from the RV *Tangaroa*, operated by NIWA. Sampling took place across and along the Chatham Rise between 31<sup>st</sup> March and 29<sup>th</sup> April 2007. Sampling stations, where DTIS was deployed, were within the CREST region of the Chatham Rise Benthos (OS20/20) Survey (Figure 2-2). See Nodder (2007) for further details about the survey.

## 2.3 Multibeam echo-sounder data acquisition

During the CRP Environmental Survey, Multi-beam echo-sounder (MBES) data were collected from the wider survey area using a ship-board Reson 8160 (50 kHz) system, as well as high-resolution MBES data from transects with the survey areas using a Reson 7125 (400 kHz) system mounted on a remotely operated vehicle (see below). MBES bathymetry data were edited and gridded with PDS2000 software by Odyssey Marine Exploration during the survey.

During the Chatham Rise Benthos and Chatham-Challenger (OS20/20) Surveys, MBES data were collected from individual survey areas using a ship-board Kongsberg EM302 (30 kHz) and Kongsberg EM300 (30 kHz) system, respectively. MBES bathymetry data were edited and gridded with CARIS HIPS, and C&C HydroMap software by NIWA during the surveys (respectively).

Data from the MBES surveys were collected to characterise the habitat for use in the benthic community analysis, and subsequently for habitat suitability modelling (see sections 2.6, 2.7, and 2.8).

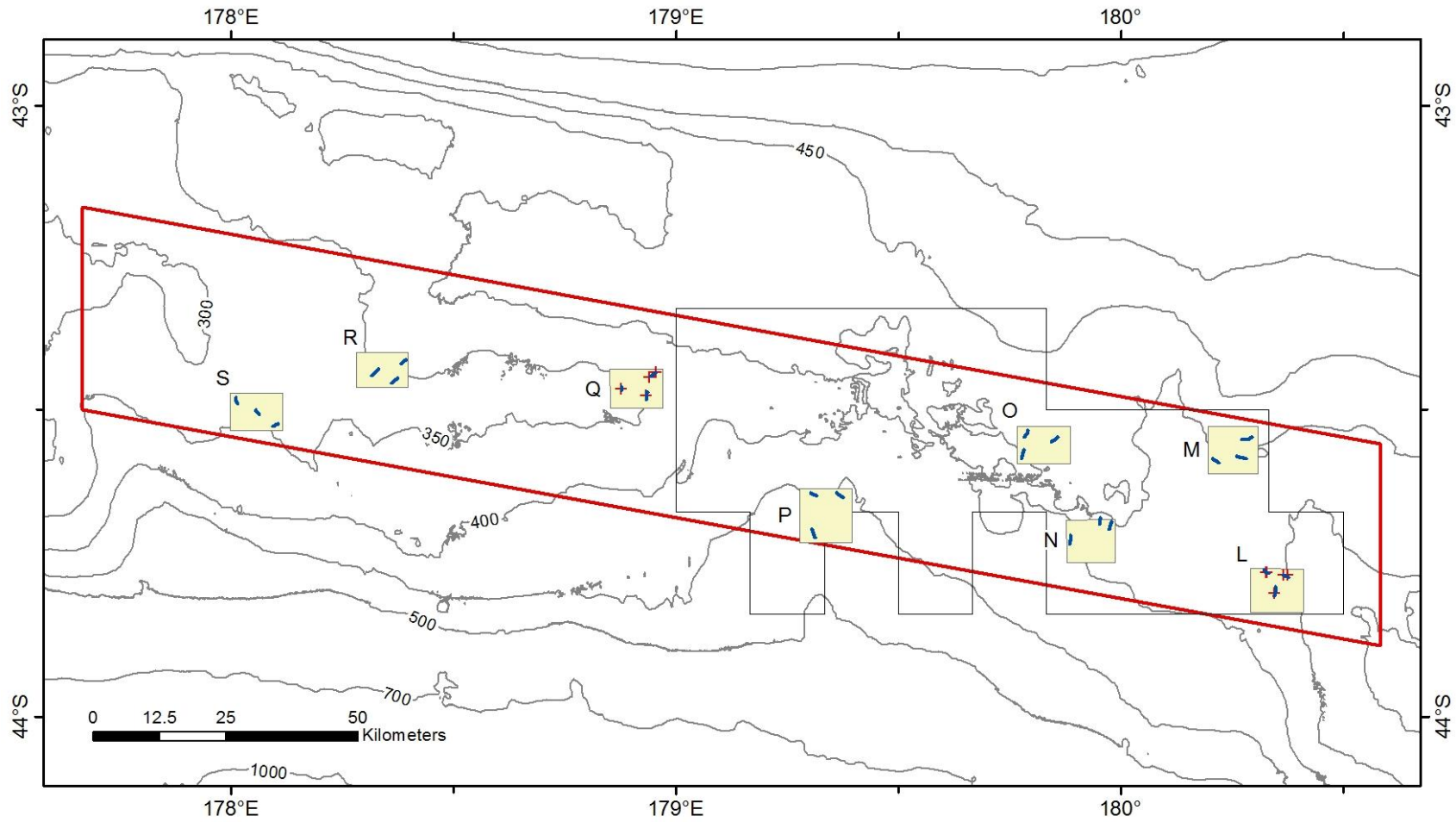


**Figure 2-5: Map showing the location of the DTIS transects (blue lines) and box-core stations (red crosses) within the survey areas (small shaded boxes) and CREST region (red box) of the Chatham Rise Benthos (OS20/20) Survey. [also shown is mining permit area].**

## 2.4 Biological sampling methods

### 2.4.1 Seafloor imaging on the CRP Environmental Survey

Video and still images taken by cameras on a remotely operated vehicle (ROV) were used to characterise benthic habitat and to sample mega- and macro-benthic communities. The ROV, *Zeus II* (Figure 2-6), was ‘flown’ at a target height of 2 m above the seafloor and at a speed of 0.5 knot along transects of approximately 1 nautical mile. Transects were initially completed in order of priority, then later in the most operationally efficient sequence. The ROV’s video and still cameras were inclined towards the seafloor at an angle of 45°. Still images were triggered manually at least every 15 seconds. The seabed position, depth and altitude of the ROV was continuously logged.



**Figure 2-6: Remotely operated vehicle (ROV) *Zeus II* used to take images of the seafloor and obtain multi-beam echo sounder data.** [photo: Emily Jones, Golder Associates].

The live video feed from the ROV was viewed on-board the research vessel by two biologists who logged their observations of benthic and pelagic organisms to the lowest taxonomic level possible in a hierarchical Access database. The biologists also logged observations of ‘lebensspuren’ (animal live traces) as they occurred on soft sediments. A geologist simultaneously logged seafloor features and bottom type in another Access database. If the biologists wanted to take video and still photographs at closer range or recover a sample, then progress along the transect was suspended while the ROV manoeuvred to complete the task. The ROV resumed the transect when the task was completed, and all camera settings were returned to transect defaults.



The manipulator arms of the ROV were used to sample animals where the identification of particular taxa was uncertain, and of small rocks or coral heads that provided habitat for biota that were unlikely to be observable in video and still images. Some use was made of net attachments in retrieving the specimens but most were collected directly using the ROV manipulator arm. Time of capture was recorded along with video and still images of the collection process. Retrieved samples were preserved on-board for later processing. Stopping the ROV during transects to obtain these samples was time consuming and therefore this type of sampling was infrequent.

During the ROV transect, the biologists assessed the suitability of box coring sites chosen prior to the voyage to determine whether they were representative of the benthic habitats imaged along the transect, and identified alternative sites nearby if necessary.

#### **2.4.2 Seafloor imaging on the Chatham Rise Benthos and Chatham-Challenger (OS2/20) Surveys**

Video and still images taken by cameras on NIWA's Deep Towed Imaging System (DTIS) (Figure 2-7) were used to characterise benthic habitat and to sample mega- and macro-benthic communities. DTIS transects were of 1 hour duration at target speed of  $0.25 \text{ ms}^{-1}$  and altitude of 2.5 m above the seabed. The camera's seabed position was tracked using R/V *Tangaroa*'s ultra-short baseline HiPAP system, and plotted in real time against the MBES bathymetry maps using Ocean Floor Observation Protocol software (OFOP, [www.ofop-by-sams.eu](http://www.ofop-by-sams.eu)), with the officer of the watch using the OFOP repeater screen on the bridge for precise positioning of DTIS in relation to seabed features. DTIS recorded continuous HD video (1080i format) with high-resolution still images taken every 15 s (Canon 350D 8 megapixel single lens reflex camera). Pairs of parallel red lasers spaced 20 cm apart were projected into the image frame of both the video and the still image cameras to enable scaling of images.

Seabed video was monitored in real time, and spatially referenced observations of substrate type and benthic megafauna were logged using OFOP. These real-time observation files were used to generate initial distribution plots for common fauna and seabed characteristics.

DTIS video tapes were rendered as uncompressed high definition (1080 50i HDV) \*.m2t files using non-linear video editing software (Sony Moviestudio PE) and saved to a dedicated hard disc drive (HDD) for back-up. Still images were downloaded from DTIS immediately on recovery of the vehicle and file names and metadata were written using the 'batch edit' tool in ACDSee Pro. All images were then saved to the OFOP PC data drive and backed up to the DTIS video HDD. OFOP log files were checked for completeness and consistency after each deployment and backed up to the ship's server. Ashore, all video, image, and log files were uploaded to secure servers and the videotape originals (MiniDV format) archived at NIWA's Wellington site.

After each DTIS deployment, the high-resolution still images were examined by NIWA analysts on board. All visible taxa were identified to the finest practicable taxonomic resolution and a presence-only record was kept of taxa in each transect. Counts of observations made in real time from the shipboard DTIS video feed (i.e., the OFOP logs) were used to generate preliminary distribution maps showing occurrence and relative abundance of common taxa and observations across all study areas.



**Figure 2-7: NIWA's Deep Towed Imaging System used to take images of the seafloor during OS20/20 surveys.** [photo: NIWA]

### 2.4.3 Box-coring

Upon completion of the ROV and DTIS transects, two box core stations were occupied on each transect of the CRP Environmental Survey and on transects in the CREST region of the OS20/20 Survey. A Reineck type box-corer with a core of 200 (w) x 300 (l) x 450 (d) mm was used to sample the macro-benthic communities and to characterise the habitat on the CRP survey, and an USNEL type box-corer with a core of 500 (w) x 500 (l) x 500 (d) mm on the OS20/20 survey. On recovery of the box-core sample, the quality of the sample was categorised as 'good', 'fair' or 'poor'. A good quality sample showed surface features such as burrow openings, pits and mounds, had a relatively horizontal surface (i.e., not slumped in one direction), and evenly distributed surface fauna if present (i.e., not piled in one corner). A poor quality sample had slumping, large holes that clearly drained away to the base of the sample, no intact surface features or a 'washed out' look. A fair quality sample showed most of the features of a good quality box sample, with a few of the poor quality indicators (i.e., a small part of the core surface was 'washed out' but the majority was intact).

Where large nodules and hardground fragments were observed on the seafloor by the ROV video prior to the box-corer deployment, box-core samples were seldom undisturbed. This disturbance was primarily due to the large rocks catching between the box and the spade, which disrupted the seal at the base of the sample. In these instances 'fair' samples were often retained for processing as the frequency of 'good' samples recovered in areas other than soft sediment was very low. As the voyage progressed, time constraints dictated that repeat sampling to obtain good or fair quality samples was only possible once per site.

After the sample quality assessment, the surface of the sample was labelled and photographed and biological observations noted. Macrofauna observed on the surface, e.g., polychete worms or small urchins, were removed and preserved separately. When possible, a 10 cm diameter plastic core up to 40 cm long was inserted into the sample to recover a sub-sample for later sediment characterisation analysis. If the box-core sample was more than 15 cm thick it was further processed in two parts. The upper 15 cm was removed from the box using a small plastic trowel. This sediment was gently homogenised using filtered seawater (100 µm) and washed through a 300 µm sieve. The material (fauna and sediment) retained on the sieve was preserved in 10% buffered formalin solution. The portion of the sample below 15 cm was washed on a 1 mm sieve and the retained material preserved as above. For ease of processing and to prevent damage to the fauna, the larger phosphorite nodules in the sample were separated by hand and retained in a labelled bag. These nodules were preserved with the respective sieved sample. Often the samples that were unsuitable for biological processing, i.e., those categorised as 'poor', were kept as geological samples. Potentially interesting fauna among these rejected samples were sometimes retained. These samples were photographed and described on board.

## 2.5 Laboratory sample treatment

### 2.5.1 Seafloor images

More images were taken than could be practically analysed. Typically, at the frequency at which images were taken on the survey (every 15 seconds), NIWA would analyse every 4<sup>th</sup> image (an unpublished NIWA study has shown that this level of analysis is sufficient to identify >50% of the total number of taxa identified by the analysis of all images on a transect), however, for the CRP Environmental Survey the number of images analysed equated to every 8<sup>th</sup> image. In order to determine if this frequency was likely to lead to a poor understanding of the fauna in the survey areas, a trial analysis of all images from a single survey transect of the CRP Environmental Survey was conducted. The trial indicated that at a frequency of every 8<sup>th</sup> image the analyses would identify only ~40% of the total number of taxa identified by the analysis of all images on a transect (a result similar to the unpublished study). This issue arises because of the patchy nature of the seafloor habitat (i.e., substrate) and the high likelihood that images of small patches of habitat would not be analysed, and therefore species that might be particular to these habitats would go unrecorded. In order to overcome this issue, rather than analyse images on a strictly regular frequency of every 8<sup>th</sup> image, images were selected for analysis with respect to substrate type (i.e., stratified sampling).

A substrate descriptor was recorded for each image as a string of descriptions of all the substrate categories observed, without information about the proportions in each category (because there was insufficient time to calculate these data). Substrate categories were based on the basic substrate type descriptors typically used for habitat characterisation (mud/sand, cobbles/pebbles, boulders) with the addition of categories specific to the location (nodules, chalk patches, chalk hard-ground, scour, ledges, 'dark patches' (interpreted as recently exposed sub-surface layer of small-sized nodules, exposed through an unknown form of disturbance, Kudrass & von Rad 1984b)).

After each image had been analysed to characterise the substrate, this information was used to select images for the faunal analysis based on a simple stratification. Images were

identified from each transect that were taken of broadly soft (mud/sand, dark patches, chalk patches, scour) or hard (cobbles/pebbles, nodules, chalk hard-ground) seafloor habitat, and also small and distinct habitat types that are likely to be under represented if images were selected at regular intervals of every 8<sup>th</sup> image. These latter habitats were the substrate categories boulder and ledges.

All images within the strata boulders and ledges were selected for identification of fauna. Typically, only one or two images were taken of each occurrence of these habitats on a transect. For the hard substrate strata, the 2<sup>nd</sup> image was selected at the start of each habitat patch and every subsequent image taken at intervals of 2 minutes (i.e., every 8<sup>th</sup> image) until the end of the habitat patch. A similar selection process was used for the soft substrata, except that the first image to be selected was the 3<sup>rd</sup> image in the habitat patch and the subsequent frequency of selection was an image every 3 minutes (i.e., every 12<sup>th</sup> image) until the end of the habitat patch. This selection process meant that small patches of soft or hard habitat were not sampled (i.e., where < 10 images in total were taken). The use of the 2<sup>nd</sup>/3<sup>rd</sup> image, rather than the 1<sup>st</sup> image, to begin the selection process reflects the desire to avoid including images at the boundary of habitat patches (which are more indeterminate for soft than hard substrate, hence 3<sup>rd</sup> compared to 2<sup>nd</sup> image). The difference in the sampling frequency for images in the hard and soft strata reflects the relative homogeneity of the latter habitat, and therefore fewer images were deemed necessary to capture the biodiversity of this substrate.

Counts of fauna observed on the selected images were made using the software package ImageJ (<http://rsbweb.nih.gov/ij/>). Images were initially colour balanced and adjusted for contrast and brightness where necessary. For images from the CRP Environmental Survey, the upper fifth of the image area was not analysed because the 45 degree camera angle caused loss of image illumination at the top of the image frame, depending on the ROV height and pitch. Images from the OS20/20 Survey were planer and illumination constant, and the entire image was analysed. To economise on analysis time, image area was not calculated. However, the images analysed were taken at a relatively consistent height above the seabed (e.g., CRP Environmental Survey: 2.01 ±0.14 m, n=3,033) and, therefore, the observable area of the seafloor was very similar across all images for each survey (CRP Environmental Survey: approximately 6 m<sup>2</sup> total area, 4 m<sup>2</sup> analysed area; OS20/20 Surveys: approximately 2 m<sup>2</sup> analysed area).

Faunal identifications (to lowest possible taxonomic level) and counts were made by experienced observers who analysed images from separate transects. Identification of the fauna observed was standardised between observers by maintaining a common working 'pick-list' of fauna names. This list was based on identifications from NIWA's 'working guide' to identifying fauna from seafloor images (which is supported by a 'library' of example images of fauna) and published identification resources. Unknown or unidentifiable animals were initially tagged with a placeholder identification on the faunal pick-list, and representative images were sent to taxonomic experts for identification. The faunal pick-list and working guide/library was updated during the analysis by adding names for fauna newly encountered during the analysis. These names were based on a consensus among observers or as advised by taxonomic experts.

An audit of the faunal identifications among observers was undertaken, including a formal annotated review by one observer of all the images identified by the other observers for one

transect. After fauna on all images were identified, a meeting among observers was held to discuss the resulting data and any potential identification issues and to carry out any necessary identification reconciliation.

### **2.5.2 Box-core samples (for all surveys)**

On return to the laboratory, the box-core samples were sieved on two stacked sieves (1 mm and 300  $\mu$ m mesh) and the remaining material stained with 0.2 % Rose Bengal (to aid the visual recognition of macrofauna among the retained material). Material retained on the 1 mm sieve was sorted by eye on a white tray. Macrofauna were removed, separated into major taxonomic groups and preserved in 80% ethanol. The coarse sediment fraction (> 1 mm) was retained for separate analysis (see below). The material retained on the 300  $\mu$ m sieve was also sorted by eye in a white tray. The macrofauna from this fraction were removed, separated into major taxonomic groups using a dissecting microscope, added to those collected from the 1 mm sieve and preserved in 80% ethanol. Some of the box core samples contained a large amount of fine sediment (300  $\mu$ m – 1 mm). For these samples an elutriation process was used to first separate the macrofauna and lighter material prior to sorting in a white tray. The elutriation process was repeated three times. The remaining sediment of the first 10 samples processed in this manner were checked for any remaining macrofauna. This check revealed that more than 90% of the macrofauna was retained in the elutriate and no major taxonomic bias was noted. The fine sediment fraction (300  $\mu$ m – 1 mm) was not retained for any additional analysis.

The macrofauna sorting was carried out by three trained technicians and a quality assurance check was carried out by another technician (the most experienced sorting technician on site) on 10% of the samples sorted. No sorting inconsistency or macrofauna recovery issues were identified by this audit.

Sorted macrofauna were then identified to the lowest possible/practical taxonomic level by taxonomists or parataxonomists, counted and stored in 80% ethanol.

Data for infauna were not analysed and reported upon here (see Rowden et al. (2013) for results of the analysis conducted on infaunal data from the CRP Environmental Survey), but the methodology is noted here because it involved the recovery of sediment data used in the present analysis.

Sediment retained on the 1 mm sieve (i.e., > very coarse sand particle size) from each box-core sample was first sorted into chalk and non-chalk material, and then wet weighed separately on a balance ( $\pm$  0.001 g). The non-chalk material was predominantly phosphorite nodules, and the weight of this fraction was considered to equate to the weight of nodules in a sample.

Sediment sub-cores taken from the box-cores during the CRP Environmental Survey were processed by Royal Boskalis and Hill Laboratories on behalf of CRP.

Phosphorite nodule data resulting from the above were used for characterising the habitat of the study area (see section 2.6.2).



## 2.6 Habitat characterisation

### 2.6.1 Bathymetry and seafloor morphology

About 3 km<sup>2</sup> of ROV-mounted 7125 system MBES data and more than 500 km<sup>2</sup> of ship-mounted 8160 system MBES data were collected during the CRP Environmental Survey. The former data were gridded at 10 cm and the latter data were gridded at 25 m resolution. Data were exported from the PDS2000 software as ASCII files prior to laboratory processing.

All bathymetry data, including OS2020 multibeam echo-sounder (MBES) data were processed using CARIS HIPS. The contours were then added to the NIWA bathymetry database. From this data a seamless, 25m cell size grid of the study area was generated using ESRI ArcGIS. All analysis were run on the local MBES grids and on the combined, regional grid.

Corresponding backscatter data for the whole study area was not available. The absence of the backscatter data was a significant impediment to deriving robust estimates of the spatial variation in benthic habitat, and for use in benthic community analysis and subsequent habitat suitability modelling. As a consequence, effort was focused on characterising the habitats using seafloor morphology derivatives from the MBES bathymetry data.

These metrics were: depth, slope (steepest gradient to any neighbouring cell); aspect (direction of slope); curvature (change of slope); plan curvature (curvature of the surface perpendicular to the slope direction); profile curvature (curvature of the surface in the direction of slope). In addition a further set of derivatives were calculated for the standard deviation of depth, depth range, standard deviation of the slope, and terrain rugosity from focal mean analysis in ArcGIS.

The Focal Mean analysis finds the average of the values for each cell location within a specified neighbourhood and outputs these data to the corresponding cell location. Four different neighbourhood sizes (3x3, 5x5, 7x7 and 15x15 neighbourhood cells) were computed to produce more generalised datasets. The different neighbourhood cell sizes were selected to mimic a range of spatial scales at which seafloor bathymetry and topography may affect the distribution of benthic communities (e.g., 3x3 cells = 75 x 75 m; 5x5 = 125 x 125 m; 7x7 = 175 x 175 m; 15x15 = 375 x 375 m).

### 2.6.2 Substratum characteristics

#### *Sediment datasets*

For the purposes of improving and extending the characterisation of the seafloor substrates in the study area, the grain-size dataset of Nodder et al. (2013) was revised and updated.

The physical particle-size attribute data for surface sediments were provided by CRP, with data averaged over the top 10-15 cm, as well as archived data by NIWA (Nodder et al. 2013), including box core samples collected during the Chatham Rise Benthos (OS20/20) Survey. Percent mud (<0.063 mm), percent sand (2-0.063 mm) and percent gravel (>2 mm) are used to broadly characterise the surface sediments, rather than summarising more detailed textural information.

All replicates with zero gravel values, especially where the >2 mm fraction was not analysed, were excluded, as were all the archived RV *Sonne* (SO-17) data because there was no

quantitative way of extracting percent sand and percent mud values from these data, which were only provided as a (percent sand + percent mud, <1 mm) fraction. An attempt was made to derive a proxy for these two grain-size components by undertaking a linear correlation of all the other percent sand and percent mud data and applying this to the RV *Sonne* data, but the relationships of these parameters with percent gravel only had correlation coefficients ( $r^2$ ) of 0.30-0.40, so could not be utilised effectively as proxies. In addition, all replicates that also had a full grain-size analysis undertaken by Royal Boskalis were excluded to restrict the final data-set largely to samples analysed using approximately the same method as applied by the Royal Boskalis laboratories for CRP. There were, however, other samples (designated as TI, Waikato-TI and NIWA samples) that weren't analysed by Royal Boskalis and these were included in the final data-set (e.g., Nodder et al. 2013). Finally, a set of samples from the CRP Environmental Survey (numbered DD 186-213) were excluded since it became apparent that many of the samples from the same station were actually from deeper horizons below the seabed.

Additional grain-size data were provided from five box core samples (0-15 cm) collected on the Chatham Rise Benthos (OS20/20) Survey. These samples were analysed using a Coulter laser particle-sizer and the software program GRADISTAT V8 (Blott, 2010) to derive granulometric measures and statistics of sediment texture (size fractions, mean, modes, etc). Only two of these samples (TAN1306/128 and 129) had a conspicuous gravel (>2 mm) component, which was excluded from the laser particle-sizer samples prior to analysis, so this fraction was re-combined with the final size fractions and re-analysed in GRADISTAT V8.

The final grain-size data-set, with complete percent gravel, percent sand and percent mud components from CRP and the Chatham Rise Benthos (OS20/20) Survey, comprised 127 samples, with an additional 631 samples from the NIWA sediment archives, making a total of 758 samples to be used in the subsequent GIS approaches to derive grain-size data layers for the study area (see below).

The phosphorite nodule data used in the previous study of benthic communities (Rowden et al. 2013) was a measure of nodule density ( $\text{kg m}^{-2}$ ), derived almost solely samples taken by RV *Valdivia* and RV *Sonne* (Nodder et al. 2013), and was therefore largely restricted to the immediate area covered by CRP's mining permit area. In order to obtain a data-set with more regional coverage, data for the percent phosphorite nodule content of the substratum was utilised. These data were provided by Kenex Ltd. In addition, estimates of percent phosphorite content for five Chatham Rise Benthos (OS20/20) Survey box core samples (TAN1306/95, 97, 99, 128 and 129) were made based on qualitative determinations of the retained >1 mm size-fraction following macrofauna processing (J. Halliday, NIWA, pers. comm.). Additional estimates of percent phosphorite content were made for two other Chatham Rise Benthos (OS20/20) Survey samples (TAN1306/126 and 127), for which no macrofauna samples were retained, by comparing deck photographs of these samples with those collected using a large grab on CRP's mineral exploratory voyages using RV *Dorado Discovery*. The TAN1306/126 and 127 samples were ascribed phosphorite contents of 33% to indicate they were at the maximum range of comparable values from CRP, specifically samples collected at stations DD 38-40.



### *Derived sediment data layers*

Following the compilation of the point-source sediment grain-size and percent phosphorite nodule content data, ArcGIS was used to generate a gridded surface using the Natural Neighbour Interpolation method. This process determines the closest subset of input samples to a query point and applies weights to them based on proportionate areas in order to interpolate a value (Sibson, 1981). The same method was used by Nodder et al. (2013) for the previous study of benthic communities (Rowden et al. 2013).

Using this interpolation method, contour plots of percent gravel, sand, mud and phosphorite nodules were generated for the sample domain. These gridded surface data were then clipped to the model domain (between latitudes 42° 50'S and 44°30'S and longitudes 177°30'E and 178°W, and the area shallower than the 500 m isobath) used for the habitat suitability modelling analyses (see section 2.8).

In order to test the veracity of the interpolation method, independent grain-size data were collated from stations that were occupied on the Chatham-Challenger (OS20/20) Survey in 2007 (TAN0705). This independent sampling was conducted within the model domain used in the habitat suitability modelling analyses. While there were a total of five stations within this domain, only two grain-size samples from TAN0705/174 and 257 were available, with other stations (TAN0705/183, 185 and 254) not returning any sediment samples. The interpolated values at the locations of TAN0705/174 and 257 were within 5% of the actual values reported in Nodder et al. (2013), indicating that the modelled grid for each of the grain-size parameters within the model domain was likely predicting percentages close to those observed in reality. It is recognised, however, that these two samples had very similar compositions (i.e., 40-50% mud and 50-60% sand + gravel, with ~1% in the greater than 500 µm fraction (coarse sand and above)), and did not include a significant coarse gravel fraction, representative of the phosphorite nodule-rich areas on the central Chatham Rise crest.

### **2.6.3 Regional environmental variables**

Gridded data layers for environmental variables that describe the regional habitat characteristics of the Chatham Rise were obtained from those used to generate New Zealand's Marine Environmental Classification (MEC) (Snelder et al. 2007 and sources references therein). The layers selected are known or presumed to influence the distribution of benthic fauna over the spatial scale of the study area (see references in Tracey et al. 2011), and as such were deemed useful to include in the benthic community and habitat suitability analysis (see sections 2.7 and 2.8). These variables were: Bottom temperature (a variable that has a fundamental influence on the distribution of benthic fauna; for example by influencing reproduction and other metabolic functions), Primary productivity, Dissolved organic matter (DOM), Particulate organic carbon (POC) flux (all indicators of potential food availability for benthic fauna), Bottom current speed, Tidal current speed, Dynamic topography (three measures of water currents that can influence benthic fauna directly or indirectly; for example, through the delivery of food material or structuring of substratum characteristics), and Sea Surface Temperature (SST) gradient (an indication of the position of oceanographic fronts, which can represent areas of increased surface productivity and downwelling which can enhance food delivery to the benthos).

The data layers for these regional environmental variables were clipped to the model domain for the habitat suitability analysis.

## 2.7 Benthic community analysis

### 2.7.1 Pre-analysis treatment

In order to construct a dataset suitable for the final analysis, data were first subjected to assessment and modification.

Some taxa from the image data records were removed prior to any analysis. Fish and cephalopod species respond differently to the presence of a ROV or DTIS and their lights (e.g., avoidance response), and therefore a complete record of the demersal or benthic fish and cephalopod communities is not reliably obtained by just using these methods of data capture. Thus, fish and cephalopod taxa records were not included in the final dataset, leaving the focus of the analysis on the invertebrate communities alone. Some invertebrate taxa were also removed from the data because they were infaunal taxa (e.g., echinurans), or were ill-defined and/or could be confused with other taxa (e.g., polychaetes).

Data for lebenspuren (life traces of animals) were also not included in the datasets to be analysed because records that relate to infauna were too sparse to allow for a meaningful community analysis. Originally it was intended for these data to be analysed separately as another means to characterise the infauna community, particularly those animals not well-sampled by a box-corer (i.e., large animals that exist in low densities and/or live in deep burrows). Lebenspuren records that related to epifauna were never intended to be analysed, and so they too were excluded from the image datasets used in the final analysis.

### 2.7.2 Merging datasets

To generate the most complete summary of benthic epifaunal distributions currently possible for the central crest region of the Chatham Rise, the ROV photographic transect data collected during the CRP Environmental Survey were merged with DTIS image data from selected transects from the Chatham Rise Benthos and Chatham-Challenger (OS20/20) Surveys. The CRP dataset was derived from analysis of 2,767 images in 39 ROV transects across 13 survey areas. The Chatham Rise Benthos (OS20/20) Survey dataset was from 935 images in 24 transects across 8 survey areas within the CREST region, and the Chatham-Challenger (OS20/20) Survey dataset from 206 images in 6 transects selected for their proximity to the permit area on the crest of the rise.

Direct comparisons between ROV and DTIS images were complicated by differences in the image resolution and camera angle of the two camera platforms: ROV images were of lower resolution than DTIS images, and the ROV and DTIS cameras were angled at ca. 45° and 90° to the seabed, respectively. As a result, more taxa could be reliably identified from the DTIS images than the ROV images, particularly in the smaller size range, and the imaged seabed area was larger in the ROV images.

Large taxa unlikely to have been missed in ROV images, such as the large sea cucumber *Bathyploetes moseleyi* and distinctive sponge *Seriocolophus*, were left in the dataset (11 taxa in total, all from Chatham Rise Benthos (OS20/20) Survey). By contrast, forty small and/or cryptic taxa, including isopods (Serolidae) and the alcyonacean *Taiaroa tauhou*, were not included in the merged dataset because they were not detectable in the lower quality ROV

images. Thirty-eight individual taxa that were discriminated in Chatham Rise Benthos (OS20/20) Survey DTIS images were merged with existing CRP taxa at coarser taxonomic levels. For example, the colonial ascidian taxa *Aplousobranchia*, *Botrylloides*, and Polycitoridae, which were identified in DTIS images, were merged under the general grouping Encrusting bryozoan/sponge/ascidian in final analyses. Some common taxa, which were originally kept separate in the CRP dataset, were also merged in order to minimise any bias associated with potential misidentification. For example, juvenile *Paramaretia peloria*, adult *P. peloria* and Spatangidae were merged under the general taxon heading of “Irregular urchins”. Details of how each taxon originally identified from the three datasets were treated in the final analyses are shown in Appendix A. A total of 77 taxa were included in the final merged dataset.

Differences in image quality between ROV and DTIS images also caused differences in population density estimates, i.e., more individuals could be discriminated in the higher-resolution DTIS images, particularly for relatively small and abundant taxa. Data were compared from selected transects in survey areas from the CRP Environmental Survey and Chatham Rise Benthos (OS20/20) Survey that were (1) located in close proximity to each other (7-32 km), and (2) characterised by similar physical substrata and habitat-forming sessile fauna. Multivariate analyses of community structure between these transects showed significant differences between the CRP Environmental Survey and the Chatham Rise Benthos (OS20/20) Survey transects (PERMANOVA,  $P < 0.01$ , square root-transformed data,) and SIMPER analysis showed that the difference was caused by higher abundance of small taxa in the OS20/20 survey images relative to the CRP Environmental Survey dataset. The abundance of these taxa was ‘corrected’ in all images from the two OS20/20 surveys by dividing by their corresponding correction factors (Table 2-1) prior to conducting the final analyses.

|   | <i>CRP<br/>Environmental<br/>Survey<br/>Abundance</i> | <i>OS20/20 survey<br/>Abundance</i> | <i>Dissimilarity/<br/>SD</i> | <i>% contribution<br/>to similarity</i> | <i>Correction<br/>factor</i> |
|---|---|-------------------------------------|------------------------------|---|------------------------------|
| Encrusting organisms<br>(bryozoan/sponge/ascidians) | 119   | 174                                 | 1.6                          | 22                                      | 1.5                          |
| Branching organisms<br>(bryozoan/hydroid/other)     | 9   | 201                                 | 1.5                          | 21                                      | 22                           |
| <i>Goniocorella dumosa</i>                          | 100   | 46                                  | 1.1                          | 14                                      | -                            |
| Galatheidae/Chyrostylidae                           | 7   | 137                                 | 1.4                          | 14                                      | 20                           |
| <i>Paramaretia peloria</i>                          | 75  | 59                                  | 0.9                          | 9                                       | -                            |
| Brachiopoda   | 22  | 33                                  | 0.9                          | 7                                       | 1.5                          |
| Cup corals (stalked)                                | 1.6   | 31                                  | 1.2                          | 3                                       | 20                           |
| <i>Goniocidarid</i>                                 | 6   | 20                                  | 1.5                          | 2                                       | 7                            |

**Table 2-1: Results of SIMPER analysis showing the taxa responsible for the difference in community structure between selected transects from the CRP Environmental Survey and the Chatham Rise Benthos (OS/20/20) Survey, and derived correction factor.** Data were from survey areas O and N (CRP dataset,  $n = 6$ ) and 6 and 14 (OS20/20 dataset,  $n = 6$ ). Correction factors were only applied to small taxa likely to have been overlooked in the CRP images taken with ROV relative to OS20/20 images taken with DTIS.

### 2.7.3 Statistical approach

The merged image dataset represented 3,908 individual images, a substantial proportion of which (21%) contained no observable fauna. Analyses of the epifauna dataset were therefore conducted using both individual images and transects (i.e., pooling all images

within each transect). These transect-level analyses helped avoid problems associated with the large number of observations with low (or no) abundance, and enabled the investigation of patterns at larger spatial scales (~ 6000 m<sup>2</sup> at transect level vs ~1-4 m<sup>2</sup> at image level).

Analyses of community structure were conducted using statistical routines in the multivariate software package PRIMER v6 (Clarke & Gorley 2006). Analyses were based on similarity matrices built using Bray-Curtis similarity (Clarke et al. 2006) of square root-transformed abundance data. The square root transformation was used to decrease the influence of highly abundant taxa on community patterns (Clarke & Warwick 2001).

The following procedure was used for the analysis: first, natural group structure in the samples was identified using a similarity profile test, and the results of the analysis were superimposed on a map of the study area for graphical representation and description of spatial patterns in community distribution. The taxa contributing most to within-group similarity were also identified using a similarity percentage routine. The contribution of the different spatial scales to variation in community structure were compared using a multivariate version of ANOVA. Finally, the relationship between three sets of predictor variables and benthic community structure were investigated using a form of multivariate multiple-regression. The three sets of predictor variables were (1) local substrate variables (from ROV/DTIS images), (2) topographical variables (derived from the MBES bathymetry), and (3) regional environmental layers (from modelled data layers, including regional substrate variables). The nature and number of variables differed between image- and transect-level analyses, and details of analyses conducted are given below.

#### **2.7.4 Epifauna (image-level)**

A total of 3908 images were analysed for epifauna community structure from 69 transects across 21 survey areas. Spatial patterns in community structure were described using group-average hierarchical cluster analysis in the routine CLUSTER (Clarke & Warwick 2001). A similarity profile test (SIMPROF) was performed to identify natural group structure in the samples, i.e., communities (Clarke et al. 2008). The SIMPROF routine conducts a series of permutation tests to find clusters of samples with statistically significant internal structure (P set at 0.01; Clarke & Warwick 2001). SIMPROF could not be performed directly on the epifaunal image data because of the high number of samples and associated high computing power required. Instead, a first classification of the still images was conducted based on the epifauna data and using k-means grouping with the Calinski-Harabasz stopping statistic (Milligan & Cooper 1985, Calinski & Harabasz 1974). This process classified all images into 111 classes. Fauna abundances across all images in each of those classes were then averaged and SIMPROF was performed on those values (P set at 0.01). The SIMPER routine was used to identify the five taxa contributing most to within-group similarity for each SIMPROF group (Clarke and Warwick 2001).

The PERMANOVA routine in PRIMER was used to compare the effects of different spatial scales (i.e., survey area and transect) on benthic community structure (Anderson et al. 2008). PERMANOVA is a semi-parametric, permutation-based routine for analysis of variance based on any similarity measure (e.g., Bray-Curtis). Analyses were conducted using the fixed factor Survey Area and random factor Transect nested within Survey Area (Quinn & Keough 2009). P-values for individual predictor variables were obtained using 9999 permutations. Because PERMANOVA is sensitive to differences in multivariate dispersion

among groups, the PERMDISP routine in PRIMER was used to test for homogeneity of dispersion when significant factor effects were found (Anderson et al. 2008). The square root of estimates of components of variation was used for comparing the amount of variation attributable to the two factors (i.e., Survey Area and Transect) in the multivariate PERMANOVA models (Anderson et al. 2008).

Because many of the images (21%) contained no faunal data (i.e., no fauna were observed) the similarity matrix for PERMANOVA (and DistLM, see below) was built by adding a “dummy” taxon to avoid undefined similarities between pairs of images (Clarke & Warwick 2001). This procedure assumes that images without any fauna are 100% similar to each other, which in the case of epifauna is a reasonable assumption.

Relationships between epifauna community structure and predictor variables were investigated using Distance-based Linear Models (DistLMs) in PERMANOVA+ (Anderson et al. 2008). The DistLM routine is based on an approach called distance-based redundancy analysis (dbRDA) first developed by Legendre & Anderson (1999). It is a semi-parametric, permutation-based method that does not rely on the assumption of normally distributed data, and is a form of multivariate multiple regression that can be performed directly on a distance or dissimilarity matrix of choice (Anderson et al. 2008). The analyses conducted in DistLM are based on the individual samples, thereby allowing straight-forward interpretation of partial regression tests (Anderson et al. 2008). In contrast, other approaches, which treat the individual distances as a single univariate response, are problematic for the interpretation of multiple regression analyses (e.g., the Mantel approach, Dutilleul et al. 2000, Legendre et al. 2005, Anderson et al. 2011).

Variability in benthic community structure was partitioned according to three sets of predictor variables in DistLM, i.e., substrate (visual observations of sediment physical characteristics derived from ROV/DTIS images; i.e., the substrate variables mud/sand, nodules, chalk, dark patches, boulders, cobbles, scour, and ledge, and an additional substrate variable (habitat diversity) was derived by adding substrate observations for each image, topography variables (19 bathymetry-derived variables derived from ship-based MBES data consisting of 9 derivatives at two spatial scales; see below and section 2.6.1), and regional environmental variables (12 variables derived from modelled environmental layers; see section 2.6.3). Some data were missing from the ship data, but only for 83 images in the CRP dataset (which represent < 3% of all CRP images); these images were therefore removed from the dataset prior to DistLM analyses. DistLM analyses were conducted using a set of nine bathymetry-derived variables (one for each derivative), using the smallest and largest spatial scale (18 variables in total). The smallest scale consisted of the smallest neighbourhood size (1 grid cell of size 25x25 m), whereas the largest spatial scale consisted of the largest neighbourhood size (15x15 grid cells of size 25x25 m). The set of variables providing the strongest overall correlations ( $R^2$ ) was selected.

Relationships between predictor variables and benthic community structure were initially examined by analysing each variable in marginal tests. Sequential tests using a step-wise selection procedure and using the Akaike Information Criterion (AIC) as selection criterion were then used to determine which set of variables were most strongly correlated with benthic community structure (Quinn & Keough 2009). P-values for individual predictor variables were obtained using 500 permutations of raw data.

### 2.7.5 Epifauna (transect-level)

Faunal data from all analysed images were pooled for each of the 69 transects prior to analyses ( $n = 10\text{--}99$  images per transect, mean number of images per transect = 57). The SIMPROF routine was used to identify natural groupings ( $P$  set at 0.01). Variability in community structure was partitioned according to three main sets of predictor variables in DistLM, i.e., substrate (mud/sand, nodules, chalk, dark patches, boulders, cobbles, scour, ledge, and habitat diversity (calculated using the Shannon–Wiener diversity index (Etter & Grassle, 1992)), topography variables (19 bathymetry-derived variables based on MBES data; see above and section 2.6.1), and regional environmental variables (12 variables derived from modelled environmental layers; see section 2.6.3). For each transect, substrate observations from all analysed images were added and divided by the total number of images analysed, and the mean and standard deviation of each topography and regional environmental variable were used as predictor variables in the DistLM analysis (see above). The transect-level DistLM was run using 999 permutations (compared to 500 for image-level analyses) because of the lower computing power required (69 transects vs 3908 images).

Relationships between within-transect heterogeneity (i.e., mean deviation from centroid based on image data within each transect) and four sets of predictor variables (spatial, substrate, topography, and environmental) were investigated using DistLM as described above for transect-level community structure analyses.

## 2.8 Habitat suitability modelling

### 2.8.1 Datasets

The results of the benthic community analysis provided the location of epifauna communities in the study area (see section 3.2).

Data for the predictor variables were provided by the habitat characterisation layers described in section 3.1.

### 2.8.2 Modelling approach

Boosted regression tree (BRT) models were generated to interpret the distribution of benthic communities relative to environmental variability, and to predict the distribution of benthic communities across the study area.

BRT is an ensemble method that interprets complex relationships between species (or groups of species/communities) and their environment by partitioning similar observations into groups based on many simple classification or regression trees (Elith et al. 2006, Leathwick et al. 2006). The first of two algorithms implemented in BRT partitions the response variable (species or groups of species/communities) into groups with similar characteristics using regression or classification trees. Boosting is the second algorithm and stems from machine learning where trees are fitted iteratively, emphasizing observations that poorly fit the existing collection of trees (Friedman et al. 2000). Boosting combines these trees to minimize misclassification errors and improve predictive performance over a single tree model (Leathwick et al. 2006). Additional advantages to BRT are its ability to include continuous and categorical data, handle missing and outlying data, cope with irrelevant and correlated predictor (environmental) variables, and automatically fit interactions between predictors.



Boosting is optimized by the learning rate (lr) that considers residual variation during tree building, and tree complexity (tc) that estimates interactions between predictor variables. Model fit and predictive performance are balanced to reduce overfitting by jointly optimizing the number of trees (nt), lr, and tc (Elith et al. 2008).

The relative importance of predictor variables in a model is determined by its contribution to the model as measured by the number of times it is selected for tree splitting. The contribution of each variable is scaled so that the sum equals 100, with higher numbers reflecting stronger influence on the response variable (Elith et al. 2008). Fitted-functions are produced by BRT that show the effect of a focal predictor on the response while controlling for the average effect of all other variables in the model (Buston & Elith 2011).

BRT models of species distribution have been shown to be an effective method to understand the ecological drivers of species distribution patterns, and a reliable approach to generate predictions of species distributions across many scales (Buston & Elith 2011, Elith et al. 2006, Leathwick et al. 2006, Torres et al. 2013), including benthic communities (Compton et al. 2012).

### 2.8.3 Model analysis

The 'gbm' package version 1.6-3.1 (Ridgeway 2007) implemented in R (R Development Core Team 2011), plus custom code available online (Elith et al. 2008), was used to generate BRT models of the epifauna and infauna benthic communities.

Models were not generated for communities for which there were insufficient data to make robust models. This meant that no models were made for the four less observed epifauna communities at the image-level scale ( $n = < 40$  images). Models of epifauna communities at the transect-level scale were also not generated due to insufficient explanatory capacity of the predictor variables. BRT models for these communities could not be generated without error, likely due to the high environmental variation along single transects which could not be used to describe communities based on averaged data.

Binomial (presence/absence) BRT models were generated, using a bernoulli distribution, for the remaining benthic communities: 9 epifauna communities (Communities *b*, *f*, *g*, *j*, *m*, *n*, *o*, *p*, *q*). Additionally, a presence and abundance model (using a poisson distribution) for the stony coral *Goniocorella dumosa* were generated.

For each community and the two *Goniocorella dumosa* models, two initial models were generated with the response variable, either presence/absence or abundance, related to a suite of environmental predictor variables at one of two different spatial scales: sampling point and 15x grid cell focal mean (gcfm). Predictor variable values of depth, the four substrate variables (%nodules, %mud, %gravel, %sand) and the twelve regional environmental variables (see above) at the sampling point were included in all models. The topographical variables in each model were aspect, curvature, plan curvature, profile curvature, depth range (3x or 15x gcfm), standard deviation of depth (3x or 15x gcfm), slope, standard deviation of slope (3x or 15x gcfm), and rugosity (3x or 15x gcfm).

The predictive performance of these two scale models were compared based on area under the receiver operating curve (AUC), and cross-validation per cent deviance explained (CVdev). AUC is widely used to evaluate binomial models (Fawcett 2006) by measuring the

ability to discriminate between areas with species/community presence or absence. AUC ranges from 0 to 1: 1 = perfect discrimination, < 0.5 = worse than random, > 0.7 is considered “useful” (Swets 1988). Although AUC has limitations for measuring model performance (Austin 2007, Lobo et al. 2008), it can be used as a relative metric of model performance because it provides a single value that is easy to interpret. CVdev is estimated by a cross-validation procedure run during the modelling process that withholds a subset of data at each tree. CVdev is a measure of the goodness of fit between the predicted and raw values and indicates how well the model predicted the subsets of withheld data (Buston & Elith 2011). As well as this ‘internal’ model cross-validation, an independent validation was performed by withholding 10% of the available data for each model, and AUC and CVdev metrics of performance calculated for this ‘external’ validation procedure.

Once the appropriate scale for each model was determined, each model was optimized based on the above described performance metrics (AUC and CVdev) by varying the tree complexity (number of interactions allowed between variables) and only including predictor variables that contributed more than 3% to the model (Buston & Elith 2011). Fitted-functions of the optimized models were produced to show the effect of each predictor variable in the model on the response while controlling for the average effect of all other variables in the model (Buston & Elith 2011).

#### **2.8.4 Predictive mapping**

Predictive maps were made for the habitat suitability (scaled low (0) to high (1)) of each benthic epifauna community. A predictive map of *Goniocorella dumosa* probability of occurrence was also derived from the optimal model of abundance. Mapped predictions were produced using the function `predict.gbm` (Ridgeway 2007) and the package `Raster` (Hijmans 2010) in R (R Development Core Team 2011). The output prediction `ascii` file was converted to a raster in ArcGIS (version 10, ESRI) and projected into UTM 60S for display. Due to the highly skewed nature of the raster data (many more low values of community presence), map illustration was optimised using a two-standard deviation ‘stretch’ (the default setting in ArcGIS for raster datasets that have statistics). This approach is used to brighten raster datasets that normally appear dark, by preventing pixel values being stretched to the extremes, and overemphasising the areas of low values. This form of illustration was chosen to, in effect, highlight those areas that have a greater proportion of individual pixels with relatively high habitat suitability. With the colour ramp used, these areas appear as conspicuous red patches on the output maps and thereby aid the visual appreciation of where generally in the study area suitable habitat is more likely to be found. It must be noted that within these areas, there are individual pixels that are not predicted to be suitable habitat (see Appendix B for a more detailed explanation and illustration).

### **3 Results**

#### **3.1 Habitat characterisation**

The bathymetry, topographic, substratum and regional environmental variables that characterise the habitat of the study area are figured in Appendix C. These figures show that the habitat across the study area varies considerably and that particular areas have a features or a combination of distinctive features that are likely to influence the structure and distribution of benthic communities.

## 3.2 Benthic community analysis

### 3.2.1 Epifauna (image-level)

A total of 36,018 individuals belonging to 77 epifauna taxa were identified from the ROV and DTIS images (see Appendix A). The most diverse group was the echinoderms (28 taxa), followed by sponges (17), and cnidarians (13). The most abundant taxon (based on final dataset corrected for image size and small taxon abundance, see section 2.7.2) was Encrusting bryozoan/sponge/ascidian (5714 counts), followed by Irregular urchins (2295), *Goniocorella dumosa* (stony coral, 1897), Brachiopoda (lampshells, 1361), Branching bryozoan/hydroid/other (859), Actinaria/Ceriantharia (sea anemones, 422), and Galatheidae/Chirostylidae (squat lobsters, 367).

The 3908 analysed images were classified into 13 communities by k-means followed by SIMPROF; four of the 111 k-means groups were left unclassified (Figure 3-1). One of these unclassified groups (*b*) comprised 1142 images with either no (74% of images) or little fauna (26% of all images, 1-2 counts image<sup>-1</sup>). The other unclassified groups only contained 1-7 images and are not discussed further. Of the 13 communities identified by SIMPROF, 9 comprised at least 40 images. Unclassified communities comprising less than 40 images were not included in the following discussion of SIMPER results.

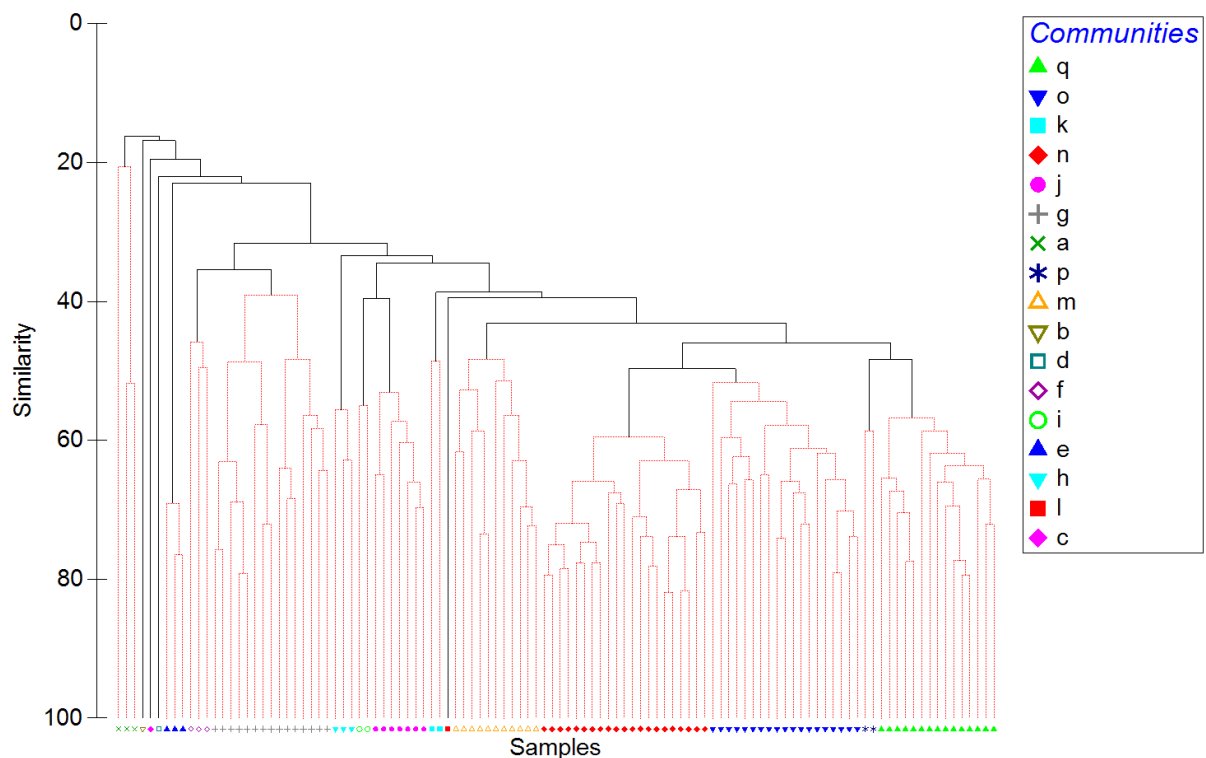


**Figure 3-1: Dendrogram showing groups of samples identified as epifauna communities (image-level) by SIMPROF (after initial k-means classification).**

The largest classified community (Community *g*,  $n = 1001$  images) was characterised by relatively low average similarity (29.1%) and was mainly characterised by the presence of Irregular urchins in low density (mean = 1.2 counts image<sup>-1</sup>) (Table 3-1). The second largest group (Community *q*,  $n = 829$ ) comprised images characterised by low density of Encrusting bryozoan/sponge/ascidian. Community *o* was mainly characterised by the presence of *Goniocorella dumosa* (stony coral), and, to a lesser extent, Branching bryozoan/hydroid/other and Encrusting bryozoan/sponge/ascidian. Community *n* comprised images with relatively high abundance of Encrusting bryozoan/sponge/ascidian (8.2 image<sup>-1</sup>) and presence of *Goniocorella dumosa*. Community *m* was mainly characterised by the presence of Brachiopoda (lamp shells), whereas community *j* was dominated by Actinaria/Ceriantharia (sea anemones) and Paguridae (hermit crabs). The two smallest communities (*f* and *p*,  $n = 56$  and  $42$ , respectively), were characterised by low densities of both Encrusting bryozoan/sponge/ascidian as well as Irregular urchins and Branching bryozoan/hydroid/other, respectively (Figure 3-2). The highest mean dissimilarities were observed between Community *n* and Communities *g* and *f* (>90% dissimilarity) (Table 3-2). Communities *n* and *o* (both dominated by *Goniocorella dumosa* and Encrusting bryozoan/sponge/ascidian) showed the lowest mean dissimilarity.

| Taxa  | Av. Abund | Av.Sim | Sim/SD | Contrib% | Cum%  |
|---|-----------|--------|--------|----------|-------|
| <b>Community g</b> (n = 1001, Av. Sim. = 29.1%) |           |        |        |          |       |
| Irregular urchins                               | 1.2       | 16.51  | 0.80   | 56.82    | 56.82 |
| Branching bryozoan/hydroid/other                | 0.4       | 8.24   | 0.57   | 28.36    | 85.18 |
| Encrusting bryozoan/sponge/ascidian             | <0.1      | 1.55   | 1.3    | 5.34     | 90.52 |
| <b>Community q</b> (n = 829, Av. Sim. = 51.1%)  |           |        |        |          |       |
| Encrusting bryozoan/sponge/ascidian             | 2.1       | 39.13  | 2.46   | 76.59    | 76.59 |
| Irregular urchins                               | 0.2       | 3.17   | 0.82   | 6.20     | 82.79 |
| Galatheidae/Chyrostylidae                       | 0.1       | 1.78   | 1.31   | 3.49     | 86.28 |
| Branching bryozoan/hydroid/other                | 0.1       | 1.75   | 0.55   | 3.42     | 89.70 |
| <i>Goniocidaris</i> spp                         | 0.1       | 1.12   | 1.54   | 2.19     | 91.89 |
| <b>Community o</b> (n = 262, Av. Sim. = 43.7%)  |           |        |        |          |       |
| <i>Goniocorella dumosa</i>                      | 4.3       | 21.82  | 1.67   | 49.94    | 49.94 |
| Encrusting bryozoan/sponge/ascidian             | 1.5       | 6.86   | 0.93   | 15.69    | 65.64 |
| Branching bryozoan/hydroid/other                | 0.5       | 3.5    | 1.52   | 8.00     | 73.64 |
| Galatheidae/Chyrostylidae                       | 0.3       | 1.98   | 1.17   | 4.53     | 78.17 |
| <i>Goniocidaris</i> spp                         | 0.3       | 1.90   | 1.34   | 4.36     | 82.53 |
| Brachiopoda                                     | 0.3       | 1.70   | 1.34   | 3.88     | 86.41 |
| Irregular urchins                               | 0.1       | 0.83   | 1.20   | 1.90     | 88.31 |
| Actinaria/Ceriantharia                          | 0.2       | 0.76   | 0.79   | 1.73     | 90.04 |
| <b>Community n</b> (n = 240, Av. Sim. = 53.7%)  |           |        |        |          |       |
| Encrusting bryozoan/sponge/ascidian             | 8.2       | 36.96  | 2.43   | 68.82    | 68.82 |
| <i>Goniocorella dumosa</i>                      | 2.6       | 6.21   | 0.61   | 11.57    | 80.39 |
| Brachiopoda                                     | 2.0       | 6.2    | 0.91   | 11.55    | 91.94 |
| <b>Community m</b> (n = 180, Av. Sim. = 39.9%)  |           |        |        |          |       |
| Brachiopoda                                     | 3.8       | 23.57  | 1.74   | 59.15    | 59.15 |
| Irregular urchins                               | 0.6       | 6.62   | 0.61   | 16.63    | 75.78 |
| Encrusting bryozoan/sponge/ascidian             | 0.7       | 3.8    | 1.15   | 9.53     | 85.31 |
| Branching (bryozoan/hydroid/other               | 0.3       | 1.66   | 1.21   | 4.18     | 89.49 |
| Galatheidae/Chyrostylidae                       | 0.2       | 1.04   | 1.08   | 2.6      | 92.09 |
| <b>Community j</b> (n = 164, Av. Sim. = 44.2%)  |           |        |        |          |       |
| Actinaria/Ceriantharia                          | 1.8       | 20.75  | 2.37   | 46.91    | 46.91 |
| Paguridae                                       | 0.7       | 8.09   | 2.26   | 18.29    | 65.2  |
| Irregular urchins                               | 0.3       | 2.65   | 0.7    | 5.99     | 71.19 |
| Branching bryozoan/hydroid/other                | 0.2       | 2.62   | 3.29   | 5.92     | 77.11 |
| Galatheidae/Chyrostylidae                       | 0.2       | 2.52   | 2.87   | 5.71     | 82.82 |
| Encrusting bryozoan/sponge/ascidian             | 0.1       | 1.72   | 1.99   | 3.88     | 86.69 |
| <i>Goniocorella dumosa</i>                      | 0.2       | 0.95   | 0.75   | 2.15     | 88.84 |
| <i>Suberites</i> n. spp.                        | <0.1      | 0.83   | 1.41   | 1.88     | 90.72 |
| <b>Community f</b> (n = 56, Av. Sim. = 30.7%)   |           |        |        |          |       |
| Encrusting bryozoan/sponge/ascidian             | 0.2       | 10.88  | 34.33  | 35.41    | 35.41 |
| Irregular urchins                               | 0.1       | 6.69   | 111.19 | 21.77    | 57.18 |
| Galatheidae/Chyrostylidae                       | 0.5       | 5.68   | 4.87   | 18.49    | 75.67 |
| Branching bryozoan/hydroid/other                | 0.1       | 4.08   | 13.11  | 13.28    | 88.95 |
| <i>Hymedesmia (Stylopus)</i> n. sp. 1           | <0.1      | 0.97   | 7.67   | 3.15     | 92.1  |
| <b>Community p</b> (n = 42, Av. Sim. = 37.2%)   |           |        |        |          |       |
| Encrusting bryozoan/sponge/ascidian             | 0.3       | 11     | -      | 29.6     | 29.6  |
| Branching bryozoan/hydroid/other                | 0.3       | 5.64   | -      | 15.17    | 44.77 |
| <i>Suberites</i> n. spp.                        | 0.7       | 4.46   | -      | 12.01    | 56.78 |
| <i>Goniocidaris</i> spp.                        | 0.1       | 3.64   | -      | 9.79     | 66.57 |
| Galatheidae/Chyrostylidae                       | 0.1       | 2.69   | -      | 7.25     | 73.81 |
| Actinaria/Ceriantharia                          | 0.1       | 2.14   | -      | 5.76     | 79.58 |
| Irregular urchins                               | 0.1       | 1.79   | -      | 4.8      | 84.38 |
| Paguridae                                       | 0.1       | 1.52   | -      | 4.08     | 88.46 |
| <i>Goniocorella dumosa</i>                      | 0.1       | 1.26   | -      | 3.4      | 91.87 |

**Table 3-1: Results of the SIMPER analysis showing taxa accounting for >90% of the within group similarity for epifauna communities (image-level) identified by SIMPROF.** [Only communities with >40 images are shown. Av. Abund = Average abundance, Av. Sim = Average similarity, Sim/SD = Similarity/Standard Deviation, Contrib% = % contribution to overall similarity, Cum% = % cumulative similarity].



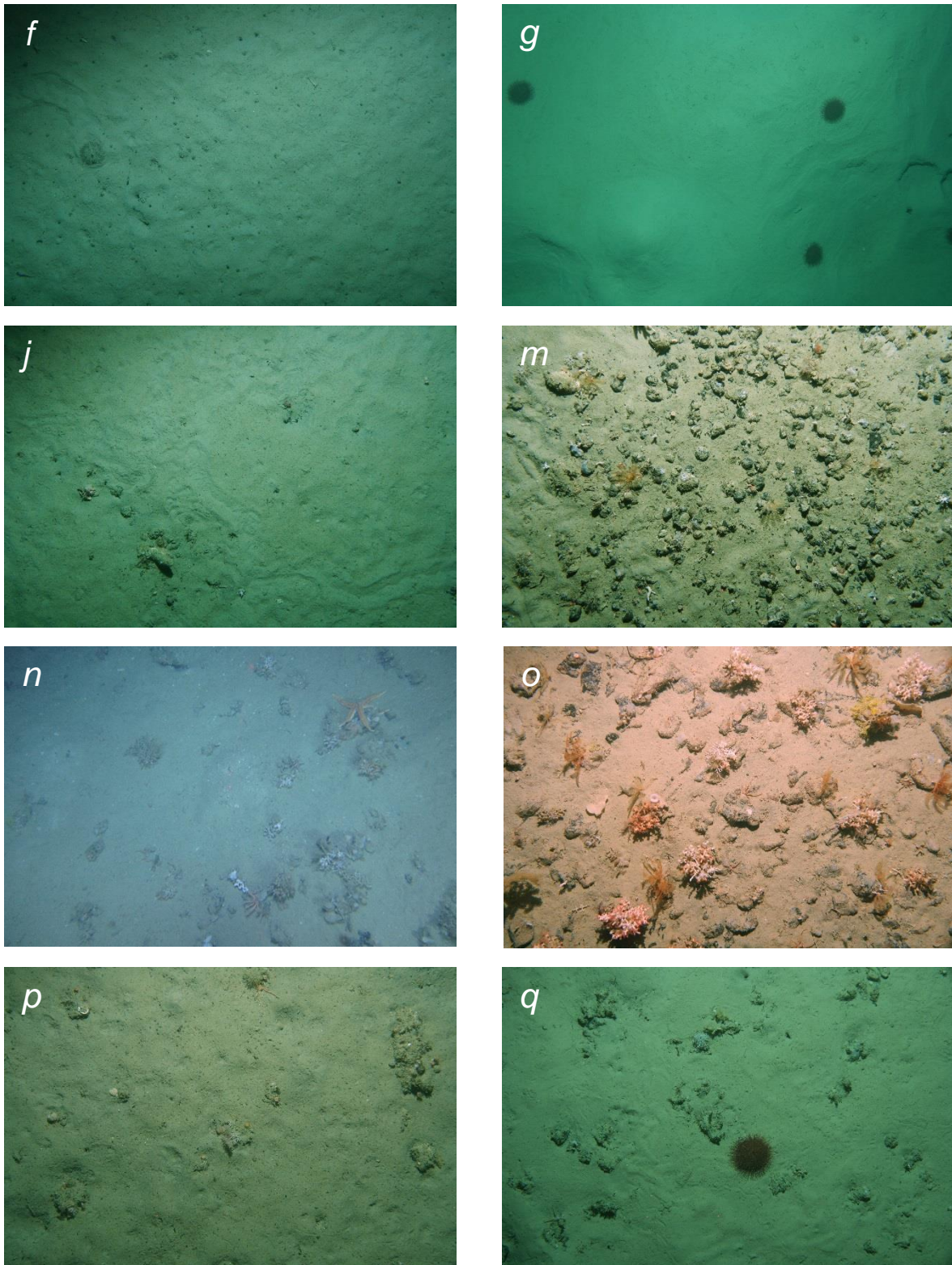


**Figure 3-2: Seafloor images representative of the epifauna communities (image-level) identified by SIMPROF (Communities *f, g, j, m, n, o, p, q*). [Only communities with >40 images shown].**



| <b>Community</b> | <b>f</b> | <b>g</b> | <b>j</b> | <b>m</b> | <b>n</b> | <b>o</b> | <b>p</b> |
|------------------|----------|----------|----------|----------|----------|----------|----------|
| <i>g</i>         | 84.8     |          |          |          |          |          |          |
| <i>j</i>         | 78.9     | 85.2     |          |          |          |          |          |
| <i>m</i>         | 85.8     | 82.9     | 77.2     |          |          |          |          |
| <i>n</i>         | 91.3     | 93.3     | 88.3     | 74.7     |          |          |          |
| <i>o</i>         | 84.2     | 88.7     | 78.1     | 80.3     | 69.6     |          |          |
| <i>p</i>         | 71.7     | 81.7     | 79.1     | 82.2     | 89.0     | 77.2     |          |
| <i>q</i>         | 78.4     | 82.9     | 85.3     | 78.4     | 68.8     | 73.6     | 74.9     |

**Table 3-2: Mean dissimilarity (%) between epifauna community groups (image-level) identified by SIMPROF.**

Each transect comprised images classified as belonging to several community groups, although some transects were more heterogeneous than others. Transects in survey area L, for example, showed lower levels of heterogeneity in community structure than transects in survey area Q. Heterogeneity also varied between transects of the same box (e.g., survey area O) (see maps in Appendix D).

There were significant effects of the factors Survey Area and Transect on epifauna community structure (PERMANOVA,  $P = 0.001$ ). There was a significant difference in multivariate dispersion between survey areas (PERMDISP,  $P = 0.001$ ), indicating that among-survey area differences in community structure may be due to differences in multivariate dispersion. Transects in the survey areas 4, 5, 6, 14, M and Q were characterised by the highest multivariate dispersion (mean distance to centroid > 39), whereas transects in survey area 16, L and S, and all five Chatham-Challenger (OS20/20) Survey transects were characterised by the lowest mean multivariate dispersion (mean distance to centroid < 20) (Figure 3-3). Comparison of the square root of estimates of components of variation shows that the factor Survey Area (13.40) explained 20% more of the variation in community structure than the factor Transect (11.2), meaning that among-survey area (~5 - 280 km scale) variability was greater than within-transect (~1 - 5 km) variability.

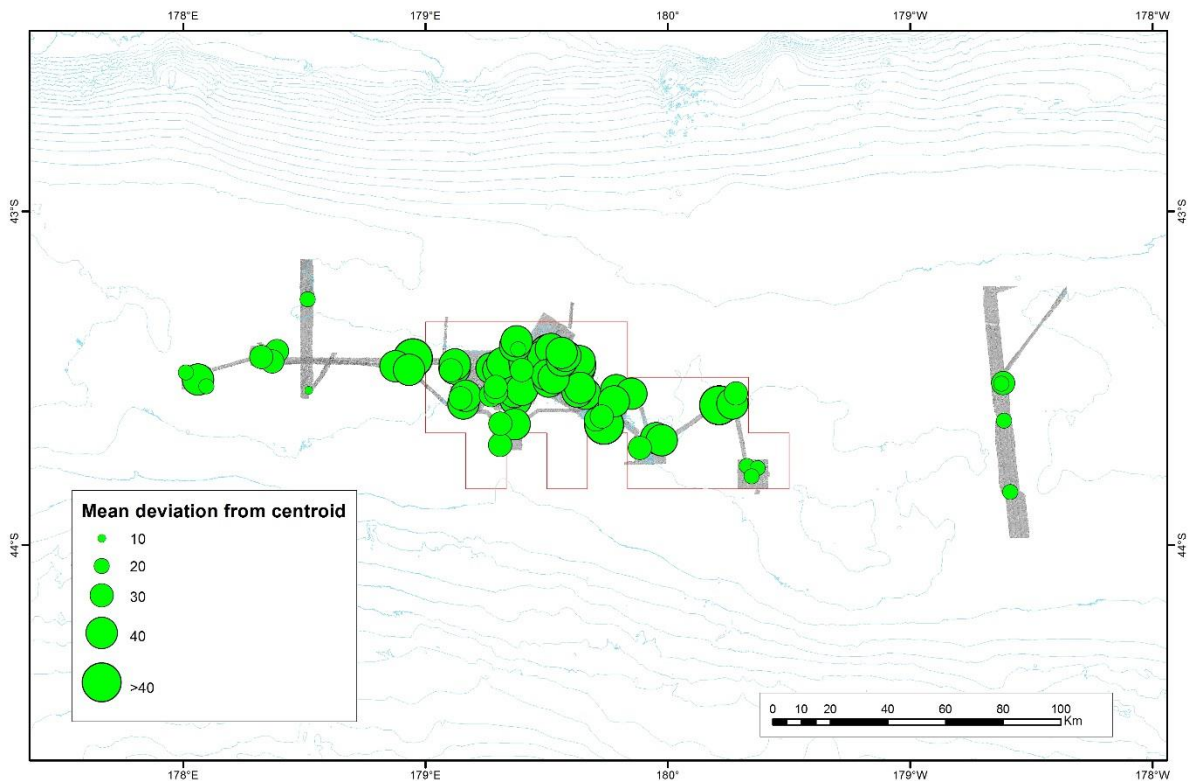


**Figure 3-3: Distribution of within-transect heterogeneity in epifauna community structure across the study area.** (i.e., mean deviation from centroid based on image-level data within each transect).

DistLM results show that epifaunal community structure was significantly correlated with 40 of the 44 predictor variables included in the model. Most of the predictor variables, however, explained only a small proportion ( $R^2 \leq 0.05$ ) of the variability in community structure in marginal tests, the only two exceptions being the substrate variables Mud/sand and Nodules which explained 15 and 14% of the variability in community structure, respectively. In sequential tests, the variables Mud/sand, Nodules, Boulders, and SST gradient were selected as the main predictors, and together explained 23% of the variability in epifauna community structure (Table 3-3).

| <i>Variable</i>           | <i>AIC</i> | <i>SS</i> | <i>Pseudo-F</i> | <i>P</i> | <i>R<sup>2</sup></i> | <i>R<sup>2</sup><br/>(cumul.)</i> | <i>res.df</i> |
|---------------------------|------------|-----------|-----------------|----------|----------------------|-----------------------------------|---------------|
| <i>Marginal</i>           |            |           |                 |          |                      |                                   |               |
| Mud/Sand                  | -          | 901000    | 701.51          | 0.002    | 0.15                 | -                                 | -             |
| Nodules                   | -          | 848000    | 653.46          | 0.002    | 0.14                 | -                                 | -             |
| Boulders                  | -          | 293000    | 203.23          | 0.002    | 0.05                 | -                                 | -             |
| SST gradient              | -          | 292000    | 202.81          | 0.002    | 0.05                 | -                                 | -             |
| Dark patch                | -          | 257000    | 177.60          | 0.002    | 0.04                 | -                                 | -             |
| Bottom current<br>speed   | -          | 147000    | 99.78           | 0.002    | 0.03                 | -                                 | -             |
| Dynamic<br>topography     | -          | 113000    | 75.93           | 0.002    | 0.02                 | -                                 | -             |
| Sand (regional)           | -          | 106000    | 70.95           | 0.002    | 0.02                 | -                                 | -             |
| Depth range (15x<br>gcfm) | -          | 94937     | 63.65           | 0.002    | 0.02                 | -                                 | -             |
| Depth SD (15x<br>gcfm)    | -          | 86904     | 58.19           | 0.002    | 0.01                 | -                                 | -             |
| <i>Sequential</i>         |            |           |                 |          |                      |                                   |               |
| Mud/sand                  | 27810      | 901000    | 701.51          | 0.002    | 0.15                 | 0.15                              | 3883          |
| Nodules                   | 27626      | 233000    | 189.94          | 0.002    | 0.04                 | 0.19                              | 3882          |
| Boulders                  | 27540      | 107000    | 89.19           | 0.002    | 0.02                 | 0.21                              | 3881          |
| SST gradient              | 27468      | 88004     | 74.91           | 0.002    | 0.02                 | 0.23                              | 3880          |
| DOM                       | 27405      | 75656     | 65.47           | 0.002    | 0.01                 | 0.24                              | 3879          |
| Gravel (regional)         | 27372      | 40113     | 35.02           | 0.002    | <0.01                | 0.25                              | 3878          |
| Dynamic<br>topography     | 27349      | 27615     | 24.25           | 0.002    | <0.01                | 0.25                              | 3877          |
| POC                       | 27329      | 25379     | 22.41           | 0.002    | <0.01                | 0.25                              | 3876          |
| Cobbles/pebbles           | 27309      | 25331     | 22.49           | 0.002    | <0.01                | 0.26                              | 3875          |
| Ledge                     | 27289      | 23565     | 21.032          | 0.002    | <0.01                | 0.26                              | 3874          |

**Table 3-3: Results of the DistLM analysis showing correlations between predictor variables and epifauna community structure (image-level).** [Only the variables with the ten highest  $R^2$  values are shown. AIC = Aikake Information Criterion, SS = Sum of Squares, Pseudo-F = Pseudo-F Statistic, P = probability,  $R^2$  = proportion of explained variation attributable to each variable,  $R^2$  (cumul.) = cumulative proportion of variation, res.df = residual degrees of freedom].

### 3.2.2 Epifauna (transect-level)

SIMPROF analysis of the transect-level data classified the 69 transects into 12 communities (each comprising 2-21 transects), except for two transects that were left unclassified (Figure 3-4). Results of SIMPER analyses for the four communities comprising only two transects are not included in the following descriptions. The largest group (Community *l*,  $n = 21$ ) comprised transects with high epifaunal abundance (mean = 388 counts transect<sup>-1</sup>) dominated by Encrusting bryozoan/sponge/ascidian and *Goniocorella dumosa* (stony coral) (Table 3-4). Community *j* ( $n = 13$ ) comprised transects with lower faunal abundance (153 counts transect<sup>-1</sup>) and dominated by Encrusting bryozoan/sponge/ascidian, Irregular urchins, and Branching bryozoan/hydroid/other. Transects in Community *a* ( $n = 11$ ) were characterised by low faunal abundance (17 transect<sup>-1</sup>) of mostly Actinaria/Ceriantharia (sea anemones), Galatheidae/Chyrostylidae (squat lobsters), and Paguridae (hermit crabs), whereas transects in Community *d* ( $n = 8$ ) were characterised by moderate abundance (137 transect<sup>-1</sup>) of Encrusting bryozoan/sponge/ascidian, Actinaria/Cerantharia, Brachiopoda (lamp shells), and Paguridae. Community *b* was the smallest community ( $n = 4$ ) and was characterised by low abundance (23 transect<sup>-1</sup>) of mostly Irregular urchins (Table 3-4) (Figure 3-5). The highest mean dissimilarities were observed between community *a* communities *j*

and *l* (>94% dissimilarity) (Table 3-5). Communities *j* and *l* (both dominated by Encrusting bryozoan/sponge/ascidian) showed the lowest mean dissimilarity.

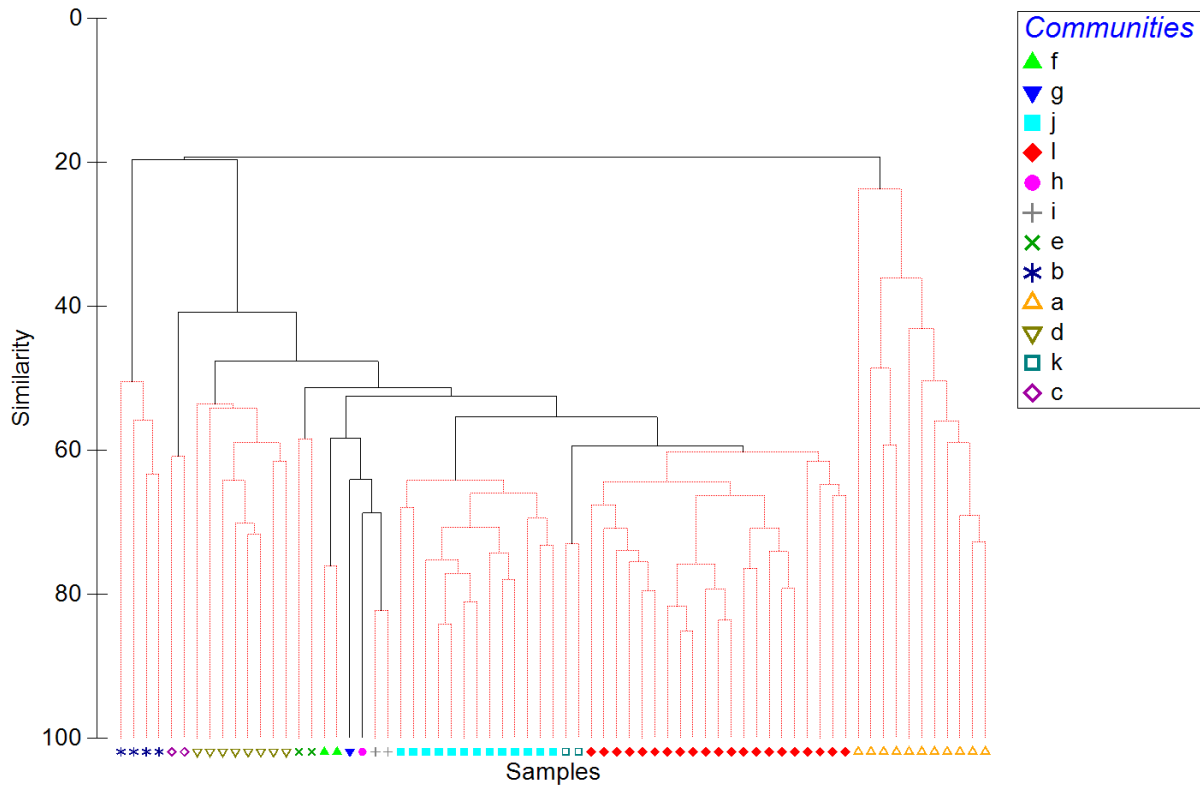


**Figure 3-4: Dendrogram showing groups of samples identified as epifauna communities (transect-level) by SIMPROF.**

| <i>Taxa</i>   | <i>Av. Abund</i> | <i>Av.Sim</i> | <i>Sim/SD</i> | <i>Contrib%</i> | <i>Cum%</i> |
|---|------------------|---------------|---------------|-----------------|-------------|
| <b>Community <i>l</i></b> (n = 21, Av. Sim = 57.5%) |                  |               |               |                 |             |
| Encrusting bryozoan/sponge/ascidian                 | 169.4            | 30.91         | 2.43          | 53.80           | 53.80       |
| <i>Goniocorella dumosa</i>                          | 72.1             | 7.99          | 0.97          | 13.90           | 67.70       |
| Irregular urchins                                   | 38.0             | 7.00          | 1.99          | 12.18           | 79.88       |
| Brachiopoda   | 33.7             | 3.65          | 0.99          | 6.35            | 86.23       |
| Branching bryozoan/hydroid/other                    | 18.1             | 2.50          | 1.07          | 4.35            | 90.58       |
| <b>Community <i>j</i></b> (n = 13, Av. Sim = 67.8%) |                  |               |               |                 |             |
| Encrusting bryozoan/sponge/ascidian                 | 76.0             | 39.04         | 3.88          | 57.54           | 57.54       |
| Irregular urchins                                   | 44.9             | 20.40         | 2.32          | 30.07           | 87.61       |
| Branching bryozoan/hydroid/other                    | 7.7              | 2.28          | 0.95          | 3.37            | 90.97       |
| <b>Community <i>a</i></b> (n = 11, Av. Sim = 35.3%) |                  |               |               |                 |             |
| Actinaria/Ceriantharia                              | 6.9              | 20.17         | 1.38          | 57.18           | 57.18       |
| Galatheidae/Chyrostylidae                           | 1.2              | 4.40          | 1.60          | 12.46           | 69.64       |
| Paguridae   | 2.6              | 3.91          | 0.61          | 11.08           | 80.72       |
| Gastropoda  | 1.1              | 2.93          | 0.63          | 8.32            | 89.04       |
| Encrusting bryozoan/sponge/ascidian                 | 1.3              | 1.86          | 0.47          | 5.27            | 94.32       |
| <b>Community <i>d</i></b> (n = 8, Av. Sim = 47.9%)  |                  |               |               |                 |             |
| Encrusting bryozoan/sponge/ascidian                 | 49.0             | 18.3          | 1.47          | 38.19           | 38.19       |
| Actinaria/Ceriantharia                              | 14.8             | 7.99          | 1.84          | 16.68           | 54.87       |
| Brachiopoda   | 23.1             | 5.60          | 2.14          | 11.69           | 66.56       |
| Paguridae   | 11.1             | 5.25          | 1.23          | 10.96           | 77.52       |
| Galatheidae/Chyrostylidae                           | 5.9              | 3.12          | 1.95          | 6.51            | 84.03       |
| Irregular urchins                                   | 11.3             | 2.48          | 0.89          | 5.18            | 89.21       |
| Branching bryozoan/hydroid/other                    | 4.5              | 1.58          | 1.42          | 3.30            | 92.51       |
| <b>Community <i>b</i></b> (n = 4, Av. Sim = 48.9%)  |                  |               |               |                 |             |
| Irregular urchins                                   | 19.8             | 48.32         | 2.42          | 98.89           | 98.89       |

**Table 3-4: Results of SIMPER analysis showing taxa accounting for >90% of within group similarity for the epifauna communities (transect-level) identified by SIMPROF.** [Only the communities comprising at least three transects are shown. Av. Abund = Average abundance (transect<sup>-1</sup>), Av. Sim = Average similarity, Sim/SD = Similarity/Standard Deviation, Contrib% = % contribution to overall similarity, Cum% = % cumulative similarity].

| <i>Community</i> | <i>a</i> | <i>b</i> | <i>d</i> | <i>j</i> |
|------------------|----------|----------|----------|----------|
| <i>b</i>         | 87.7     |          |          |          |
| <i>d</i>         | 80.4     | 87.2     |          |          |
| <i>j</i>         | 94.3     | 79.4     | 56.4     |          |
| <i>l</i>         | 96.1     | 90.6     | 66.9     | 52.3     |

**Table 3-5: Mean dissimilarity (%) between epifauna community groups (transect-level) identified by SIMPROF.** [Only communities comprising at least 3 transects are shown].



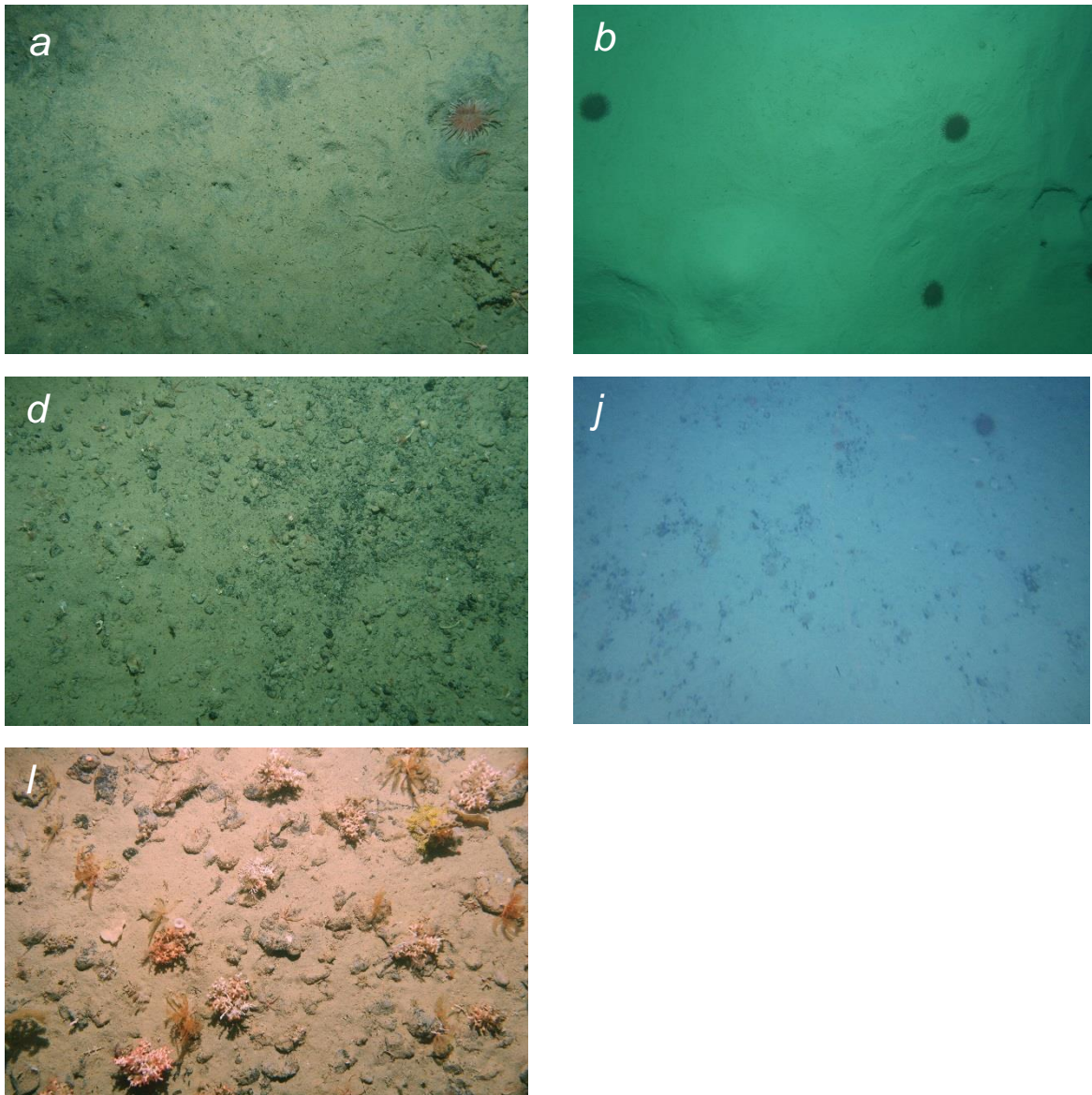


**Figure 3-5: Seafloor images representative of the epifauna communities (transect-level) identified by SIMPROF (Communities a, b, d, j, l).**

The stony coral *Goniocorella dumosa* was most abundant in the centre of the permit area, but was also present in lower abundance at the eastern and western edges of the permit area. *Goniocorella dumosa* was absent from all transects situated outside the permit area, except for two transects located immediately to the west of the permit area (survey area Q, 1 and 58 counts per transect) (Figure 3-6). Similarly, Community *l* (characterised by high abundance of *Goniocorella dumosa*) was mostly restricted to the centre of the permit area, with only one transect outside of the permit area characterised by this community type (Figure 3-7). Communities *a*, *b* and *d* were found more evenly represented inside and outside the permit area. The remaining communities were only found within the permit area. The most commonly observed transect-level communities observed only inside the permit area was community *j*, the community characterised by encrusting bryozoan/sponge/ascidian and irregular urchins. The other communities unique to the permit area occurred at a small number of transects (Figure 3-7).



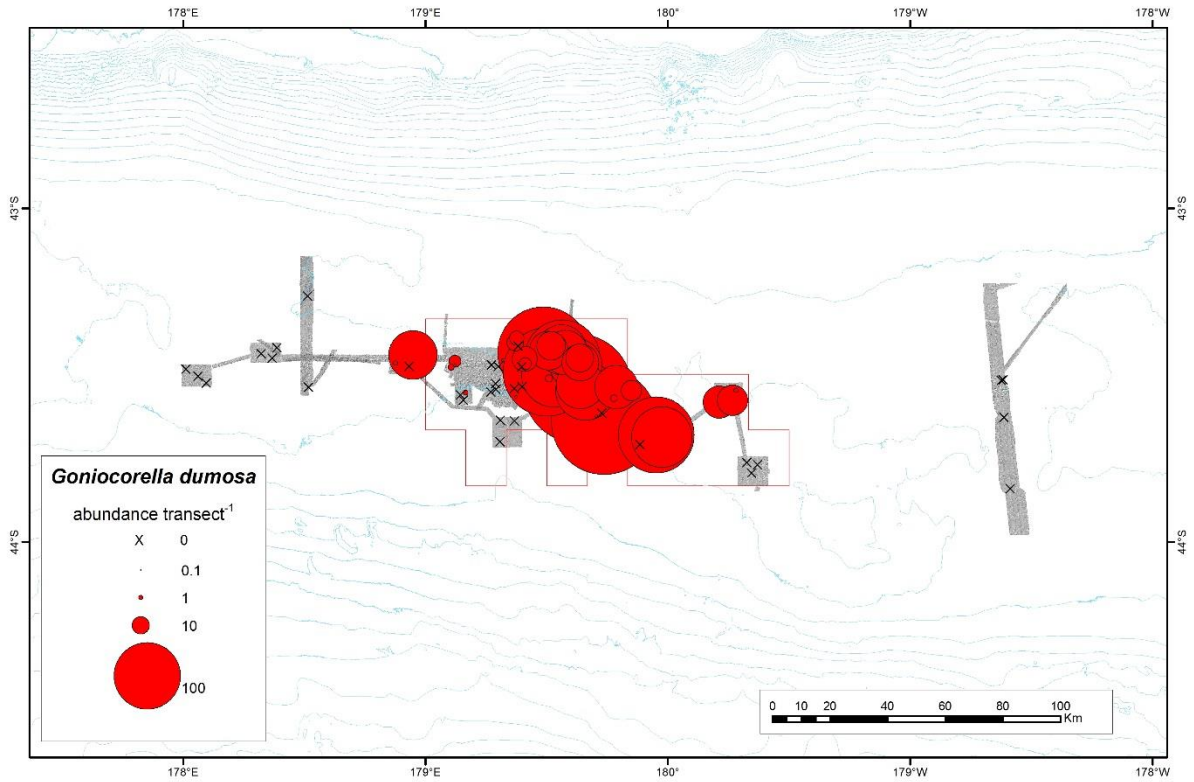


**Figure 3-6: Distribution of the relative abundance of the stony coral *Goniocorella dumosa* in the study area. [Abundance equals number of colonies imaged per transect].**

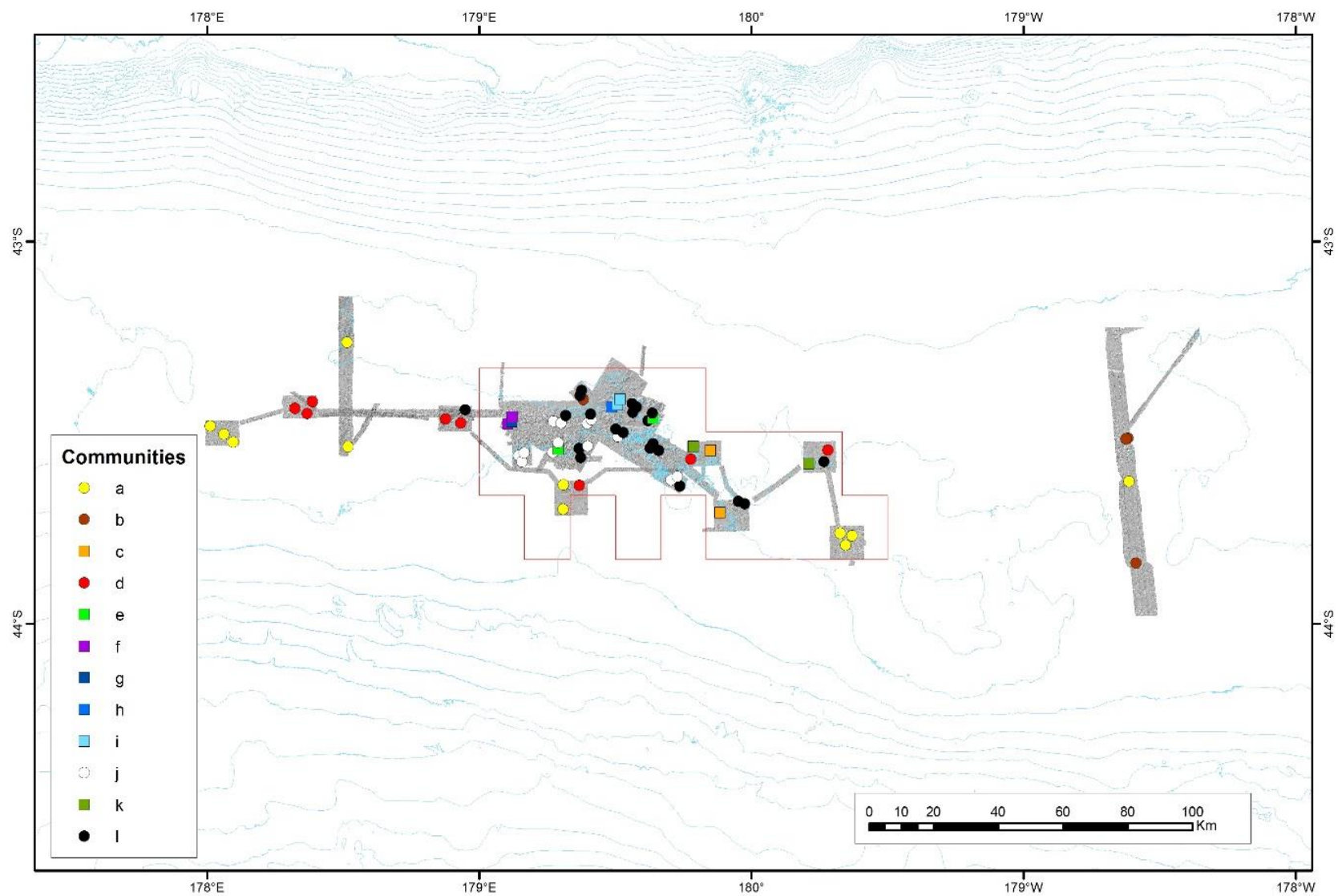


Figure 3-7: Distribution of epifauna communities (transect-level) in the study area.

Epifauna community structure at the transect-level was significantly correlated with 53 out of the 75 predictor variables entered in the DistLM model (Table 3-6). Community structure was most strongly correlated with SST gradient, Nodules, Habitat diversity, Mud/sand and Bottom current speed in marginal tests ( $R^2 > 0.17$ ). In sequential tests, community structure was most strongly correlated with SST gradient and Habitat diversity, which together explained about a quarter of variability in community structure (combined  $R^2 = 0.28$ ). The other variables explained relatively small proportions of variability in sequential tests ( $R^2 < 0.04$ ).

| <i>Variables</i>               | <i>AIC</i> | <i>SS</i> | <i>Pseudo-F</i> | <i>P</i> | <i>R<sup>2</sup></i> | <i>R<sup>2</sup><br/>(cumul.)</i> | <i>res.df</i> |
|--------------------------------|------------|-----------|-----------------|----------|----------------------|-----------------------------------|---------------|
| <i>Marginal</i>                |            |           |                 |          |                      |                                   |               |
| SST gradient                   | -          | 27632     | 17.844          | 0.001    | 0.21                 | -                                 | -             |
| Nodules                        | -          | 25387     | 16.047          | 0.001    | 0.21                 | -                                 | -             |
| Habitat diversity              | -          | 24129     | 15.073          | 0.001    | 0.18                 | -                                 | -             |
| Mud/sand                       | -          | 23622     | 14.687          | 0.001    | 0.18                 | -                                 | -             |
| Bottom current speed           | -          | 22549     | 13.882          | 0.001    | 0.17                 | -                                 | -             |
| Sand (regional)                | -          | 15256     | 8.802           | 0.001    | 0.12                 | -                                 | -             |
| Depth (SD)                     | -          | 13496     | 7.670           | 0.001    | 0.10                 | -                                 | -             |
| Sand (SD) (regional)           | -          | 12131     | 6.815           | 0.001    | 0.09                 | -                                 | -             |
| Depth SD (15x gcfm)<br>(mean)  | -          | 11170     | 6.225           | 0.001    | 0.09                 | -                                 | -             |
| Dynamic topography             | -          | 11169     | 6.224           | 0.001    | 0.09                 | -                                 | -             |
| <i>Sequential</i>              |            |           |                 |          |                      |                                   |               |
| SST gradient                   | 508.78     | 27632.0   | 17.844          | 0.001    | 0.21                 | 0.21                              | 67            |
| Habitat diversity              | 504.05     | 9644.1    | 6.763           | 0.001    | 0.07                 | 0.28                              | 66            |
| Nodules                        | 501.69     | 5761.6    | 4.239           | 0.001    | 0.04                 | 0.33                              | 65            |
| Dynamic topography             | 499.87     | 4754.6    | 3.6403          | 0.001    | 0.04                 | 0.36                              | 64            |
| POC (SD)                       | 498.24     | 4285      | 3.404           | 0.001    | 0.03                 | 0.40                              | 63            |
| Bottom current speed<br>(SD)   | 496.84     | 3817.7    | 3.1355          | 0.002    | 0.03                 | 0.43                              | 62            |
| Primary Productivity<br>(mean) | 495.83     | 3219.8    | 2.7177          | 0.003    | 0.02                 | 0.45                              | 61            |
| Mud/sand                       | 494.83     | 3077.3    | 2.6685          | 0.005    | 0.02                 | 0.47                              | 60            |
| Slope (15x gcfm) (SD)          | 494.33     | 2460      | 2.175           | 0.021    | 0.02                 | 0.49                              | 59            |
| Depth SD (15x gcfm)<br>(SD)    | 493.52     | 2657.6    | 2.4056          | 0.013    | 0.02                 | 0.51                              | 58            |

**Table 3-6: Results of DistLM analyses showing correlations between predictor variables and epifauna community structure (transect data).** [Only the variables with the ten highest  $R^2$  values are shown. AIC = Aikaie Information Criterion, SS = Sum of Squares, Pseudo-F = Pseudo-F Statistic, P = probability,  $R^2$  = proportion of explained variation attributable to each variable,  $R^2$  (cumul.) = cumulative proportion of variation, res.df = residual degrees of freedom].

Among-transect multivariate dispersion was significantly correlated with 34 out of the 75 predictor variables entered in the DistLM model. Multivariate dispersion was most strongly correlated with Nodules, SST gradient, Habitat diversity and Bottom current speed in marginal tests ( $R^2 > 0.29$ ) (Table 3-7). In sequential tests, community structure was most strongly correlated with Nodules and SST gradient, which together explained half of variability in multivariate dispersion (combined  $R^2 = 0.50$ ). The other variables explained relatively small proportions of variability in sequential tests ( $R^2 < 0.07$ ).

| <i>Variables</i>                    | <i>AIC</i> | <i>SS</i> | <i>Pseudo-F</i> | <i>P</i> | <i>R<sup>2</sup></i> | <i>R<sup>2</sup></i><br><i>(cumul.)</i> | <i>res.df</i> |
|-------------------------------------|------------|-----------|-----------------|----------|----------------------|---|---------------|
| <i>Marginal</i>                     |            |           |                 |          |                      |   |               |
| Nodules                             | -          | 1787.0    | 45.23           | 0.001    | 0.40                 | -                                       | -             |
| SST gradient                        | -          | 1707.9    | 41.977          | 0.001    | 0.39                 | -                                       | -             |
| Habitat diversity                   | -          | 1369.8    | 29.952          | 0.001    | 0.31                 | -                                       | -             |
| Bottom current speed                | -          | 1302.9    | 27.881          | 0.001    | 0.29                 | -                                       | -             |
| Dynamic topography                  | -          | 953.19    | 18.348          | 0.001    | 0.21                 | -                                       | -             |
| Mud/sand                            | -          | 888.30    | 16.786          | 0.001    | 0.20                 | -                                       | -             |
| Depth (SD)                          | -          | 832.97    | 15.499          | 0.001    | 0.19                 | -                                       | -             |
| Depth SD (15x gcfm)<br>(mean)       | -          | 704.72    | 12.661          | 0.003    | 0.16                 | -                                       | -             |
| Depth range (15x gcfm)<br>(SD)      | -          | 686.98    | 12.284          | 0.002    | 0.15                 | -                                       | -             |
| Depth SD (15x gcfm)<br>(SD)         | -          | 677.53    | 12.085          | 0.001    | 0.15                 | -                                       | -             |
| <i>Sequential</i>                   |            |           |                 |          |                      |   |               |
| Nodules                             | 255.64     | 1787.00   | 45.2340         | 0.001    | 0.40                 | 0.40                                    | 67            |
| SST gradient                        | 244.86     | 447.58    | 13.4320         | 0.002    | 0.10                 | 0.50                                    | 66            |
| Aspect (SD)                         | 236.18     | 315.45    | 10.8840         | 0.003    | 0.07                 | 0.58                                    | 65            |
| Shell hash                          | 231.72     | 168.28    | 6.2776          | 0.016    | 0.04                 | 0.61                                    | 64            |
| Gravel                              | 226.86     | 162.52    | 6.5925          | 0.013    | 0.04                 | 0.65                                    | 63            |
| Plan curvature (15x<br>gcfm) (mean) | 222.11     | 144.72    | 6.3712          | 0.016    | 0.03                 | 0.68                                    | 62            |
| Bottom temperature                  | 221.56     | 51.04     | 2.2942          | 0.121    | 0.01                 | 0.69                                    | 61            |
| Tidal current speed                 | 219.69     | 74.04     | 3.4616          | 0.070    | 0.02                 | 0.71                                    | 60            |
| DOM                                 | 217.63     | 73.25     | 3.5716          | 0.064    | 0.02                 | 0.73                                    | 59            |
| Plan curvature (SD)                 | 216.61     | 51.89     | 2.5986          | 0.121    | 0.01                 | 0.74                                    | 58            |

**Table 3-7: Results of DistLM analyses showing correlations between predictor variables and multivariate dispersion (mean deviation from centroid) among transects.** [Only the variables with the ten highest R<sup>2</sup> values are shown. AIC = Akaike Information Criterion, SS = Sum of Squares, Pseudo-F = Pseudo-F Statistic, P = probability, R<sup>2</sup> = proportion of explained variation attributable to each variable, R<sup>2</sup> (cumul.) = cumulative proportion of variation, res.df = residual degrees of freedom].

### 3.3 Habitat suitability modelling

#### 3.3.1 Overall model performance

The performance of models at the sampling point and 15x gcfm scale were very similar (differences in measures of CVdev and AUC were < 0.023 and < 0.034, respectively) and only the point scale models are considered and presented hereafter.

The BRT models at the point scale for each community or *Goniocorella dumosa* included different predictor variables, and had varying learning rates (range: 0.000938-0.0075) and tree complexities (range: 2-4) (Table 3-8). The epifauna community models had external validation CVdevs ranging from 0.096 to 1.094, with all models but one (Community *m*) having AUC values greater than 0.70 (the AUC threshold at which models are considered 'useful'). The AUC score for the Community *m* model was just below the threshold (0.68) and had a CVdev higher than some of the other models, and is therefore still considered reliable. The abundance model for *Goniocorella dumosa* was zero-inflated and considered unreliable, therefore only the presence model for this coral is considered further.

Appendix E provides the fitted functions for the BRT models of the epifauna (image-level) communities, and the presence model for *Goniocorella dumosa*.

| <b>Community</b> | <b>Parameters<br/>(contribution %)</b>  | <b>tc</b> | <b>lr</b> | <b># of<br/>trees</b> | <b>CVdev<br/>(internal)</b> | <b>AUC<br/>(internal)</b> | <b>CVdev<br/>(external)</b> | <b>AUC<br/>(external)</b> |
|------------------|---|-----------|-----------|-----------------------|-----------------------------|---------------------------|-----------------------------|---------------------------|
| <b>f</b>         | Depth (52.2)<br>Bottom current speed (11.1)<br>Nodule content (10.2)<br>Slope (6.4)<br>Curvature (4.9)<br>Depth SD [3x gcfm] (4.5)<br>Aspect (4.4)<br>Plan curvature (3.8)<br>Profile curvature (2.6)   | 2         | 0.000938  | 1950                  | 0.117                       | 0.786                     | 0.123                       | 0.93                      |
| <b>g</b>         | Depth (11.5)<br>Aspect (11.3)<br>Profile curvature (9.5)<br>DOM (9.0)<br>Nodule content (8.8)<br>Dynamic topography (8.4)<br>SST gradient (7.9)<br>Bottom current speed (7.6)<br>Depth SD (7.2)<br>Tidal current speed (6.9)<br>Temperature (6.8)<br>Primary productivity (5.1) | 3         | 0.00375   | 2000                  | 0.087                       | 0.7                       | 0.997                       | 0.72                      |
| <b>j</b>         | DOM (17.1)<br>SST gradient (15.7)<br>POC (11.9)<br>Tidal current speed (10.9)<br>Depth (9.8)<br>Temperature (7.5)<br>Gravel (6.8)<br>Aspect (6.2)<br>Slope (5.3)<br>Profile curvature (5.1)<br>Curvature (3.6)  | 2         | 0.00375   | 1700                  | 0.287                       | 0.903                     | 0.247                       | 0.90                      |
| <b>m</b>         | SST gradient (16.5)<br>Rugosity [3x gcfm] (15.0)<br>Dynamic topography (12.0)<br>Nodule content (10.8)<br>Depth (9.7)<br>Profile curvature (9.5)<br>Slope (7.3)<br>Aspect (6.9)<br>DOM (6.4)<br>Sand (6.1)  | 4         | 0.001875  | 1650                  | 0.127                       | 0.784                     | 0.372                       | 0.68                      |
| <b>n</b>         | SST gradient (22.6)<br>Mud (18.6)<br>Depth range [3x gcfm] (8.6)<br>Bottom current speed (8.5)<br>Rugosity [3x gcfm] (8.1)<br>Slope SD [3x gcfm] (8.0)<br>Temperature (6.8)<br>Gravel (6.7)<br>Aspect (4.9)<br>Depth (4.1)<br>Sand (3.0)  | 2         | 0.0075    | 1050                  | 0.236                       | 0.872                     | 0.722                       | 0.86                      |



| <i>Community</i>                      | <i>Parameters<br/>(contribution %)</i>  | <i>tc</i> | <i>lr</i> | <i># of<br/>trees</i> | <i>CVdev<br/>(internal)</i> | <i>AUC<br/>(internal)</i> | <i>CVdev<br/>(external)</i> | <i>AUC<br/>(external)</i> |
|---------------------------------------|---|-----------|-----------|-----------------------|-----------------------------|---------------------------|-----------------------------|---------------------------|
| <b>o</b>                              | Depth (21.3)<br>SST gradient (17.6)<br>Aspect (9.7)<br>DOM (9.7)<br>Sand (8.4)<br>Slope SD [3x gcfm] (7.5)<br>Rugosity [3x gcfm] (7.0)<br>Tidal current speed (6.9)<br>Plan curvature (6.4)<br>Primary productivity (5.6)                   | 3         | 0.0075    | 1300                  | 0.309                       | 0.898                     | 0.311                       | 0.91                      |
| <b>p</b>                              | Depth (27.9)<br>Slope (17.3)<br>Plan curvature (15.6)<br>Nodule content (13.3)<br>DOM (10.2)<br>Rugosity [3x gcfm] (7.9)<br>Slope SD [3x gcfm] (7.7)  | 3         | 0.00375   | 1450                  | 0.103                       | 0.793                     | 0.096                       | 0.89                      |
| <b>q</b>                              | DOM (29.4)<br>SST gradient (16.4)<br>Sand (12.1)<br>Tidal current speed (11.0)<br>Depth (9.2)<br>POC (8.3)<br>Aspect (7.5)<br>Nodule content (6.1)  | 2         | 0.0075    | 1150                  | 0.18                        | 0.781                     | 0.846                       | 0.77                      |
| <b><i>Goniocorella<br/>dumosa</i></b> | SST gradient (23.2)<br>Depth (15.3)<br>Slope SD [3x gcfm] (8.1)<br>DOM (8.0)<br>Tidal current speed (7.6)<br>Mud (7.4)<br>Plan curvature (7.2)<br>Gravel (6.5)<br>Aspect (6.1)<br>Depth range [3x gcfm]<br>(5.6)<br>Profile curvature (4.9) | 2         | 0.0075    | 2050                  | 0.284                       | 0.875                     | 0.475                       | 0.9                       |

**Table 3-8: Model parameters and performance metrics of epifauna community (image-level) and *Goniocorella dumosa* boosted regression tree models.** [tc = tree complexity, lr = learning rate, CVdev = percent deviance explained, AUC = area under receiver operating curve, gcfm = grid cell focal mean].

### 3.3.2 Epifauna (image-level)

Suitable habitat for Community *f* (characterised by encrusting bryozoans/sponges/ascidians found on isolated hard ground and irregular urchins typical of soft sediment) is predicted to occur primarily in the western part of the study area, and in smaller areas towards the eastern side of the study area. Relatively small areas of high habitat suitability for this community are predicted to occur in the mining permit area (Figure 3-8). The distribution of suitable habitat for this community is related primarily to depth (52.2% contribution to the model), with shallower depths (<380 m) representing more suitable habitat (although smaller areas at ~470 m are also predicted to be suitable habitat). Other relatively important

variables for predicting habitat suitability (>10% contribution to the model) are bottom current speed (when higher) and the nodule content of the sediment (when not very low) (Table 3-8, Appendix E).

Community *g* (characterised by irregular urchins typical of soft sediment) is predicted to occur in patches almost throughout the study area (the exception being the areas predicted to be suitable habitat for Community *f* (see above). A relatively large part of the mining permit area is predicted to include suitable habitat for this community (Figure 3-9). Twelve environmental variables were identified as relatively equally important for predicting suitable habitat for this community, with only depth and aspect each contributing >10% to the model. Habitat suitability tended to be higher when depth was relatively deep and the aspect of the seafloor topography was between north and east (Table 3-8, Appendix E).

Suitable habitat for Community *j* (characterised by sea anemones and hermit crabs) was predicted to occur mainly along the deeper northern and southern flanks of study area, and at the shallowest depths of the study area to the west and east the mining permit area (Figure 3-10). Four environmental variables contributed >10% to the model, with DOM (17.5%) and SST gradient (15.7%) being the two most important variables for predicting the distribution of this community. Areas with relatively high and low DOM, and low SST gradient provided the most suitable habitat for Community *j* (Table 3-8, Appendix E).

Community *m* (characterised by brachiopods) is predicted to mainly occur in a large area in the northwest part of the study area, with a disjunct extension of this suitable habitat into the permit area. The model for this community also predicts that smaller patches of suitable habitat for this community exists to the west and southeast of the permit area. The remainder of the study area is largely predicted to be unsuitable habitat (Figure 3-11). The environmental variables that contribute the most to the model are SS gradient, Rugosity, Dynamic topography and Nodule content (contributing between 10.8% and 16.5% to the model). The most suitable habitat occurring where SST gradient, Dynamic topography and Nodule content are relatively high and seafloor rugosity low (Table 3-8, Appendix E).

Suitable habitat for Community *n* (characterised by high abundance of encrusting bryozoans/sponges/ascidians, and also the presence of *Goniocorella dumosa*, which are taxa typically found on isolated hard substratum) was restricted to patches with a broad area of the northwest part of the study, which included relatively small patches within the mining permit area. The majority of the study area represented unsuitable habitat for this community (Figure 3-12). SST gradient and Mud were the two most important variables for predicting suitable habitat for this community, contributing 22.6% and 18.6% to the model (respectively). The most suitable habitat occurred where SST gradient and the mud content of the substratum were relatively high (Table 3-8, Appendix E).

Community *o* (dominated by the habitat-forming coral *Goniocorella dumosa* and also characterised by an associated mix of taxa - Branching bryozoan/hydroid/other and Encrusting bryozoan/sponge/ascidian) is predicted to occur in a large area in the northwest part of the study area, as well as relatively large patches that wholly or partly occur in the mining permit area. Outside these areas the model for this community predicts only very small areas of highly suitable habitat (Figure 3-13). Depth and SST gradient are the most important contributors to the model (21.3% and 17.6%, respectively), and suitable habitat is

predicted to occur in water shallower than 400 m and where the SST gradient is high (Table 3-8, Appendix E).

Suitable habitat for Community *p* (characterised by Encrusting bryozoan/sponge/ascidian and Branching bryozoan/hydroid/other) is predicted to occur in patches of varying size throughout the study area, except the deepest areas (Figure 3-14). Four environmental variables contribute >10% to the model for this community. Depth, Slope and Plan curvature contribute the most (27.9%, 17.3%, and 15.6% respectively) and suitable habitat is predicted to occur where water depth is relatively shallow and the seafloor essentially flat. The nodule content of the substratum is another relatively important variable (contributing 13.3% to the model) for predicting habitat suitability, with the most suitable habitat occurring where nodule content is relatively high (Table 3-8, Appendix E).

Community *q* (dominated by the taxon group Encrusting bryozoan/sponge/ascidian, which colonise patches of hard substratum) is predicted to occur mostly in the western half of the study area. Within this area, suitable habitat mainly occurs in two strips to the north and south, as well as occupying a relatively large part of the western side of mining permit area (Figure 3-15). The distribution of suitable habitat for this community is primarily related to DOM, SST gradient, sand content of the substratum and tidal current speed (contributions to the model of 29.4%, 16.4%, 12.1% and 11%, respectively). The most suitable habitat is predicted to occur where levels of DOM are in the middle of their range, SST gradient is high, and where the sand content of the substratum and the tidal current speed are not high (Table 3-8, Appendix E).

### **3.3.3 *Goniocorella dumosa***

Suitable habitat for the stony coral *Goniocorella dumosa* is predicted to occur in a large area in the northwest part of the study area, as well as a patchy distribution through the central and eastern part of the mining permit area. There are no other locations predicted to be highly suitable habitat for this coral species elsewhere in the study area (Figure 3-16). The predicted distribution of *Goniocorella dumosa* is most strongly related to SST gradient (23.2% contribution to the model), with the most suitable habitat for this species occurring where the value of this variable is at its highest. Only one other environmental variable contributes >10% to the habitat suitability model for *Goniocorella dumosa*. That is, water depth (15.3% contribution), which is relatively shallow (<380m) where habitat is most suitable.

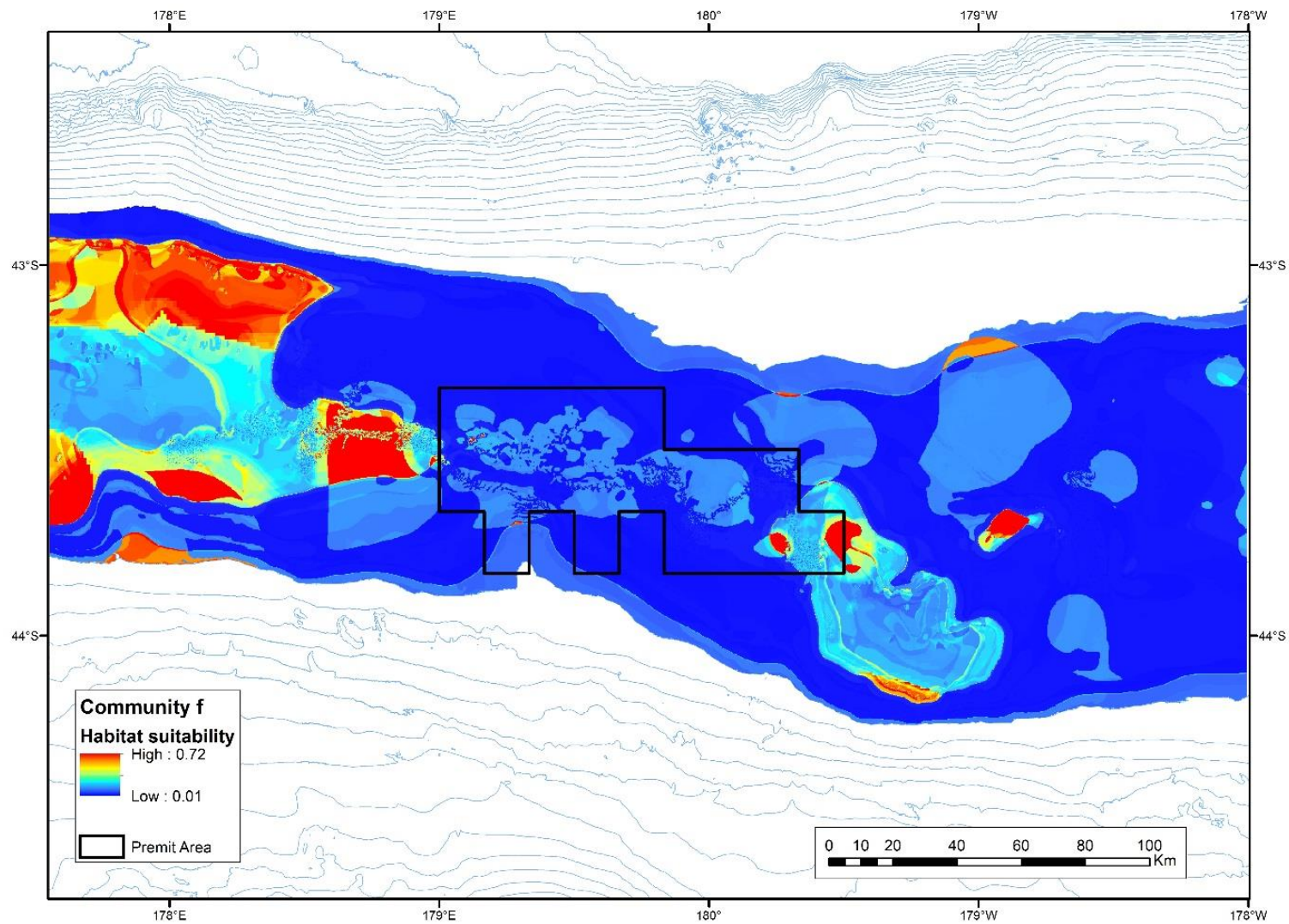


Figure 3-8: Predicted habitat suitability for epifauna Community *f* (image-level) in the study area.



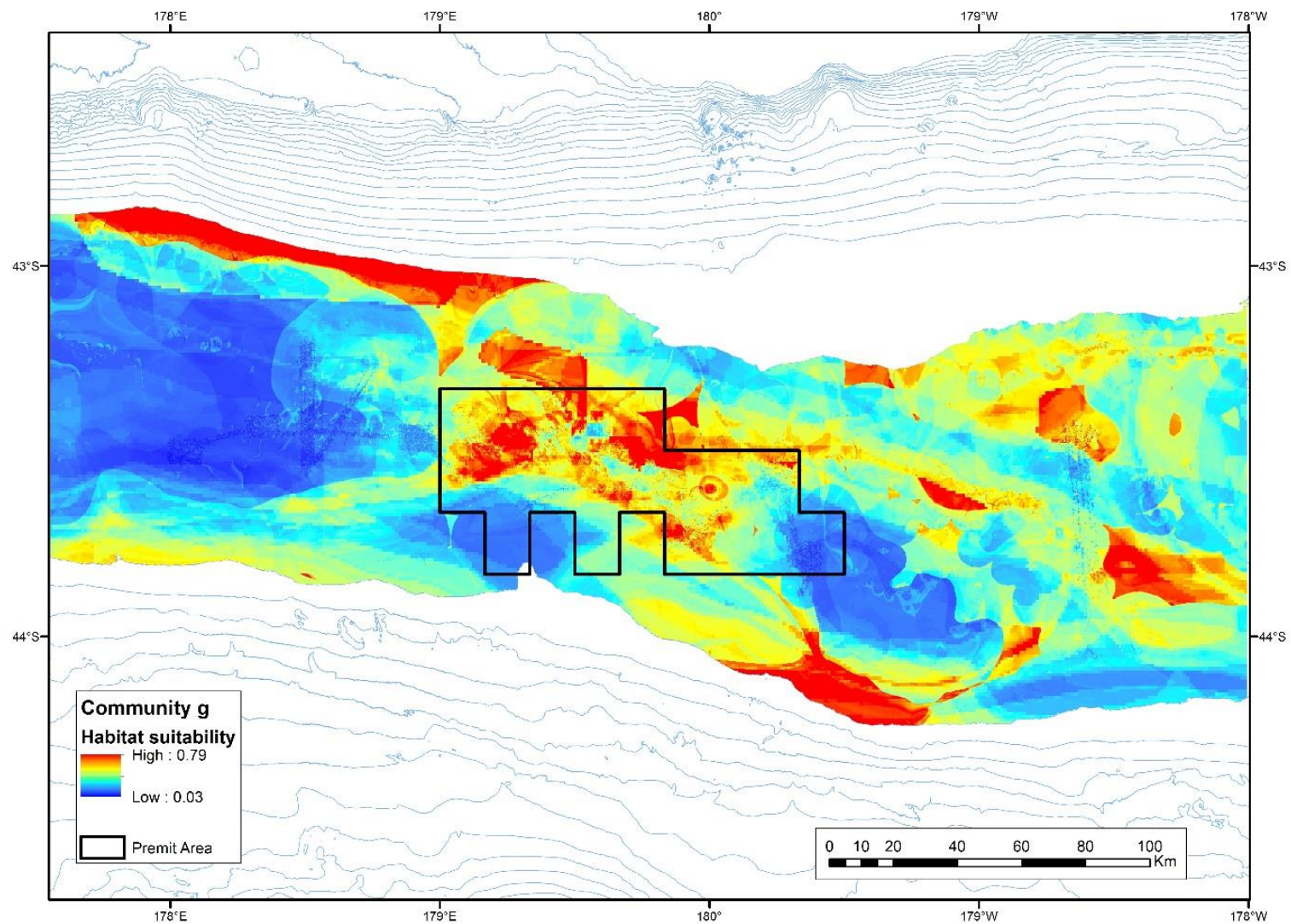


Figure 3-9: Predicted habitat suitability for epifauna Community *g* (image-level) in the study area.



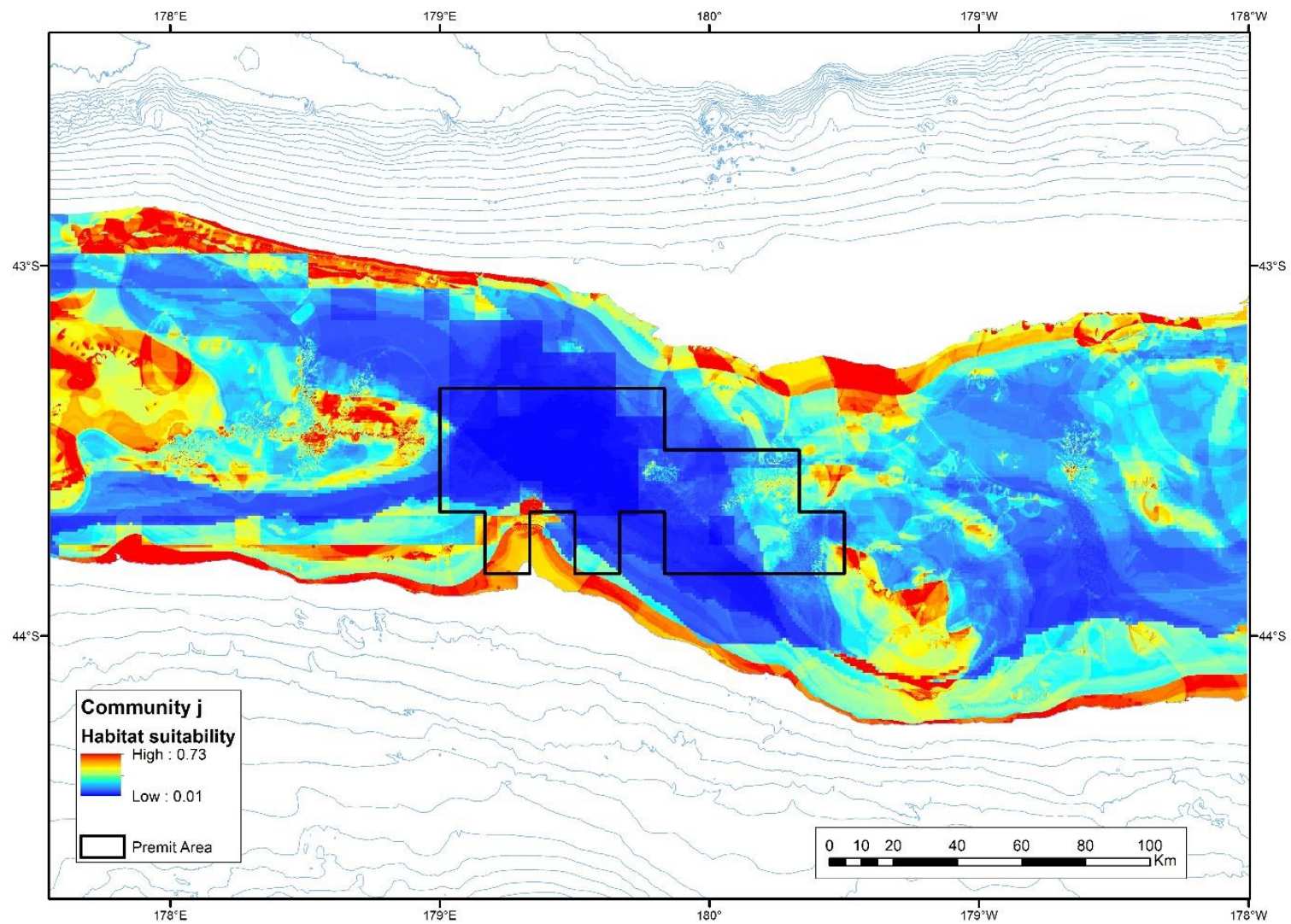


Figure 3-10: Predicted habitat suitability for epifauna Community *j* (image-level) in the study area.

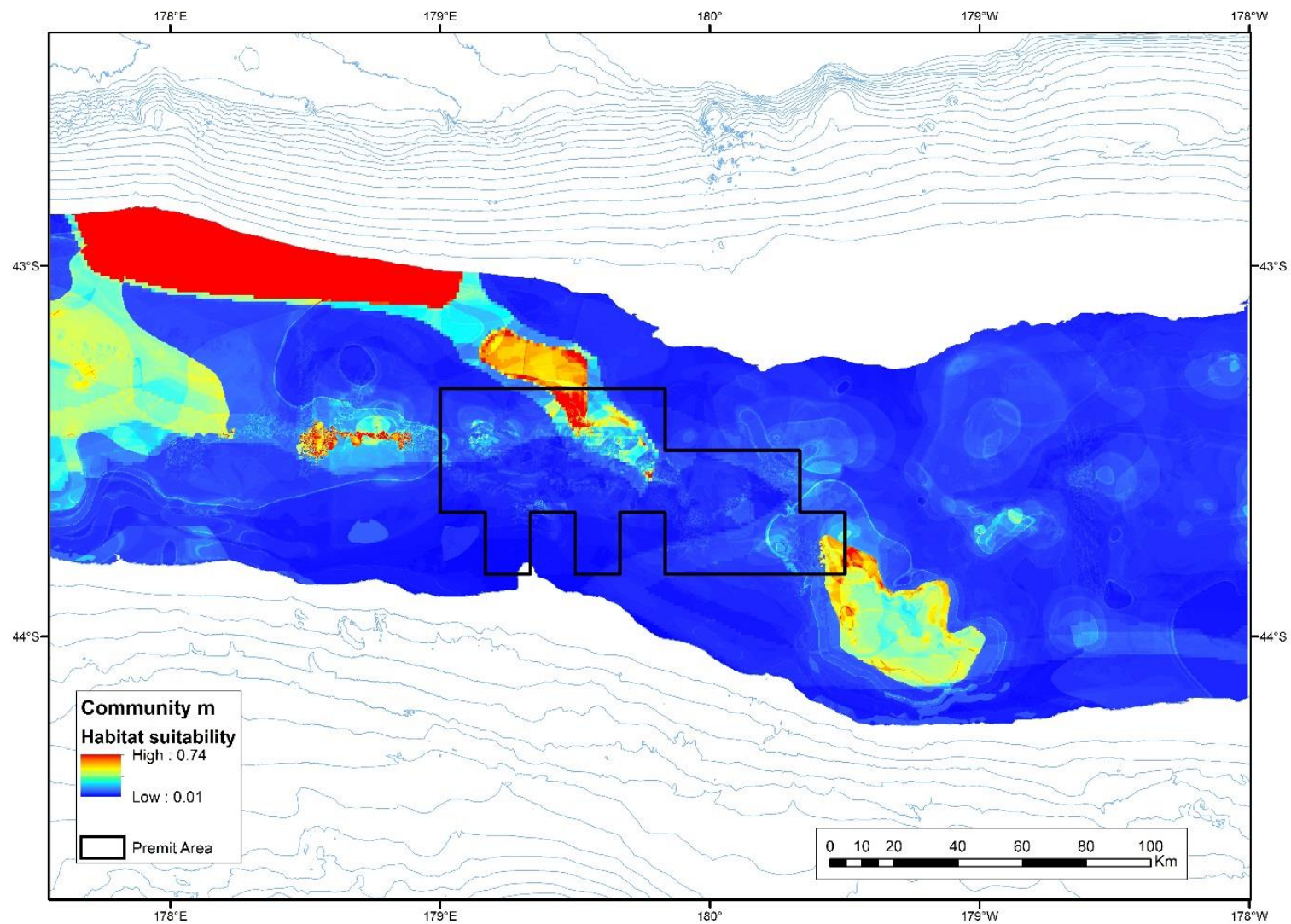


Figure 3-11: Predicted habitat suitability for epifauna Community *m* (image-level) in the study area.



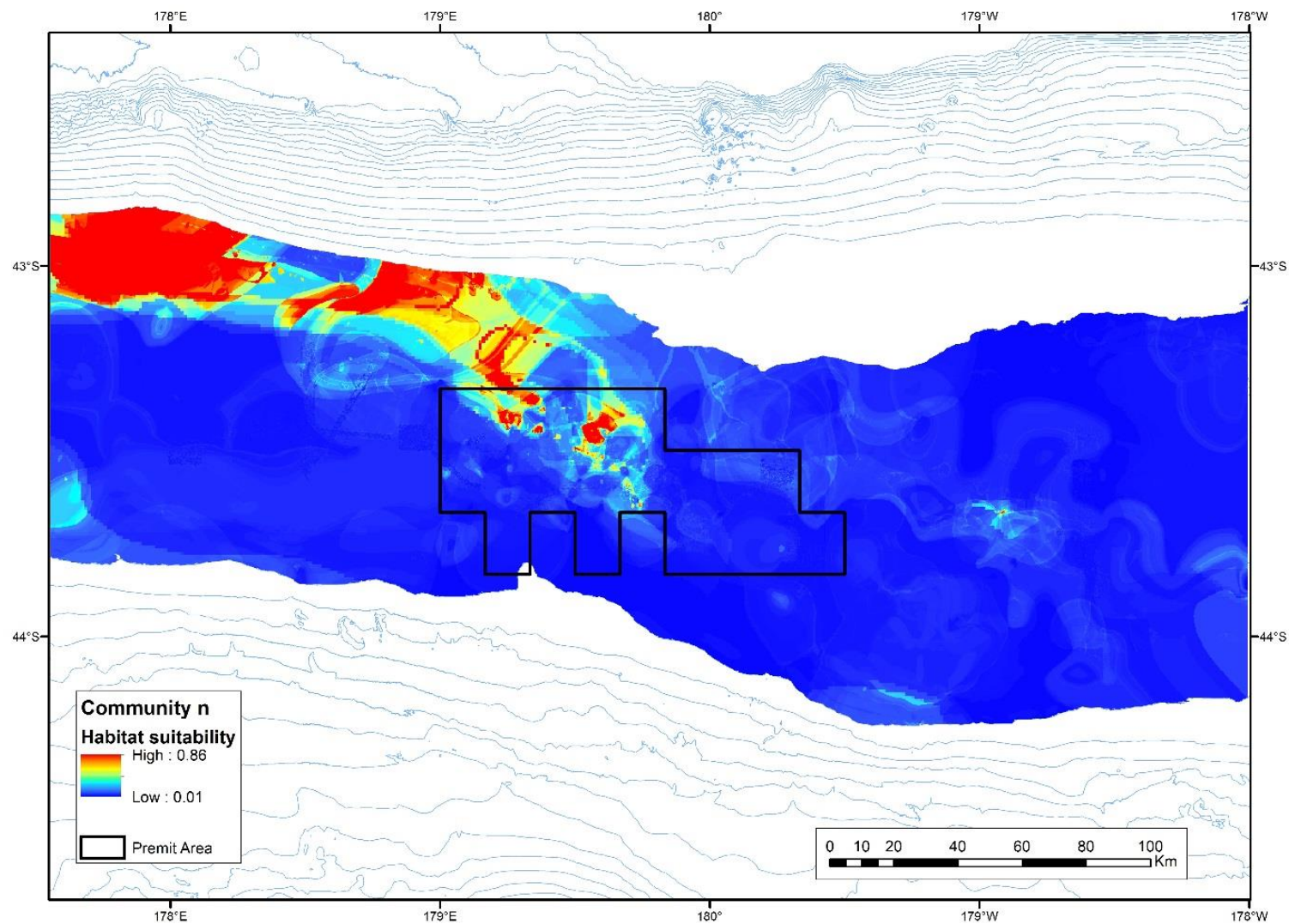


Figure 3-12: Predicted habitat suitability for epifauna Community *n* (image-level) in the study area.

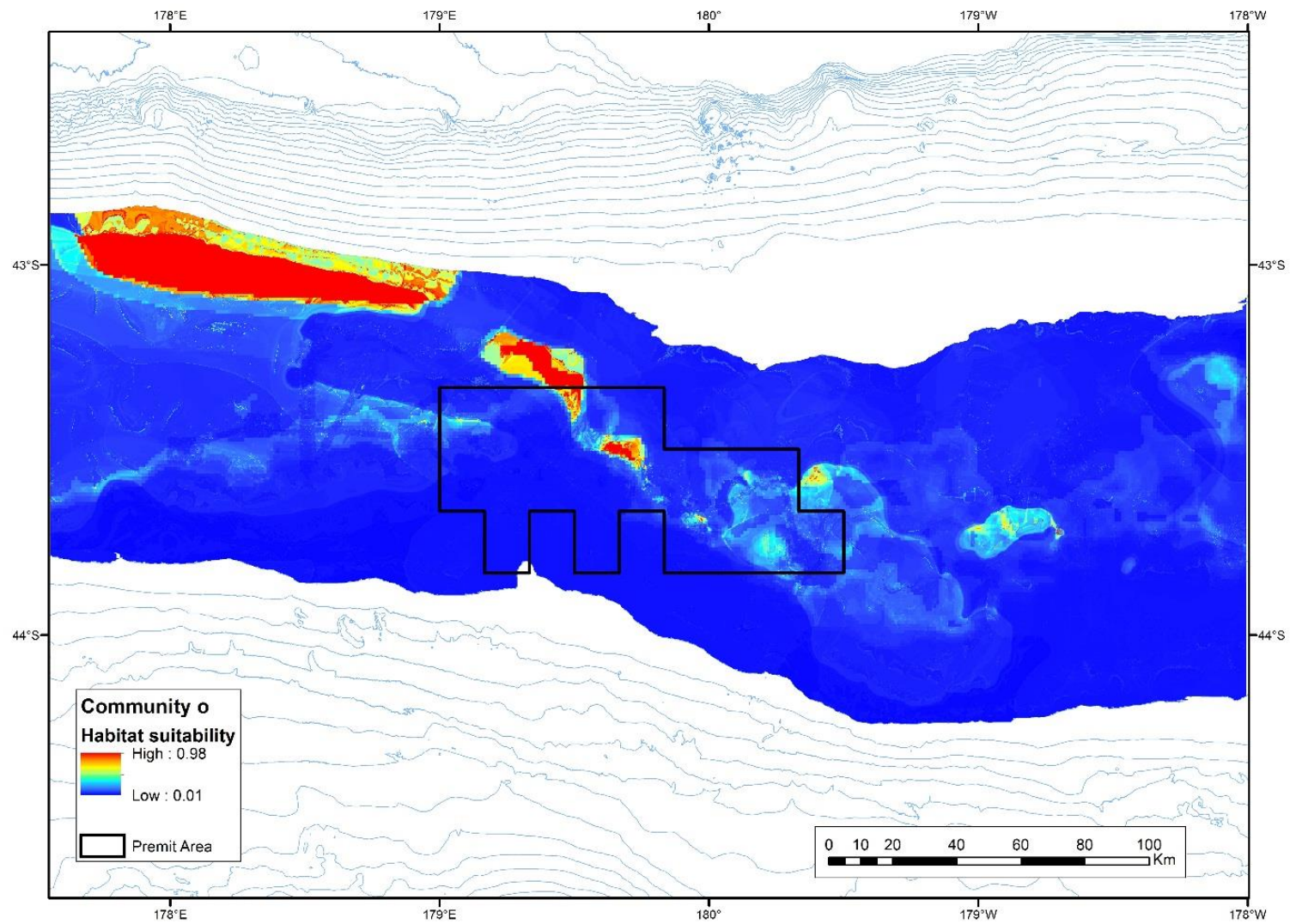


Figure 3-13: Predicted habitat suitability for epifauna Community o (image-level) in the study area.



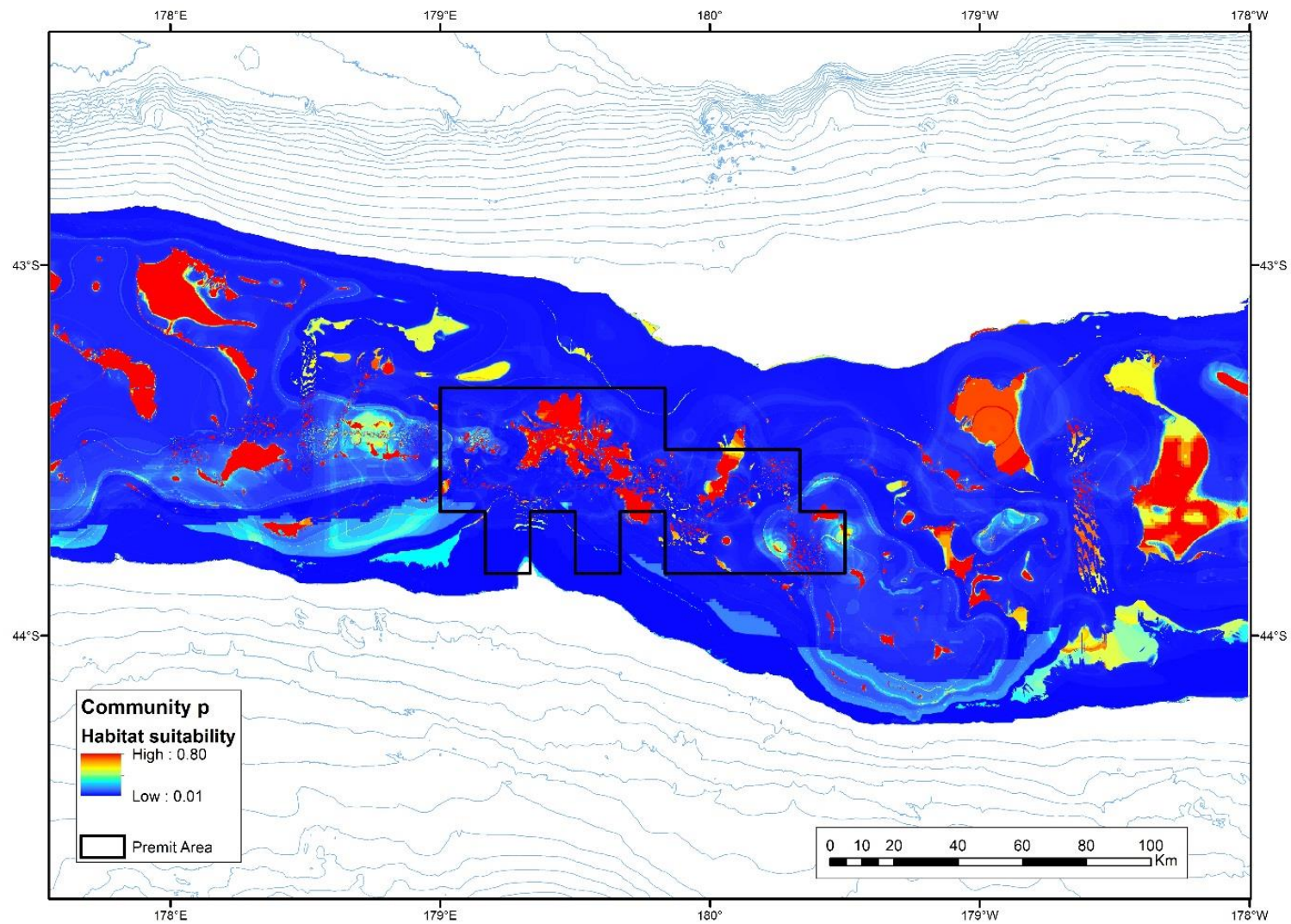
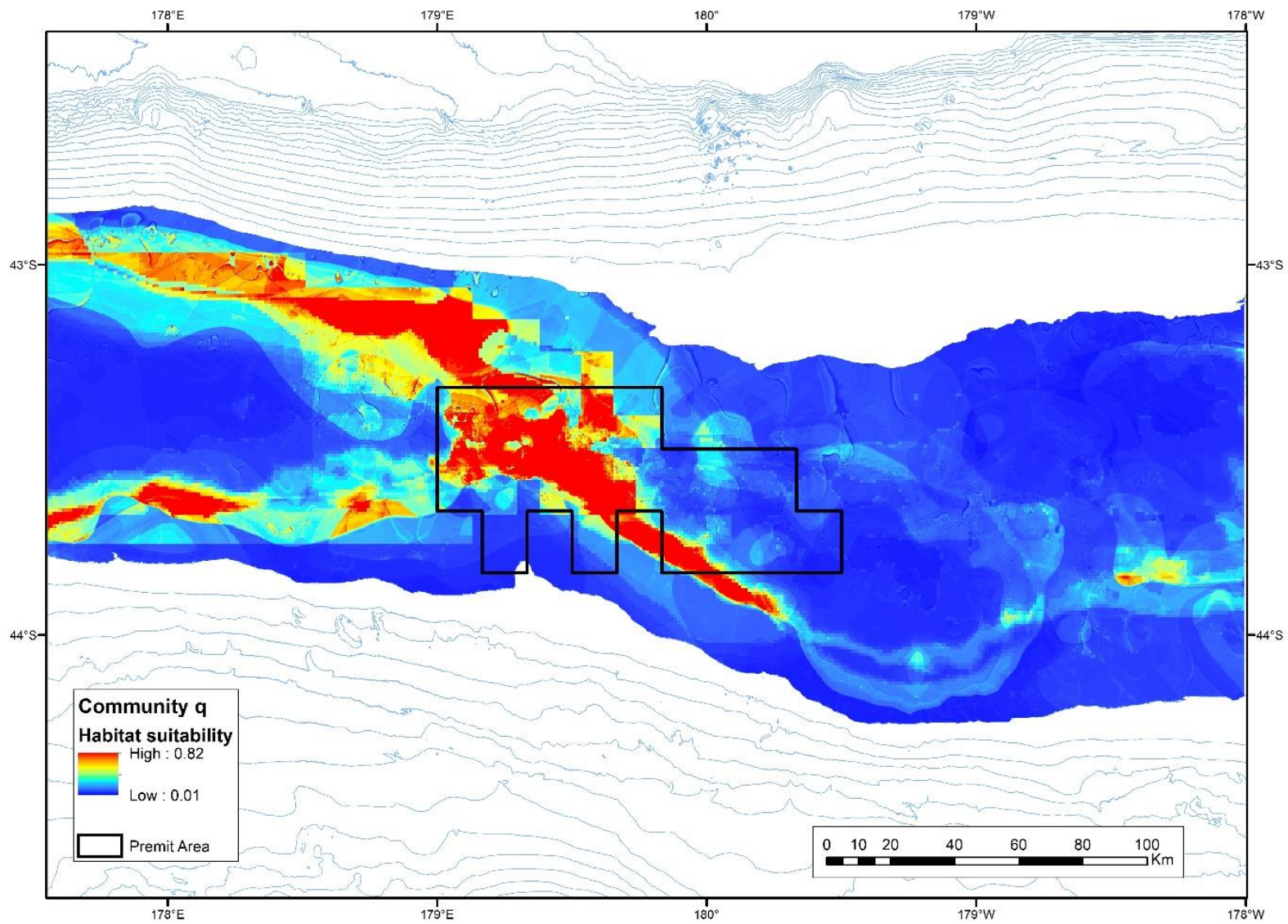


Figure 3-14: Predicted habitat suitability for epifauna Community *p* (image-level) in the study area.





**Figure 3-15: Predicted habitat suitability for epifauna Community q (image-level) in the study area.**

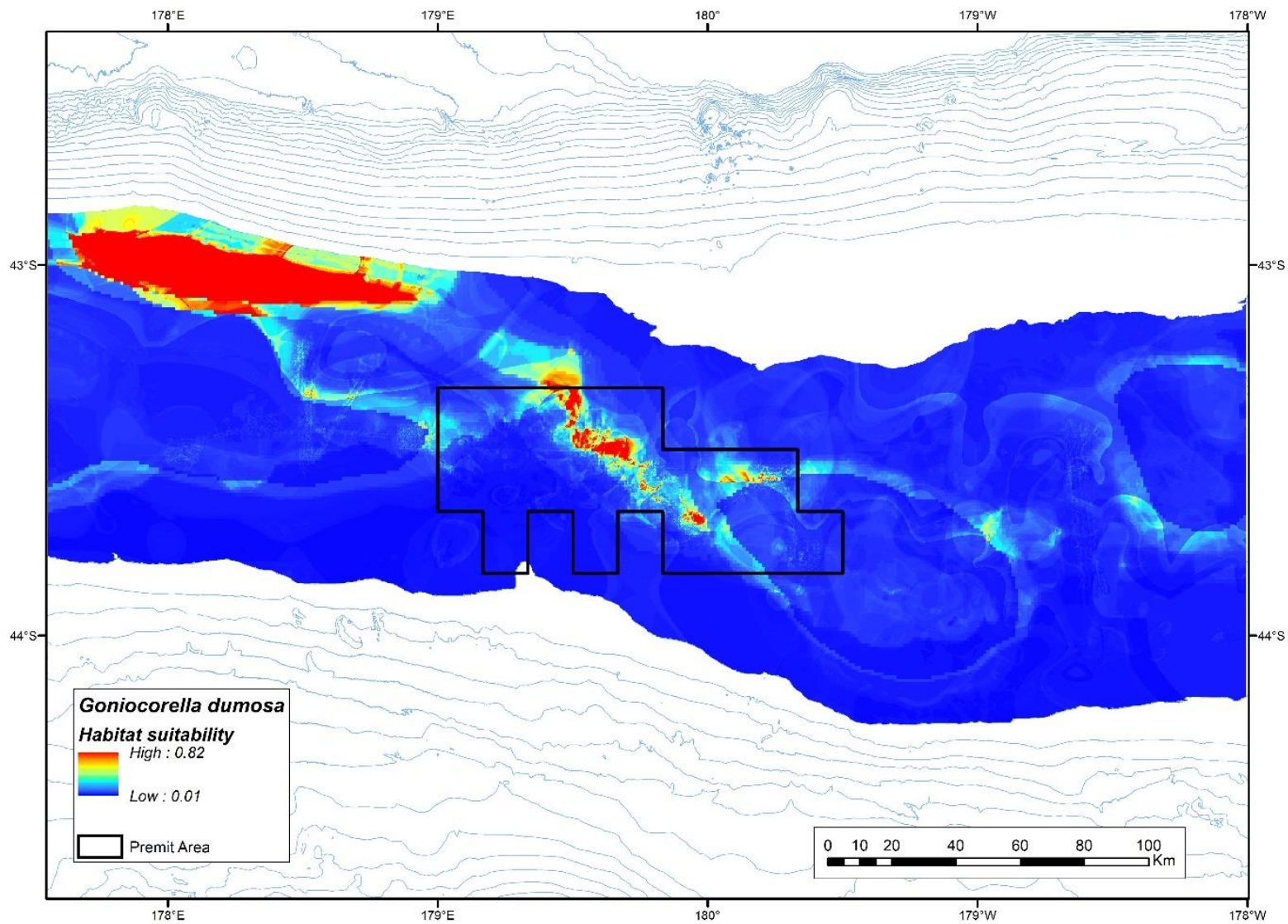


Figure 3-16: Predicted habitat suitability for the stony coral *Goniocorella dumosa* (image-level) in the study area.

## 4 Discussion

The Environmental Survey conducted by CRP, and the Chatham Rise Benthos and Chatham-Challenger (OS20/20) Surveys were successful in obtaining data to characterise the benthic communities and habitats that included the mining permit area on the Chatham Rise. ROV and DTIS photographic transects obtained images that were used to identify epifauna communities across the study area. Data were also recovered that could be used to explain the structure and distribution of these communities, and to predict the distribution of suitable habitat for these communities across the entire study area. The survey was designed to provide this information in support of CRP's Environmental Impact Assessment. The main results are summarised below and then discussed in the context of what is known about benthic community structure elsewhere on the Chatham Rise.

### 4.1 Epifauna community structure and distribution in the study area

Thirteen epifauna communities were identified by the analysis of the individual still images of the seafloor obtained by the ROV and DTIS. Community structure varied at both the among-survey area scale (~5 – 280 km) and within-survey area scale (~1 – 5 km), although the former scale accounted for more of the observed variability in structure. Overall, benthic community structure was explained by a large number of predictor variables ( $n = 40$ ). However, most variables have little explanatory power apart from Mud/sand (i.e., soft sediment) and Phosphorite nodules (i.e., hard substrate). Together with two other variables (Boulders and SST gradient), these variables explained nearly a quarter of the variability in epifauna community structure (at the image-level scale). Habitat suitability modelling allowed for an appreciation of the environmental forces that account for the structure and distribution of each of the identified epifauna communities.

The most commonly observed community type, Community *g*, was found, and was predicted to be found across much of the study area (apart from the western side), particularly in the deeper waters. A relatively large part of the mining permit area is predicted to include suitable habitat for this community. Community *g* was dominated by irregular urchins that occurred on soft sediments. Irregular urchins move on and through soft sediment when feeding, and a fairly uniform, flat sand/mud substrate with few large particles to impede their mobility is ideal habitat (Schinner 1993). The next most commonly observed epifauna community, Community *q*, was characterised by a low density of sessile taxa, primarily bryozoans, sponges and ascidians that require hard substrates to colonise. This community was found and predicted to occur mainly in the western side of the study area in two strips to the north and south, as well as the western half of the mining permit area. Suitable habitat for this community was predicted to be where variables indicate that the potential food for benthic organisms (DOM, SST gradient, POC) is relatively high in the water overlying a predominantly soft (sand) sediment seafloor, but with some surface nodules to provide sites of attachment for sessile epifauna taxa. Nodules are widespread in relatively low densities on the shallow western parts of the permit area (Nodder et al. 2013, Appendix C Figure C-13).

The predicted suitable habitat for Community *j* is in obvious contrast to the combined distribution of suitable habitat for Communities *g* and *q*. Whereby predicted suitable habitat for this community largely occupies the area deemed to be relatively unsuitable for either of the other two communities. That is, suitable habitat for Community *j* is found along the



deepest parts of the northern and southern flanks of the study area and the shallowest parts of the study area. Depth is one of the most important variables used to predict the distribution of this community, which is characterised by sea anemones and hermit crabs. Other variables contribute only a small proportion to the habitat suitability model, and so it is not straightforward to understand what environmental drivers are likely responsible for the structure and distribution of Community *j*. Of note, is that there is very little suitable habitat for this community predicted to occur in the mining permit area.

Few and small areas of suitable habitat are also only predicted to occur within the mining permit area for Community *f*. Predicted suitable habitat is concentrated in the west and generally shallower parts of the study area, and depth is by far the most important predictor included in the model. This community is characterised by encrusting bryozoans, sponges and ascidians that require hard substratum to colonise, as well as irregular urchins which are typical of soft sediment. Suitable habitat was predicted to occur when bottom current speed and nodule content were relatively high. These two variables can be related to the enhanced delivery of food material (e.g. Thiem et al. 2006) and the provision of suitable habitat for the sessile characterising taxa, respectively.

Community *p* is solely characterised by sessile taxa, including bryozoans, sponges, hydroids and ascidians. This community has a predicted distribution quite different from any of the other communities, in that suitable habitat is predicted to occur in relatively evenly dispersed patches throughout almost the entire the study area (including the mining permit area). Suitable habitat is characterised by being relatively shallow and where the seafloor is essential flat (very low slope and plan curvature). The phosphorite nodule content of the substratum is another variable that contributes to the prediction of suitable habitat. Nodules have a patchy distribution in the study area (Appendix Figure C-13), which presumably accounts to some extent for the patchy distribution of this community, whose characterising taxa require a hard substratum on which to settle and thrive (Dawson 1984, Kudrass & van Rad 1984b).

The two communities with the most similar structure, Communities *o* and *n*, are both characterised by the stony coral *Goniocorella dumosa* (Community *n* less so) as well as sessile taxa, including bryozoans, sponges, hydroids and ascidians. These two communities are predicted to have a similar distribution of suitable habitat, occurring in patches mainly in the northwestern part of the study area as well as smaller patches within the mining permit area. SST gradient is an important variable for predicting the occurrence of these communities, suitable habitat occurring where the SST gradient is relatively high. High values of SST gradient are indicative of oceanographic fronts, where surface productivity can be concentrated (compare Appendix Figures C-18 and C-21), and where associated downwelling can enhance the flux of potential food material to the benthos (Nodder et al. 2003, 2007) (Appendix Figure C-20). These are particularly suitable conditions for the sessile taxa that characterise Communities *o* and *n* to thrive.

Suitable habitat for both these communities was also relatively shallow, and topographic variables such as rugosity, aspect and variation in the slope are also implicated in explaining their distribution. The topographic variables are indicative of small-scale elevations in the seafloor (and their direction), and these would be beneficial for the sessile taxa that characterise these two communities by raising them into faster water flows that contain food material (Tong et al. 2012). These taxa also require hard substrates for attachment, and

seafloor photographs indicate that these are provided by relatively large phosphorite nodules as well as rocks of other material. Nodules have a patchy distribution in the study area, and the % nodule content of the substratum was relatively high where Communities *o* and *n* were predicted to be found in the mining permit area (Appendix Figure C-13). However, phosphorite nodules were not identified as an important variable in the habitat suitability model for either community. This result is probably because of the relative low density of data points (that were used to derive the % nodule content layer used in the modelling) in the northwestern part of the study area, which are less likely to detect the typically small scale patches of nodules. Not surprisingly, the distribution and predicted distribution of *Goniocorella dumosa* matches the predicted distribution of suitable habitat for Communities *o* and *n*.

Suitable habitat for Community *m* was also predicted to be found mainly in a relatively large patch in the northwestern part of the study area, including an area of the mining permit area. However, for this community there were additional patches of predicted suitable habitat to the west and southeast of the permit area. SST gradient was an important predictor variable of suitable habitat, as was dynamic topography (and indicator of surface water currents), rugosity, and the nodule content of the substratum. Community *m* is dominated by brachiopods which require hard substrates for attachment. As well as nodule content being identified as an important variable in the habitat suitability model, images of the seafloor show that this community is associated with pebble-sized rocks and phosphorite nodules. In contrast to the suitable habitat for Communities *o* and *n* (which have a somewhat similar predicted distribution), the most suitable habitat for Community *m* was related to low rugosity values.

No attempt was made to generate models for the remaining five epifauna communities identified at the image-level scale because of the small number of images in which they were observed. Thus, the possible reasons for the structure and likely distribution of these relatively rare epifauna communities in the study area are not known.

Analysis of the image data at the transect-level identified twelve epifauna communities. By pooling images for each transect, communities that may exist at a large spatial scale can be identified, or alternatively the scale-independent constancy of communities identified at smaller spatial scales. An examination of the taxa that characterised the five most commonly identified communities (identified at  $\geq 4$  transects, and the only ones described by the analysis), and the patterns of their observed distribution, revealed that the transect-level communities are equivalent to five of the eight main communities identified at the image-level. That is, image-level epifauna Communities *o*, *f*, *j*, *g* and *m* are re-identified at the transect-level by Communities *l*, *j*, *a*, *b* and *d* (respectively). Unfortunately it was not possible to produce robust habitat suitability models for the transect-level communities, but because of the observed scale-independence, the image-level predictive maps provide a suitable means to appreciate the likely distribution of the main and consistent epifauna communities in the study area.

In summary, epifauna community structure in the surveyed area was observed to vary at two scales, but predominantly at the larger among-survey area scale. This pattern of spatial variation reflects the observation that epifauna communities are distributed with respect to soft sediment (Communities *g* and *j*), and within some areas occupied by this substrate, the patchy distribution of hard substrate (even if the hard substrate within these patches was



small in size) – where it more (Communities *m*, *n*, *o* and *p*) or less predominates (Communities *f* and *g*). Habitat suitability modelling also revealed the importance of other environmental variables for the distribution epibenthic communities. Variation in seafloor topography is among the variables that are predicted to play a part in generating suitable habitat for some epifauna communities, as are larger scale environmental variables such as SST gradient that is related to the position of fronts and the availability and flux of potential food for the benthic fauna. The latter is known to be important in structuring benthic communities across a wider area of the central Chatham Rise (see Nodder et al. 2007 and references within). The importance of the position of a frontal feature for predicting suitable habitat in the study area was particularly noticeable for Communities *m*, *n* and *o*, which are characterised by sessile taxa such as bryozoans, sponges, hydroids and ascidians. Also notable is the observed association between the patchy distribution of hard substrate, particularly phosphorite nodules, and Communities *o* and *n* – particularly within the mining permit area. These communities are characterised by the stony coral *Goniocorella dumosa*. Community *o*, in particular, has abundances of *Goniocorella dumosa* that allow areas where this community is found to be termed “coral thickets”, a type of “sensitive environment” (MacDiarmid et al. 2013) as defined by the Continental Shelf and EEZ Environmental Effects Act regulations (<http://www.legislation.govt.nz/regulation/public/2013/0283/latest/DLM5270660.html>). Coral dominated communities found elsewhere in the world have been observed to be highly diverse in terms of their invertebrate fauna (e.g., Henry & Roberts 2007) and can also provide important habitat for juvenile or larval fish (D’Onghia et al. 2010, Baillon et al. 2012). As such these particular epifauna communities have a notable significance for ecosystem function (Dawson 1984).

## 4.2 Comparison with epifauna communities identified by Rowden et al. (2013)

The previous study, that used solely ROV data from the CRP Environmental Survey, identified up to twelve epifauna communities (Rowden et al. 2013) over a relatively small portion of the present study area (the northwestern part of the mining permit area). Using more data from a larger area, the present study identified up to thirteen communities at the image-level. Between the 6 and 8 main communities that were described and mapped by each study, respectively, there is a high level of equivalence despite the difference in sampling scale. Communities *c*, *l*, *h*, *g*, *l* and *k* identified by Rowden et al. (2013) have similar characterising taxa as Communities *g*, *q*, *o*, *n*, *m*, *p* and/or *f* identified by the present study at the image-level. Rowden et al. (2013) did not identify any main communities that parallel the main Communities *j* and *f* identified by the present study. This result is explainable, as these communities are rarely found in the mining permit area and could therefore represent one of the minor undescribed communities identified by Rowden et al. (2013).

While up to twelve epifauna communities were identified at the transect-level by the present study compared to five by the study of Rowden et al. (2013), three of the communities of the former were not observed in the portion of the study area surveyed by the earlier study. The number of main communities identified (at  $\geq 4$  or 5 transects) was the same between the two studies. However, the level of congruence between the characterising taxa and distribution of these communities were they occurred within the same area was more limited and mainly overlapping. Community *j* identified in the present study, and characterised by sessile taxa including bryozoans, sponges and ascidians as well as irregular urchins, was mostly

associated with Community *h* and *f* (7 out of 10, and 5 out of 8 transects, respectively) identified by Rowden et al. (2013). Both the latter communities included characterising taxa similar to those of Community *j* (e.g., irregular urchins). Community *l* identified in the present study, and dominated by bryozoans, sponges, ascidians and the stony coral *Goniocorella dumosa*, was mostly associated with Community *c* and *e* (5 out of 6 transects, 6 out of 7 transects, respectively) identified by the earlier study (Rowden et al. 2013). Community *e* was dominated by the stony coral, while Community *c* was mainly characterised by bryozoans and hydroids as well as *Goniocorella dumosa*. The final main epifauna community identified by Rowden et al. (2013) at the transect-level, Community *g*, was associated with minor Communities *f*, *g* and *l* identified by the present study. These patterns of less than perfect equivalence are probably a consequence of the data pooling aspect of the transect-level based analysis.

Overall, the comparison between the results of the present study and that of Rowden et al. (2013), testify to the successful merging of the image datasets from the different surveys, and consistency in the identification of epifauna community types over different sampling scales at the image-level of analysis. However, the present report does not wholly supersede the report of Rowden et al. (2013), because importantly the previous report includes the results of an analysis of infauna data obtained from box-cores as well as presenting a comparison of the distribution of infauna and epifauna communities within a part of the mining permit area.

#### **4.3 Comparison with epifauna communities elsewhere on the Chatham Rise**

The information about benthic community structure and distribution within the study area, provided by CRP's Environmental Survey and the two OS2/20 surveys, needs to be viewed alongside available information about benthic communities elsewhere on the Chatham Rise. It is important to make this comparison, principally, to determine if the communities identified by the survey are found elsewhere in the region or whether they are unique communities (or not yet known from elsewhere). However, it is important before attempting to make such a comparison to understand the limitations of any such assessment. Comparisons are impacted principally by differences in the data collection method (e.g., type of sampling gear, scale of sampling) as well as by the analysis method (e.g., different classification or ordination techniques, and subjective or objective means for identifying communities). Obviously, the ideal comparison is made using results derived from both the same sampling and analysis method, but this is not always possible (e.g., given time constraints or the availability of raw data). Reasonable comparisons can be made even if different, yet functional similar, sampling techniques have been used (e.g., grab and box-core sampling, or ROV and towed camera), particularly if there is time to first standardise the different datasets as much as possible and then analyse the standardised data by the same method (as was done here for data from the central crest region of the rise). If the same sampling gear has been used it is possible to make reasonable qualitative comparisons even if different analytical techniques have been used to identify communities, at least when the 'family' of analysis techniques is similar (e.g., classification). Any other sort of comparison is far from ideal and should be made with appropriate caution. Below, qualitative comparisons are made between the results of this study and those of previous published studies on the benthic communities of the Chatham Rise, but in the context of the limitations expressed above.

McKnight & Probert (1997) described a single epifauna community found at sites in water depths of 237-602 m, a range that includes the depth range where epifauna communities were observed in the study area (338-490 m). Their sites were within, and ~80 km to the west, of the study area. Sites were sampled using a small trawl, and sampling for their survey was over a larger-spatial scale than the present survey. While McKnight & Probert (1997) used broadly similar analytical techniques to the present study to define community identity and structure, the sampling method they used limits the meaningfulness of any comparison between the results of the two studies. The community identified by McKnight & Probert (1997) on sandy sediments of the crest of the rise was characterised by *Munida gracilis*, *Phylladorhynchus pusillus*, *Campylonotus rathbunae*, *Philocheras acutirostratus* and *Brucerolis hurleyi* (Crustacea), *Amphiura lanceolata* (Ophiuroidea), *Cuspidaria fairchildi* and *Euciroa galathea* (Bivalvia). Not surprisingly, given the difference in sampling gear (trawl versus images from ROV and towed camera transects) the characteristic species of this community are not comparable to any characterising taxa for communities identified by the present study. However, that is not to say that the same community was not sampled by the two studies, because the definition of the communities by the two studies is sampling method (gear/sampling scale) dependent.

The epifauna “groups” described by Floerl et al. (2012) were sampled and identified using similar techniques (video from the DTIS towed camera, multivariate classification) as those used in the present study. However, the analysis of these video data from the 2007 Chatham-Challenger (OS20/20) Survey encompassed a much larger area, sampling density was generally lower, and did not include the central portion of the present study area. Nonetheless a qualitative comparison between the results of the two studies is worthwhile making, particularly because still image data from six of the DTIS transect stations (towards the western and eastern sides of the study area) of the Chatham-Challenger (OS20/20) Survey were included in the present analysis of epifauna community structure. Floerl et al. (2012) identified 8 major and 9 minor epifauna groups on the Chatham Rise from the DTIS video data of Chatham-Challenger (OS20/20) Survey. The six transects included in the present analysis were deemed to belong to two epifauna groups by Floerl et al. (2012). The present analysis of still images (at the transect-level) from the same transects, as well as images from the DTIS and ROV transects from the Chatham Rise Benthos (OS20/20) Survey and CRP Environmental Survey, also identified these transects as belonging to two communities. The distribution of these two community types among the transects was consistent with the pattern for the epifauna groups identified by Floerl et al. (2012). Floerl et al. (2012) indicated that these two groups, B5 and B7, were characterised in the video images by *Hyalinoecia longibranchiata* (worm) and *Sympagurus dimorphus* (hermit crab) (B5), and *Munida gracilis* (squat lobster) (B7). The apparently parallel transect-level communities identified by the present analysis, Communities *b* and *a*, were characterised by irregular urchins (Community *b*), and anemones, squat lobsters and hermit crabs (Community *a*). The characterising taxa do not exactly match, but this is not surprising because they are identified by different images (video versus still images) which can result in the identification of slightly different characterising taxa.

Hewitt et al. (2011) used the epifauna groups identified by Floerl et al. (2012) to predict their occurrence in unsampled regions of the Chatham Rise, including the central crest of the rise (which was unsampled at the time). As such it is worth examining the results of their prediction to see how it compares with the observation of communities identified within the

study area. First it must be noted that the biological groups identified by Floerl et al. (2012) were slightly modified by Hewitt et al. (2011), before their distribution was interpolated into unsampled space. Hewitt et al. (2011), beginning with the biological groups identified by Floerl et al. (2012), used information on the location of the sample sites, species composition, and environmental gradients to re-allocate some sites to different groups – which they then termed “biotic habitats”. For the sake of this comparison, biotic habitats can be considered to be equivalent to groups identified by Floerl et al. (2012) because on the Chatham Rise only one site was re-allocated to another group. Hewitt et al. (2011) made a map showing the distribution of these biotic habitats based on the distinctive environmental characteristics specific to the biotic habitats and spatial continuity of habitats. Their map (see Figure 4 in Hewitt et al. 2011) predicts that B5 and B7 are the only biotic habitats to occur in the study area, including the mining permit area. If B5 and B7 are considered to be broadly the same as transect-level epifauna Communities *b* and *a* (see above), this prediction is partly supported by the present analysis. That is, the latter two communities are indeed found in the study area between and beyond the location of the 2007 transects where B5 and B7 were observed, including in the mining permit area. Furthermore, biotic habitat B7 can be found elsewhere on the crest of the Chatham Rise and on the Challenger Plateau between water depths of 249-587 m, while biotic habitat B5 is found between 210-682 m water depths where there are muddy sediments.

That no other biotic habitats are predicted to occur in the study area and mining permit area is perhaps not surprising given the high level of uncertainty that must be placed on the predictive map because of the interpolation method used by Hewitt et al. (2011). What is notable, however, is that none of the other epifauna communities identified by the present study are similar to any of the remaining biotic habitats identified on the Chatham Rise when the sampling and analysis techniques used are broadly comparable (Floerl et al. 2012, Hewitt et al. 2011). What this comparison suggests is either, that the identification of communities is strongly influenced by the scale of the sampling, or that the central crest region of the Chatham Rise contains epifauna communities that are not found elsewhere on the rise (or Challenger Plateau). While variation in sampling scale can influence the identity of communities, it is interesting to note that a change in sampling scale between image-level and transect-level in the present analysis did not alter the identity of the epifauna communities. Thus it is certainly possible, given that the study area is located within a large area where only a few samples were taken during the 2007 OS20/20 survey, that at least some of the epifauna communities identified by the present analysis could indeed be unique to the study area.

Some support is provided for this speculation by the distinct nature of the habitat provided by, or modified by, phosphorite nodules. For example, epifauna Community *o* (image-level) and Community *l* (transect-level) are dominated by the stony coral *Goniocorella dumosa*, the relative abundance of which relates in part to the presence of nodules on which they can live and grow. Thus these two communities are only likely to develop where nodules are in relatively high density. While *Goniocorella dumosa* can be found outside the licence area elsewhere on the Chatham Rise (Tracey et al. 2011), communities dominated by this coral have not been recorded from anywhere other than where nodules exist in relatively high densities within the permit area (Kudrass & von Rad 1984b, Dawson 1984).

## 5 Conclusions and Recommendations

Analysis of data from by the CRP Environmental Survey, the Chatham Rise Benthos (OS20/20) Survey, and the Chatham-Challenger (OS20/20) Survey provided for the identification of up to 13 epifauna communities on the central crest of the Chatham Rise. The structure, characterising taxa, and distribution of these communities was determined by statistical analysis, and suitable habitat for these communities in the study area was predicted by modelling. The environmental variables that explain the overall community structure and the distribution of the individual communities were also identified. The structure and distribution of some of the epifauna communities is related to the presence and distribution of phosphorite nodules.

Comparison of the benthic communities identified by this study and communities described from previous sampling on the Chatham Rise indicates that some epifauna communities within the mining permit area have not been found elsewhere on the rise, and maybe unique to the area. Two epifauna communities identified at the image-level, both of which show a patchy distribution almost only observed within CRP's mining permit area, are dominated by the stony coral *Goniocorella dumosa*. This coral relies upon hard substrate, such as that provided by relatively large nodules, for attachment. Similar corals, particularly when in high abundance, are known to provide habitat for a diverse community of other invertebrates and, potentially, larval or juvenile fish.

The coral *Goniocorella dumosa* is widely distributed in New Zealand waters, but has only previously been observed elsewhere at low densities of isolated colonies. The communities dominated by high abundance of *Goniocorella dumosa* identified here in the mining permit area have also not been recorded in previous surveys elsewhere; either on the Chatham Rise or at other locations in New Zealand waters. These communities satisfy the definition of a "coral thicket", and are considered to be "sensitive environments" under the regulations of the Continental Shelf and EEZ Environmental Effects Act. *Goniocorella dumosa* is also a protected species, as it belongs to the taxon Scleractinia – which is one of a group of deepwater corals afforded protection by the Wildlife Act.

However, habitat suitability modelling carried out during the present analysis predicts that all the identified epifauna communities could be more widespread within the study area, including the communities dominated by *Goniocorella dumosa*. Habitat suitability models predict a relatively large area that contains suitable habitat for *Goniocorella dumosa* and associated communities in the northwestern part of the study area. These predictions are largely driven by high values of SST gradient, that are indicative of a front in that part of study area and which extends into the mining permit area.

Information presented in this report, together with knowledge of the proposed nodule mining activities, can be used to help assess the implications of mining for benthic communities in the permit area, and to design measures to mitigate and monitor any environmental effects. However, confidence in using the habitat suitability models to design mitigation measures (i.e., identify no-mining or reserve areas) will depend upon the field validation of the models. This can be achieved by conducting additional targeted sampling using a towed camera, especially in the areas identified to be suitable habitat for *Goniocorella dumosa* dominated communities. Field validation for the stony coral dominated community models is particularly important because the relatively large area of predicted suitable habitat in the northwestern



part of the study area for these communities is in area that has been subject to bottom fishing (Appendix F).

## 6 Acknowledgements

Thanks are owed to the following people, institutions, and funders for their valuable and essential role in this project:

Malcolm Clark (NIWA) for his contribution to the design of the CRP Environmental survey.

The voyage leader of the CRP Environmental Survey Ray Wood (Geological and Nuclear Sciences, now Chatham Rock Phosphate Limited) and other members of the environmental survey team on-board the RV *Dorado Discovery*, including the ship's crew, ROV operators, and data managers and loggers. Particular thanks are owed to Emily Jones (Golders Associates Ltd) and Adrian Hellman (Odyssey Marine Explorations) for assisting with biological sampling during the survey, and Simon Nielsen (Kennex) for geological context setting.

The science team and officers and crew of the Chatham Rise Benthos (OS20/20) Survey (TAN1306), and Chatham-Challenger (OS20/2) Survey (TAN0705), and the funders of these surveys – the Ministry of Primary Industries (MPI) and Land Information New Zealand.

MPI for provision of bottom trawl data.

The taxonomic experts at NIWA that provided confirmatory identifications of the fauna observed in the seafloor images.

Julie Hall (NIWA) for managing the project efficiently and effectively.

Alison MacDiarmid (NIWA) for reviewing the report and providing constructive comment that improved the report.

Analysis of DTIS images from the Chatham Rise Benthos (OS20/20) Survey contributes to the MPI-funded project MPI13304.

## 7 References

- Anderson, M.J., Gorley, R.N., Clarke, K.R. (2008) PERMANOVA+ for PRIMER: guide to software and statistical methods. PRIMER-E, Plymouth.
- Anderson, M.J., Crist, T.O., Chase, J.M., Vellend, M., Inouye, B.D., Freestone, A.L., Sanders, N.J., Cornell, H.V., Comita, L.S., Davies, K.F., Harrison, S.P., Kraft, N.J.B., Stegen, J.C., Swenson, N.G. (2011) Navigating the multiple meanings of  $\beta$  diversity: a roadmap for the practicing ecologist. *Ecology Letters*, 14:19–28.
- Austin, M. (2007) Species distribution models and ecological theory: A critical assessment and some possible new approaches. *Ecological Modelling*, 200(1–2): 1–19.
- Baillon, S., Hamel, J-F., Wareham, V.E., Mercier, A. (2012) Deep cold-water corals as nurseries for fish larvae. *Frontiers in Ecology and the Environment*; doi:10.1890/120022.

- Beaumont, J., Baird, S. (2011) Biological and commercial fishing data within the Minerals Prospecting Licence 50270 area on the Chatham Rise. *NIWA Client Report No. WLG2011-10*: 36.
- Berkenbusch, K., Probert, P.K., Nodder, S.D. (2011) Comparative biomass of sediment benthos across a depth transect, Chatham Rise, Southwest Pacific Ocean. *Marine Ecology Progress Series*, 425: 79–90.
- Bowden, D.A. (2011) Benthic invertebrate samples and data from the Ocean Survey 20/20 voyages to Chatham Rise and Challenger Plateau, 2007. *Aquatic Environment and Biodiversity Report No. 65*, Ministry of Fisheries, Wellington, New Zealand.
- Buston, P.M., Elith, J. (2011) Determinants of reproductive success in dominant pairs of clownfish: a boosted regression tree analysis. *Journal of Animal Ecology*, 80(3): 528–538.
- Calinski, T., Harabasz, J. (1974) A dendrite method for cluster analysis. *Communications in Statistics*, 3:1–27.
- Clarke, K.R., Gorley, R.N. (2006) PRIMER v6: User Manual/Tutorial. PRIMER-E Ltd, Plymouth.
- Clarke, K.R., Warwick, R.M. (2001) Change in marine communities: an approach to statistical analysis and interpretation, 2<sup>nd</sup> edn. PRIMER-E Ltd, Plymouth.
- Clarke, K.R., Somerfield, P.J., Chapman, M.G. (2006) On resemblance measures for ecological studies, including taxonomic dissimilarities and a zero-adjusted Bray–Curtis coefficient for denuded assemblages. *Journal of Experimental Marine Biology and Ecology*, 330: 55–80.
- Clarke, K.R., Somerfield, P.J., Gorley, R.N. (2008) Testing of null hypotheses in exploratory community analyses: similarity profiles and biota-environment linkage. *Journal of Experimental Marine Biology and Ecology*, 366:56–69.
- Compton, T.J., Bowden, D.A., Pitcher, R., Hewitt, J.E., Ellis, N. (2013) Biophysical patterns in benthic assemblage composition across contrasting continental margins off New Zealand. *Journal of Biogeography*, 40: 75–89.
- Cullen, D.J. (1980) Distribution, composition and age of submarine phosphorites on Chatham Rise, East of New Zealand. *Society of Economic Paleontologists and Mineralogists Special Publication*, 29: 139–148.
- Dawson, E. (1984) The benthic fauna of the Chatham Rise: An assessment relative to possible effects of phosphorite mining. *Geologisches Jahrbuch*, D65: 209–231.
- Dell, R.K. (1951) A molluscan fauna from the Mernoo Bank, New Zealand. *New Zealand Journal of Science and Technology* B33 (1): 15–18.

- D'Onghia, G., Maiorano, P., Sion, L., Giove, A., Capezzuto, F., Carlucci, R., Tursi, A. (2010) Effects of deep-water coral banks on the abundance and size structure of the megafauna in the Mediterranean Sea. *Deep-Sea Research II*, 57: 397–411.
- Dutilleul, P., Stockwell, J.D., Frigon, D., Legendre, P. (2000) The Mantel test versus Pearson's correlation analysis: assessment of the differences for biological and environmental studies. *Journal of Agricultural, Biological, and Environmental Statistics*, 5:131–150.
- Elith, J., Graham, C.H., Anderson, R.P., Dudik, M., Ferrier, S., Guisan, A., Hijmans, R.J., Huettmann, F., Leathwick, J.R., Lehmann, A., Li, J., Lohmann, L.G., Loiselle, B.A., Manion, G., Moritz, C., Nakamura, M., Nakazawa, Y., Overton, J.M., Peterson, A.T., Phillips, S.J., Richardson, K., Scachetti-Pereira, R., Schapire, R.E., Soberon, J., Williams, S., Wisz, M.S., Zimmermann, N.E. (2006) Novel methods improve prediction of species' distributions from occurrence data. *Ecography*, 29(2): 129–151.
- Elith, J., Leathwick, J.R., Hastie, T. (2008) A working guide to boosted regression trees. *Journal of Animal Ecology*, 77(4): 802–813.
- Etter, R.J., Grassle, J.F. (1992) Patterns of species diversity in the deep sea as a function of sediment particle size diversity. *Nature*, 360: 576–578.
- Fawcett, T. (2006) An introduction to ROC analysis. *Pattern Recognition Letters*, 27(8): 861–874.
- Floerl, O., Hewitt, J., Bowden, D. (2012) Chatham-Challenger Ocean Survey 20/20 Post Voyage analyses: Objective 9 – Patterns in Species Composition. *New Zealand Aquatic Environment and Biodiversity Report No. 97*: 40.
- Friedman, J., Hastie, T., Tibshirani, R. (2000) Additive logistic regression: A statistical view of boosting. *Annals of Statistics*, 28(2): 337–374.
- Glasby, G.P., Wright, I.C. (1990) Marine mineral potential in New Zealand's Exclusive Economic Zone. *Marine Mining*, 9: 403–427.
- Grove, S.L., Probert, P.K., Berkenbusch, K., Nodder, S.D. (2006) Distribution of bathyal meiofauna in the region of the Subtropical Front, Chatham Rise, south-west Pacific. *Journal of Experimental Marine Biology and Ecology*, 330: 342–355.
- Guisan, A., Thuiller, W. (2005) Predicting species distribution: offering more than simple habitat models. *Ecology Letters*, 8(9): 993–1009.
- Henry, L-A., Roberts, J.M. (2007) Biodiversity and ecological composition of macrobenthos on cold-water coral mounds and adjacent off-mound habitat in the bathyal Porcupine Seabight, NE Atlantic. *Deep-Sea Research I*, 54: 654–672.
- Hewitt, J., Julian, K., Bone, E.K. (2011) Chatham-Challenger Ocean Survey 20/20 Post-Voyage Analyses: Objective 10 – Biotic habitats and their sensitivity to physical disturbance. *New Zealand Aquatic Environment and Biodiversity Report No. 81*: 36.

- Hijmans, R.J. (2010) Package raster. Available at: <http://cran.r-project.org/web/packages/raster/>, p.
- Hurley, D.E. (1961) The distribution of the isopod crustacean *Serolis bromleyana* Suhm with a discussion of an associated deepwater community. *New Zealand Oceanographic Institute Memoir*, 13: 225–233.
- Knox, M.A., Hogg, I.D., Pilditch, C.A., Lörz, A-N., Nodder, S.D. (2012) Abundance and diversity of epibenthic amphipods (Crustacea) from contrasting bathyal habitats. *Deep-Sea Research I*, 62:1–9.
- Kudrass, H-R., Cullen, D.J. (1980) Submarine phosphorite nodules from the central Chatham Rise off New Zealand – composition, distribution, and reserves – (Valdivia-Cruise 1978). *Geologisches Jahrbuch*, D51: 3–41.
- Kudrass, H-R., von Rad, U. (1984a) Geology and some mining aspects of the Chatham Rise phosphorite: a synthesis of SONNE-17 results. *Geologisches Jahrbuch*, D65: 233–252.
- Kudrass, H-R., Von Rad, U. (1984b). Underwater television and photography observations, side-scan sonar and acoustic reflectivity measurements of phosphorite-rich areas of the Chatham Rise (New Zealand). *Geologisches Jahrbuch*, D65: 69–89.
- Leathwick, J.R., Elith, J., Francis, M.P., Hastie, T., Taylor, P. (2006). Variation in demersal fish species richness in the oceans surrounding New Zealand: an analysis using boosted regression trees. *Marine Ecology-Progress Series*, 321: 267–281.
- Leathwick, J.R., Rowden, A.A., Nodder, S., Gorman, R., Bardsley, S., Pinkerton, M., Baird, S.J., Hadfield, M., Currie, K., Goh, A. (2012). A benthic-optimised marine environment (BOMECE) classification for New Zealand Waters. New Zealand Aquatic Environment and Biodiversity Report No. 88. 54p.
- Leduc, D., Rowden, A.A., Probert, P.K., Pilditch, C.A., Nodder, S., Bowden, D.A., Duineveld, G.C.A., Witbaard, R. (2012). Nematode beta diversity on the continental slope of New Zealand: spatial patterns and environmental drivers. *Marine Ecology Progress Series*, 545: 37–52.
- Legendre, P., Anderson, M.J. (1999) Distance-based redundancy analysis: testing multispecies hypotheses responses in multifactorial ecological experiments. *Ecological Monographs*, 69: 1–24.
- Legendre, P., Borcard, D., Peres-Neto, P.R. (2005) Beta diversity: partitioning the spatial variation of community composition data. *Ecological Monographs*, 75: 435–450.
- Lobo, J.M., Jiménez-Valverde, A., Real, R. (2008) AUC: a misleading measure of the performance of predictive distribution models. *Global Ecology and Biogeography*, 17(2): 145–151.

- Lörz, A-N. (2010) Biodiversity of an unknown New Zealand habitat: bathyal invertebrate assemblages in the benthic boundary layer. *Marine Biodiversity* DOI 10.1007/s12526-010-0064-x
- MacDiarmid, A., Bowden, D., Cummings, V., Morrison, M., Jones, E., Kelly, M., Neil, H., Nelson, W., Rowden, A. (2013) Sensitive marine benthic habitats defined. *NIWA Client Report*, prepared for Ministry for the Environment: 72.
- MacKay, K.A., Wood, B.A., Clark, M.R. (2005) Chatham Rise Bathymetry. *NIWA Miscellaneous Chart Series 82*. NIWA.
- McKnight, D.G., Probert, P.K. (1997) Epibenthic communities on the Chatham Rise, New Zealand. *New Zealand Journal of Marine and Freshwater Research*, 31: 505–513.
- Milligan, G.W., Cooper, M.C. (1985) An examination of procedures for determining the number of clusters in a data set. *Psychometrika*, 50: 159–179.
- Nodder, S.D. (2007) Ocean Survey 20/20 Chatham Rise and Challenger Plateau Hydrographic, Biodiversity and Seabed Habitats Project – Factual Voyage Report (2006/07 Season, Voyage 2). NIWA Client Report WLG2007-47, prepared for Land Information New Zealand (LINZ) and Ministry of Fisheries (MFish), Wellington (Contract No. OS2020-BS1), 66 pp.
- Nodder, S.D., Pilditch, C.A., Probert, P.K., Hall, J.A. (2003) Variability in benthic biomass and activity beneath the Subtropical Front, Chatham Rise, SW Pacific Ocean. *Deep-Sea Research I*, 50: 959–985.
- Nodder, S.D., Duineveld, G.C.A., Pilditch, C.A., Sutton, P.J., Probert, P.K., Lavaleye, M.S.S., Witbaard, R., Chang, F.H., Hall, J.A., Richardson, K.M. (2007) Physical focusing of phytodetritus deposition beneath a deep-ocean front, Chatham Rise, New Zealand. *Limnology and Oceanography*, 52: 299–314.
- Nodder, S., Pallentin, A., Mackay, K., Bowden, D. (2013) Seafloor morphology and substrate characterisation on Chatham Rise. *NIWA Client Report*, prepared for Chatham Rock Phosphate Ltd: 38.
- Norris, R.M. (1964) Sediments of Chatham Rise. *New Zealand Oceanographic Institute Memoir*, No. 26.
- Quinn, P.Q., Keough, M.J. (2009) *Experimental Design and Data Analysis for Biologists*, 1<sup>st</sup> edn. Cambridge University Press, Cambridge.
- Pasho, D.W. (1976) Distribution and morphology of Chatham Rise phosphorites. *Memoir of the New Zealand Oceanographic Institute*, 77: 27.
- Probert, P.K., McKnight, D.G. (1993) Biomass of bathyal macrobenthos in the region of the Subtropical Convergence, Chatham Rise, New Zealand. *Deep-Sea Research I*, 40: 1003–1007.



- Probert, P.K., Grove, S.L., McKnight, D.G., Read, G.B. (1996) Polychaete distribution on the Chatham Rise, Southwest Pacific. *Internationale Revue der Gesamten Hydrobiologie*, 81: 577–588.
- Probert, P.K., Glasby, C.J., Grove, S.L., Paavo, B.L. (2009) Bathyal polychaete assemblages in the region of the Subtropical Front, Chatham Rise, New Zealand. *New Zealand Journal of Marine and Freshwater Research*, 43: 1121–1135.
- von Rad & Kudrass (1987) Exploration and genesis of submarine phosphorite deposits from the Chatham Rise, New Zealand – a review. *In: Marine minerals advances in research and resource assessment*. ed. Teleki P et al. Dordrecht: Reidel, 157–175.
- R Development Core Team (2011) R: A language and environment for statistical computing. Vienna, Austria, R Foundation for Statistical Computing. p.
- Ridgeway, G. (2007) Generalized Boosted Regression Models. p.
- Rowden, A.A., Leduc, D., Torres, L., Bowden, D., Hart, A., Chin, C., Davey, N., Wright, J., Carter, M., Crocker, B., Halliday, J., Loerz, A-N., Read, G., Mills, S., Anderson, O., Neill, K., Kelly, M., Tracey, D., Kaiser, S., Gordon, D., Wilkins, S., Horn, P., Pallentin, A., Nodder, S., Mackay, K., Northcote, L. (2013) Benthic communities of MPL area 50270 on the Chatham Rise. *NIWA Client Report WLG2012-25*
- Schinner, G.O. (1993) Burrowing Behavior, Substratum Preference, and Distribution of *Schizaster canaliferus* (Echinoidea: Spatangoida) in the Northern Adriatic Sea. *Marine Ecology*, 14: 129–145.
- Snelder, T.H., Leathwick, J.R., Dey, K.L., Rowden, A.A., Weatherhead, M.A., Fenwick, G.D., Francis, M.P., Gorman, R.M., Grieve, J.M., Hadfield, M.G., Hewitt, J.E., Richardson, K.M., Uddstrom, M.J., Zeldis, J.R. (2006) Development of an ecological marine classification in the New Zealand region. *Environmental Management*, 39: 12-29.
- Snelgrove, P.V.R., Butman, C.A. (1994) Animal-sediment relationships revisited: cause versus effect. *Oceanography and Marine Biology Annual Review*, 32: 111–177.
- Sutton, P. (2001). Detailed structure of the Subtropical front over Chatham Rise, east of New Zealand. *Journal of Geophysical Research. C. Oceans*, 106(C12): 31,045–31,056.
- Swets, J.A. (1988) Measuring the accuracy of diagnostic systems. *Science*, 240: 1285–1293.
- Thiem, Ø., Ravagnan, E., Fosså, J.H., Bersten, J. (2006) Food supply mechanisms for coldwater corals along a continental shelf edge. *Journal of Marine Systems* 60:207–219.

- Tong, R., Purser, A., Unnithan, V., Guinan, J. (2012) Multivariate Statistical Analysis of Distribution of Deep-Water Gorgonian Corals in Relation to Seabed Topography on the Norwegian Margin. *PLoS ONE*, 7(8): e43534. doi:10.1371/journal.pone.0043534.
- Torres, L.G., Smith, T.D., Sutton, P., MacDiarmid, A., Bannister, J., Miyashita, T. (2013) From exploitation to conservation: habitat models using whaling data predict distribution patterns and threat exposure of an endangered whale. *Diversity and Distributions*: n/a-n/a. <<http://dx.doi.org/10.1111/ddi.12069>>
- Tracey, D.M., Rowden, A.A., Mackay, K.A., Compton, T. (2011) Habitat-forming cold-water corals show affinity for seamounts in the New Zealand region. *Marine Ecology Progress Series*, 430: 1–22.
- Tuck, I., Hartill, B., Parkinson, D., Smith, M., Armiger, H., Rush, N., Drury, J. (2011) Estimating the abundance of scampi, *Metanephrops challengeri*, from photographic surveys in SCI 3 (2009 & 2010). *NIWA Final Research Report*, prepared for Ministry of Fisheries: 29.

## Appendix A Epifauna taxa identified from seafloor images

| Phylum        | Class        | Order            | Family                    | Genus                  | Taxon name                                |
|---------------|--------------|------------------|---------------------------|------------------------|---|
| Annelida      | Polychaeta   | Eunicida         | Onuphidae                 | <i>Hyalinoecia</i>     | Quill worm (Onuphidae)                    |
| Arthropoda    | Malacostraca | Decapoda         | Goneplacidae              | <i>Pycnoplax</i>       | <i>Pycnoplax victoriensis</i>             |
| Arthropoda    | Malacostraca | Decapoda         | Majidae                   | -                      | Majidae                                   |
| Arthropoda    | Malacostraca | Decapoda         | Polychelidae              | -                      | Polychelidae                              |
| Arthropoda    | Malacostraca | Decapoda         | Atelecyclidae             | <i>Trichopeltarion</i> | <i>Trichopeltarion fantasticum</i>        |
| Arthropoda    | Malacostraca | Decapoda         | Galatheidae/Chyrostylidae |                        | Galatheidae/Chyrostylidae                 |
| Arthropoda    | Malacostraca | Decapoda         | Nephropidae               | <i>Metanephrops</i>    | <i>Metanephrops challengeri</i>           |
| Arthropoda    | Malacostraca | Decapoda         | Paguridae                 | -                      | Pagurid                                   |
| Brachiopoda   | -            | -                | -                         | -                      | Brachiopoda                               |
| Bryozoa       | Gymnolaemata | Cheilostomatida  | Bitectiporidae            | <i>Bitectipora</i>     | <i>Bitectipora retepora</i>               |
| Bryozoa       | Gymnolaemata | Cheilostomatida  | Celleporidae              | <i>Celleporina</i>     | <i>Celleporina grandis</i>                |
| Cnidaria      | Anthozoa     | Actiniaria       | -                         | -                      | Actinaria/Ceriantharia spp                |
| Cnidaria      | Anthozoa     | Alcyonacea       | Alcyoniidae               | <i>Anthomastus</i>     | <i>Anthomastus</i> sp.                    |
| Cnidaria      | Anthozoa     | Alcyonacea       | Alcyoniidae               | -                      | Alcyoniidae                               |
| Cnidaria      | Anthozoa     | Alcyonacea       | Isididae                  | -                      | Isididae                                  |
| Cnidaria      | Anthozoa     | Alcyonacea       | Primnoidae                | -                      | Primnoidae                                |
| Cnidaria      | Anthozoa     | Antipatharia     | Leiopathidae              | <i>Leiopathes</i>      | <i>Leiopathes</i>                         |
| Cnidaria      | Anthozoa     | Corallimorpharia | -                         | -                      | Corallimorpharia 2                        |
| Cnidaria      | Anthozoa     | Scleractinia     | Caryophylliidae           | <i>Goniocorella</i>    | <i>Goniocorella dumosa</i>                |
| Cnidaria      | Anthozoa     | Scleractinia     | Caryophylliidae           | <i>Stephanocyathus</i> | cup corals ( <i>Stephanocyathus</i> spp.) |
| Cnidaria      | Anthozoa     | Scleractinia     | Caryophylliidae           | -                      | cup corals (stalked)                      |
| Cnidaria      | Anthozoa     | Scleractinia     | Flabellidae               | <i>Flabellum</i>       | <i>Flabellum</i>                          |
| Cnidaria      | Hydrozoa     | Anthoathecatae   | Stylasteridae             | <i>Calyptopora</i>     | <i>Calyptopora</i> spp                    |
| Cnidaria      | Hydrozoa     | Anthoathecatae   | Stylasteridae             | <i>Lepidotheca</i>     | <i>Lepidotheca</i> spp                    |
| Echinodermata | Asteroidea   | Brisingida       | Brisingidae               | -                      | Brisingidae                               |
| Echinodermata | Asteroidea   | Forcipulatida    | Asteriidae                | <i>Sclerasterias</i>   | <i>Sclerasterias mollis</i>               |

| Phylum        | Class         | Order   | Family                          | Genus                            | Taxon name                            |
|---------------|---------------|---|---------------------------------|----------------------------------|---------------------------------------|
| Echinodermata | Asteroidea    | Forcipulatida                                   | Zoroasteridae/Asteriidae        |                                  | Zoroasteridae/Asteriidae              |
| Echinodermata | Asteroidea    | Notomyotida                                     | Benthopectinidae                | <i>Benthopecten</i>              | <i>Benthopecten</i> sp                |
| Echinodermata | Asteroidea    | Paxillosida                                     | Astropectinidae                 | <i>Dipsacaster</i>               | <i>Dipsacaster magnificus</i>         |
| Echinodermata | Asteroidea    | Paxillosida                                     | Astropectinidae                 | <i>Dipsacaster</i>               | <i>Dipsacaster</i> sp                 |
| Echinodermata | Asteroidea    | Paxillosida                                     | Astropectinidae                 | <i>Plutonaster/Dytaster</i>      | <i>Plutonaster/Dytaster</i>           |
| Echinodermata | Asteroidea    | Paxillosida                                     | Astropectinidae                 | -                                | Astromesites/Psilaster/Proserpinaster |
| Echinodermata | Asteroidea    | Paxillosida                                     | Astropectinidae                 | -                                | Astropectinidae                       |
| Echinodermata | Asteroidea    | Spinulosida                                     | Echinasteridae                  | -                                | Echinasteridae                        |
| Echinodermata | Asteroidea    | Spinulosida                                     | Pterasteridae                   | -                                | Pterasteridae                         |
| Echinodermata | Asteroidea    | Spinulosida                                     | Solasteridae                    | <i>Solaster</i>                  | <i>Solaster torulatus</i>             |
| Echinodermata | Asteroidea    | Valvatida                                       | Goniasteridae                   | <i>Lithosoma</i>                 | <i>Lithosoma novazealandiae</i>       |
| Echinodermata | Asteroidea    | Valvatida                                       | Goniasteridae                   | <i>Mediaster</i>                 | <i>Mediaster</i> sp                   |
| Echinodermata | Asteroidea    | Valvatida                                       | Goniasteridae                   | <i>Plinthaster/Ceramaster</i>    | <i>Plinthaster/Ceramaster</i>         |
| Echinodermata | Asteroidea    | Valvatida                                       | Odontasteridae                  | <i>Odontaster</i>                | <i>Odontaster benhami</i>             |
| Echinodermata | Echinoidea    | Camarodonta/<br>Spatangoida/<br>Echinothurioida | Echinidae/Spatangidae           | <i>Gracilechinus/Paramaretia</i> | Irregular urchins                     |
| Echinodermata | Echinoidea    | Cidaroida                                       | Cidaridae                       | <i>Goniocidaris</i>              | <i>Goniocidaris</i> spp               |
| Echinodermata | Echinoidea    | Echinoidea                                      | Echinidae                       | <i>Dermechinus</i>               | <i>Dermechinus horridus</i>           |
| Echinodermata | Echinoidea    | Echinoidea                                      | Echinidae                       | -                                | Echinidae                             |
| Echinodermata | Echinoidea    | Echinoidea                                      | -                               | -                                | Echinoidea                            |
| Echinodermata | Echinoidea    | Echinothurioida                                 | Echinothuriidae/Phormosomatidae |                                  | Echinothuriidae/<br>Phormosomatidae   |
| Echinodermata | Echinoidea    | Pedinoida                                       | Pedinidae                       | <i>Caenopedina</i>               | <i>Caenopedina</i> spp                |
| Echinodermata | Echinoidea    | Temnopleuroidea                                 | Temnopleuridae                  | <i>Pseudechinus</i>              | <i>Pseudechinus flemingi</i>          |
| Echinodermata | Holothuroidea | Aspidochirotida                                 | Synallactidae                   | <i>Bathyplores</i>               | <i>Bathyplores moseleyi</i>           |
| Echinodermata | Holothuroidea | Elasipoda                                       | -                               | -                                | Elasipoda                             |
| Echinodermata | Holothuroidea | Elasipodida                                     | Laetmogonidae                   | <i>Laetmogone</i>                | <i>Laetmogone</i> sp                  |
| Echinodermata | Holothuroidea | Dendrochirotida                                 | Psolidae                        | <i>Psolus</i>                    | <i>Psolus</i>                         |

| Phylum   | Class          | Order             | Family                | Genus                        | Taxon name  |
|----------|----------------|-------------------|-----------------------|------------------------------|---|
| Mollusca | Gastropoda     | Archaeogastropoda | Callostomatidae       | -                            | Callostomatidae   |
| Mollusca | Gastropoda     | Neogastropoda     | Buccinidae            | <i>Austrofusus</i>           | <i>Austrofusus glans</i>  |
| Mollusca | Gastropoda     | Neogastropoda     | Buccinidae            | <i>Penion</i>                | <i>Penion</i> sp  |
| Mollusca | Gastropoda     | Neogastropoda     | Buccinidae            | -                            | Buccinidae  |
| Mollusca | Gastropoda     | Neogastropoda     | Olividae              | -                            | Olividae  |
| Mollusca | Gastropoda     | Neotaenioglossa   | Ranellidae            | <i>Fusitriton</i>            | <i>Fusitriton magellanicus</i>                                      |
| Mollusca | Gastropoda     | -                 | -                     | -                            | Gastropoda  |
| Multiple | -              | -                 | -                     | -                            | unID Branching<br>(bryozoan/hydroid/other)                          |
| Multiple | -              | -                 | -                     | -                            | unID Encrusting organism<br>(bryozoan/sponge/ascidian)              |
| Porifera | Demospongiae   | Astrophorida      | Pachastrellidae       | -                            | Pachastrellidae   |
| Porifera | Demospongiae   | Astrophorida      | Vulcanellidae         | <i>Poecillastra</i>          | <i>Poecillastra laminaris</i>                                       |
| Porifera | Demospongiae   | Astrophorida      | -                     | -                            | Black astrophorid   |
| Porifera | Demospongiae   | Hadromerida       | Suberitidae           | <i>Suberites</i>             | <i>Suberites</i> n. spp.  |
| Porifera | Demospongiae   | Hadromerida       | Polymastiidae         | <i>Tentorium</i>             | <i>Tentorium papillatum</i>   |
| Porifera | Demospongiae   | Halichondrida     | Axinella/Pararaphoxya |                              | Axinella or Pararaphoxya  |
| Porifera | Demospongiae   | Lithistida        | Corallistidae         | <i>Awhiowhio</i>             | <i>Awhiowhio sepulchrum</i>   |
| Porifera | Demospongiae   | Poecilosclerida   | Coelosphaeridae       | -                            | Coelosphaeridae Lissodendoryx<br>(Ectyodoryx) n. sp 1?              |
| Porifera | Demospongiae   | Poecilosclerida   | Hymedesmiidae         | <i>Hymedesmia (Stylopus)</i> | <i>Hymedesmia (Stylopus)</i> n. sp. 1                               |
| Porifera | Demospongiae   | Poecilosclerida   | Dendoricellidae       | <i>Pyloderma</i>             | <i>Pyloderma demonstrans</i>  |
| Porifera | Demospongiae   | -                 | -                     | -                            | Sponges (demo)  |
| Porifera | Haxactinellida | Hexactinosida     | Aphrocallistidae      | <i>Aphrocallistes</i>        | Aphrocallistes  |
| Porifera | Hexactinellida | Amphidiscosida    | Pheronematidae        | <i>Sericolophus</i>          | <i>Sericolophus</i> n. sp. (big, flabby<br>convoluted, Kermadecs ?) |
| Porifera | Hexactinellida | Lyssacinosida     | Rossellidae           | <i>Hyalascus</i>             | <i>Hyalascus</i> n. sp  |
| Porifera | Hexactinellida | Lyssacinosida     | Rossellidae           | <i>Hyalsacus</i>             | <i>Hyalascus</i> n sp. 1  |
| Porifera | Hexactinellida | -                 | -                     | -                            | Sponges (hexact)  |



## Appendix B Displaying predicted habitat suitability

Maps of predicted habitat suitability for benthic communities in the study area were made using a two-standard deviation 'stretch' colour scale to highlight areas that contain a greater proportion of pixels of relatively high habitat suitability. Figure B-1 shows a portion of the predicted habitat suitability map for epifauna (image-level) Community *h* identified in Rowden et al. (2013) (i.e., not Community *h* of this study). In this map, the red pixels delineate an area (the central patch) where pixels of relatively high habitat suitability are more likely to be found than in areas delineated by blue pixels. This figure also shows where seafloor images were located, from which data were used to identify epifauna communities and to generate habitat suitability models for the epifauna communities described by Rowden et al. (2013).

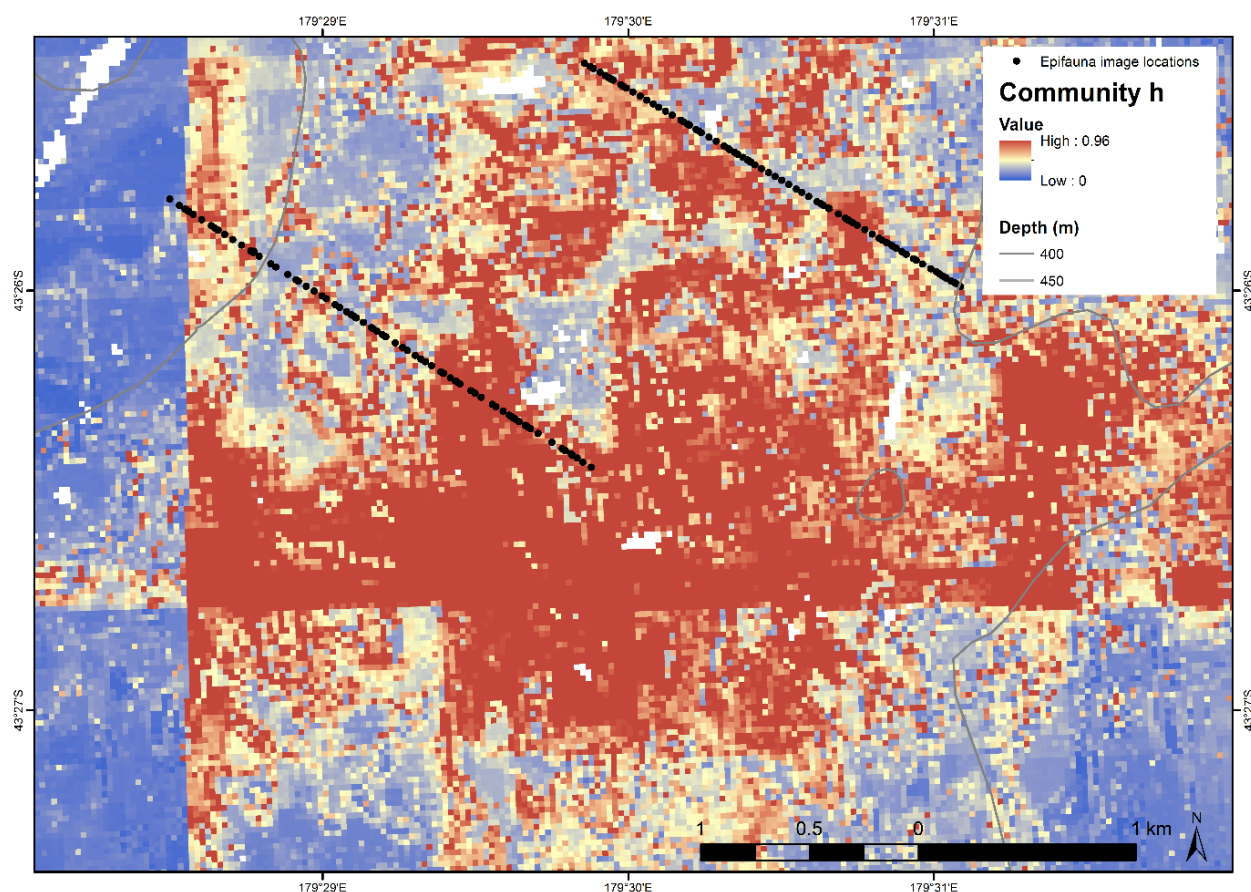


**Figure B-1: Predicted habitat suitability for epifauna Community *h* (image-level) (Rowden et al. (2013) in a portion of the study area illustrated using a two-standard deviation 'stretch' scale. [also shown are the locations of seafloor images where epifauna were observed]**

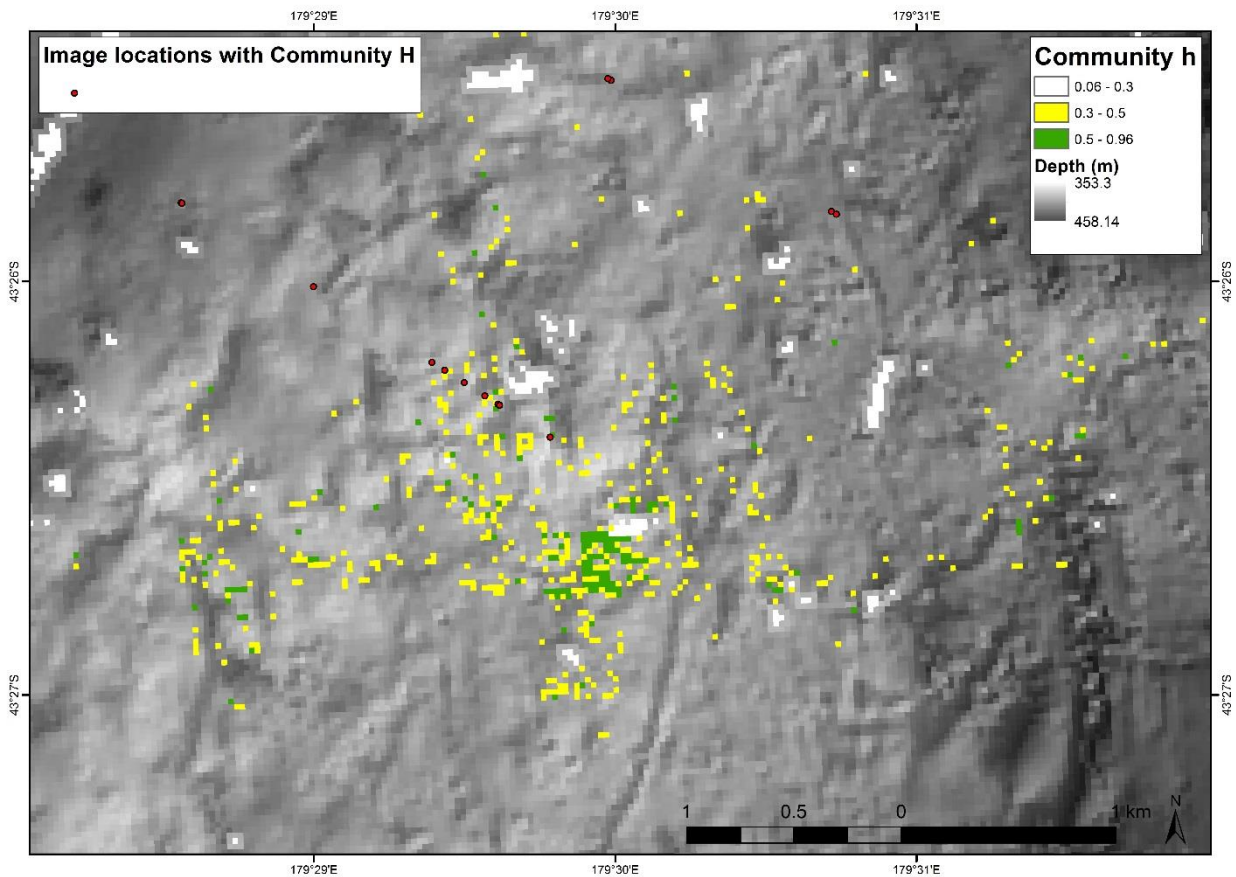


**Figure B-2: Predicted habitat suitability for epifauna Community *h* (image-level) (Rowden et al. 2013) in the study area illustrated using a three class scale (values <0.06 are not shown) overlain on a bathymetric terrain model. [also shown are the locations where Community *h* was directly observed in seafloor images]**

Figure B-2 illustrates the same spatial area as Figure B-1 but with habitat suitability classed into three groups. This figure shows that pixels of habitat suitability >0.5 (i.e., a pixel is more likely to be suitable habitat than not) are concentrated towards the centre of the red patch (of Figure B-1), but are also dispersed across the entire area delineated by the red patch using the 'stretch' scale. Furthermore this figure shows that Community *h* was directly observed at locations where the predicted habitat suitability, within the red patch, was generally <0.3.

Overall, these two figures provide an example which shows that: (1) the colour scale method adopted to illustrate the habitat suitability models in this report is useful for identifying general areas where locations of relatively high habitat suitability can be found (e.g., an area of ~15 km<sup>2</sup> in the northeastern part of the study area of Rowden et al. 2013); (2) that within these areas, habitat of relatively high habitat suitability may be restricted to small patches (e.g., < 0.01 km<sup>2</sup>), but these numerous small patches may be distributed widely across the larger general area (e.g., 25m –400m apart); and (3) communities can occur at locations within the general area that are predicted to have relatively low habitat suitability (e.g., <0.3). Together these two figures provide an indication of the likelihood of encountering a particular community if mining occurs (depending on the scale of mining) within the general areas of suitable habitat (i.e., the red patches on the model output maps).

## Appendix C Gridded layers for environmental variables

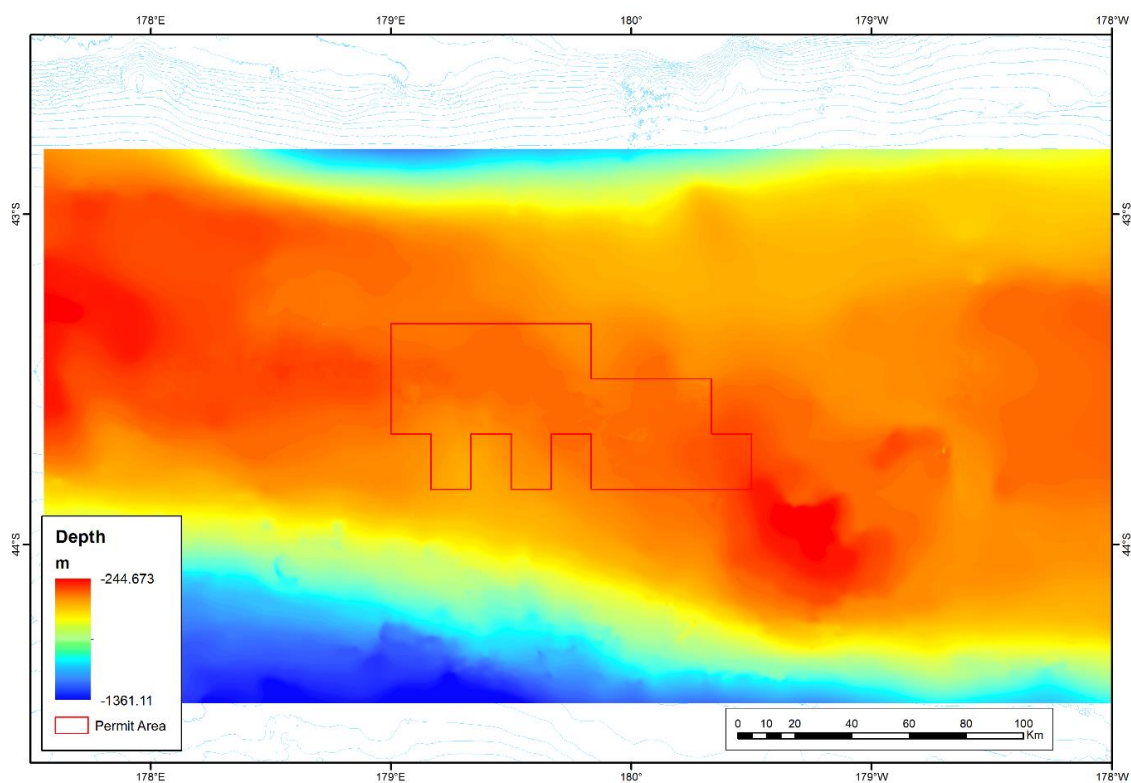


Figure C-1: Water depth

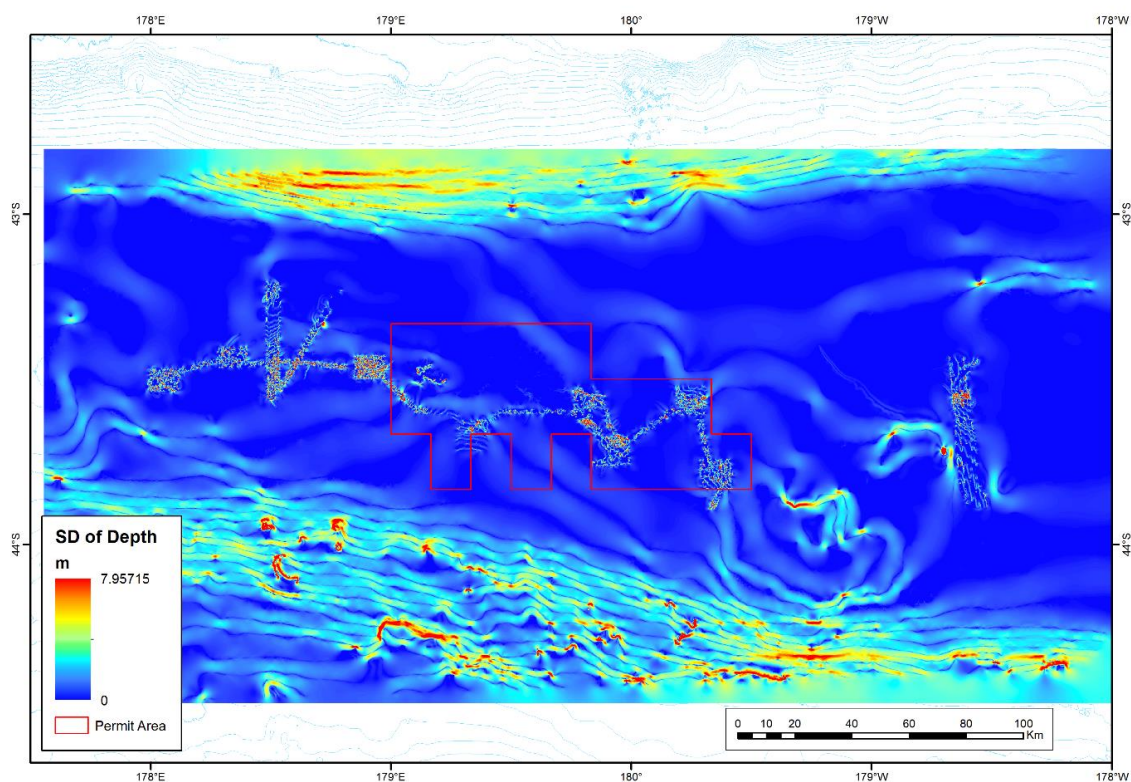
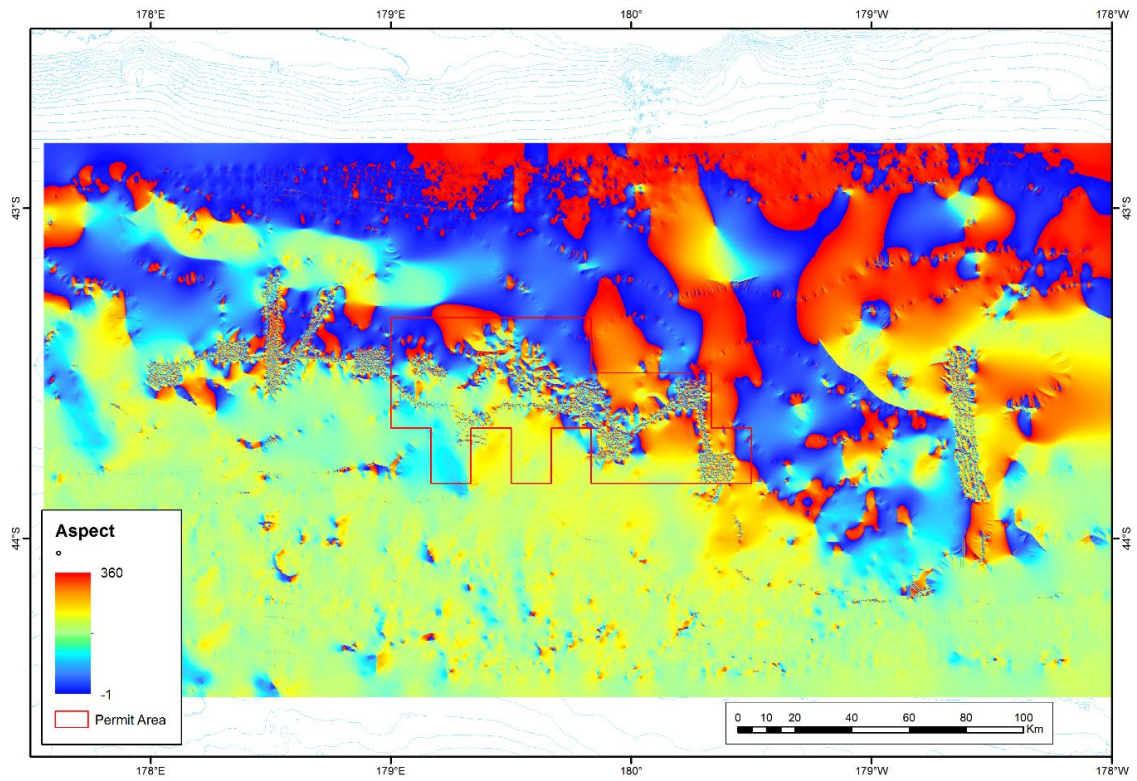
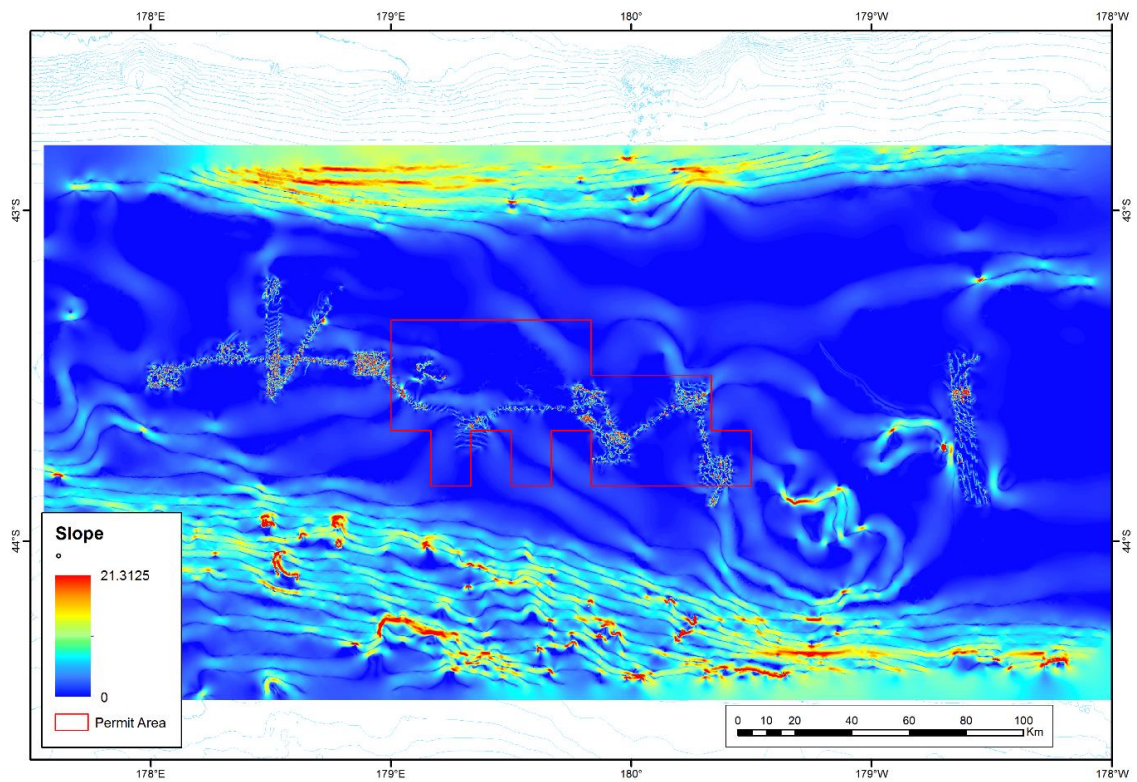


Figure C-2: Standard deviation of water depth





**Figure C-3: Seafloor aspect**



**Figure C-4: Seafloor slope**

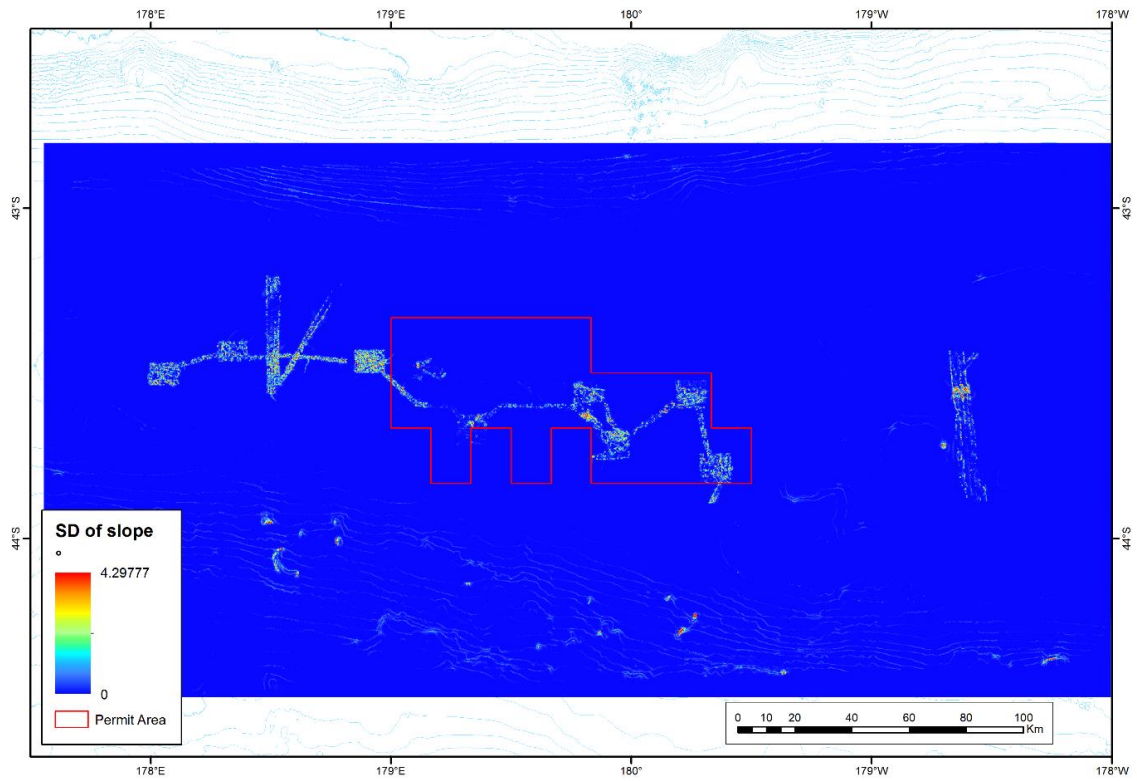


Figure C-5: Standard deviation of seafloor slope

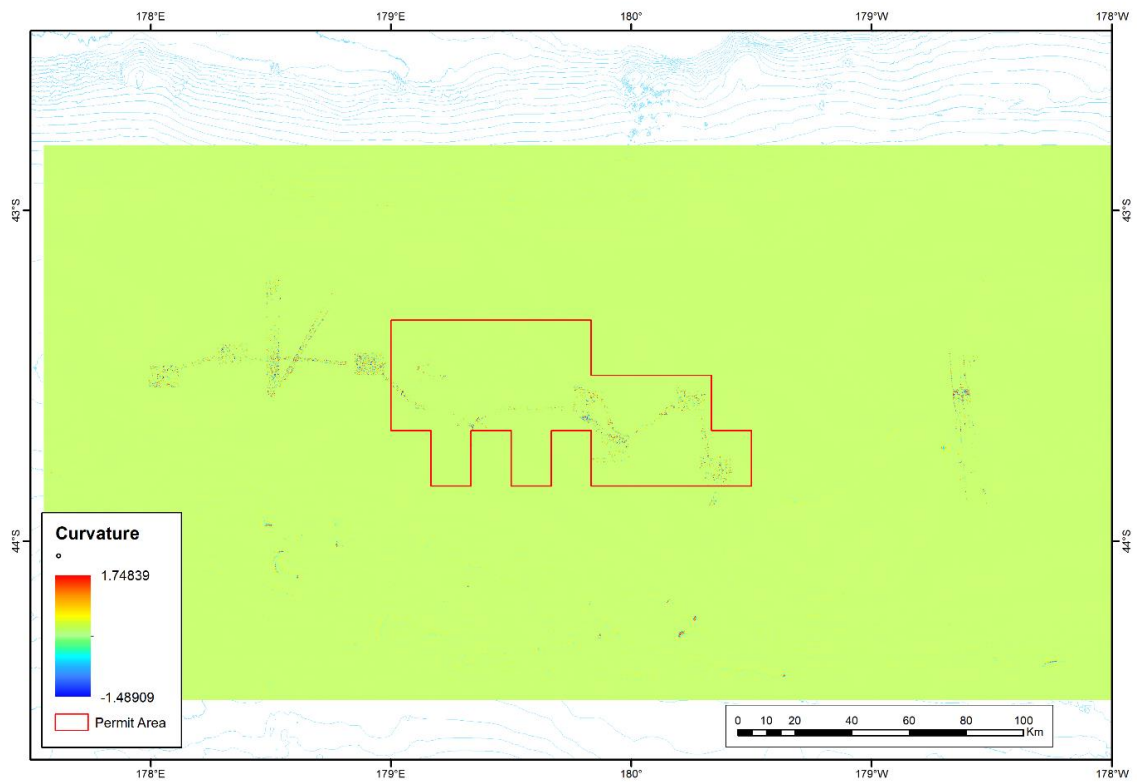
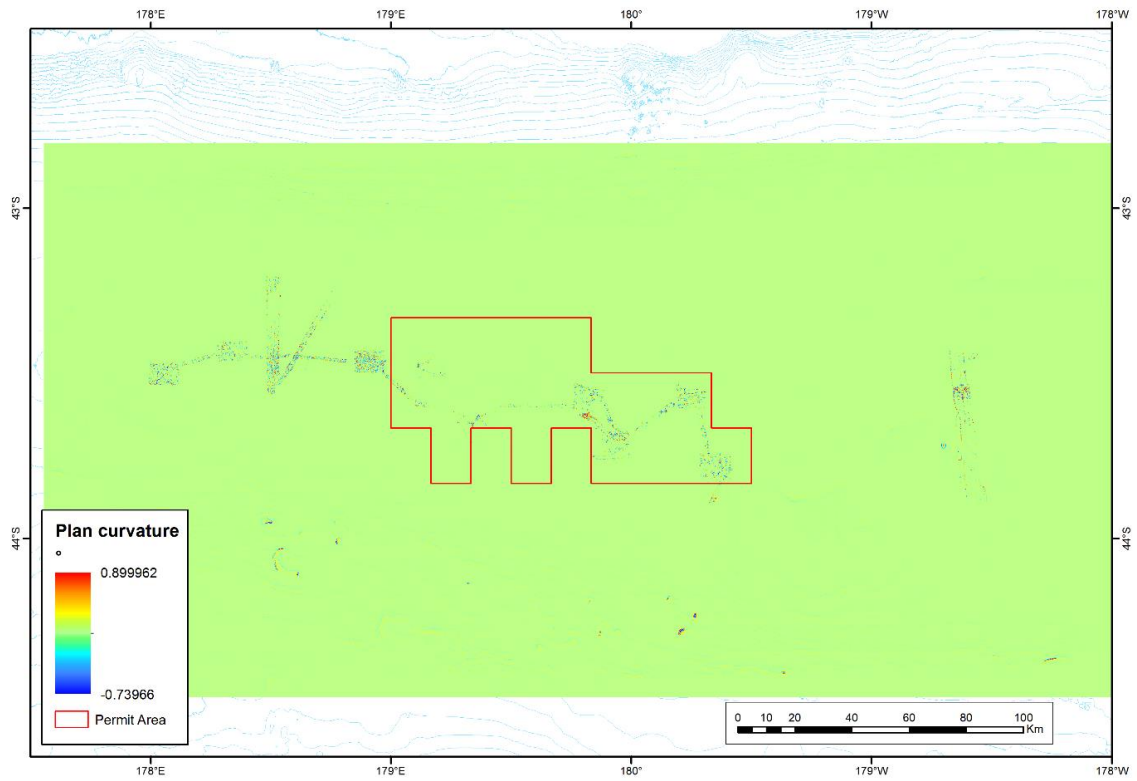
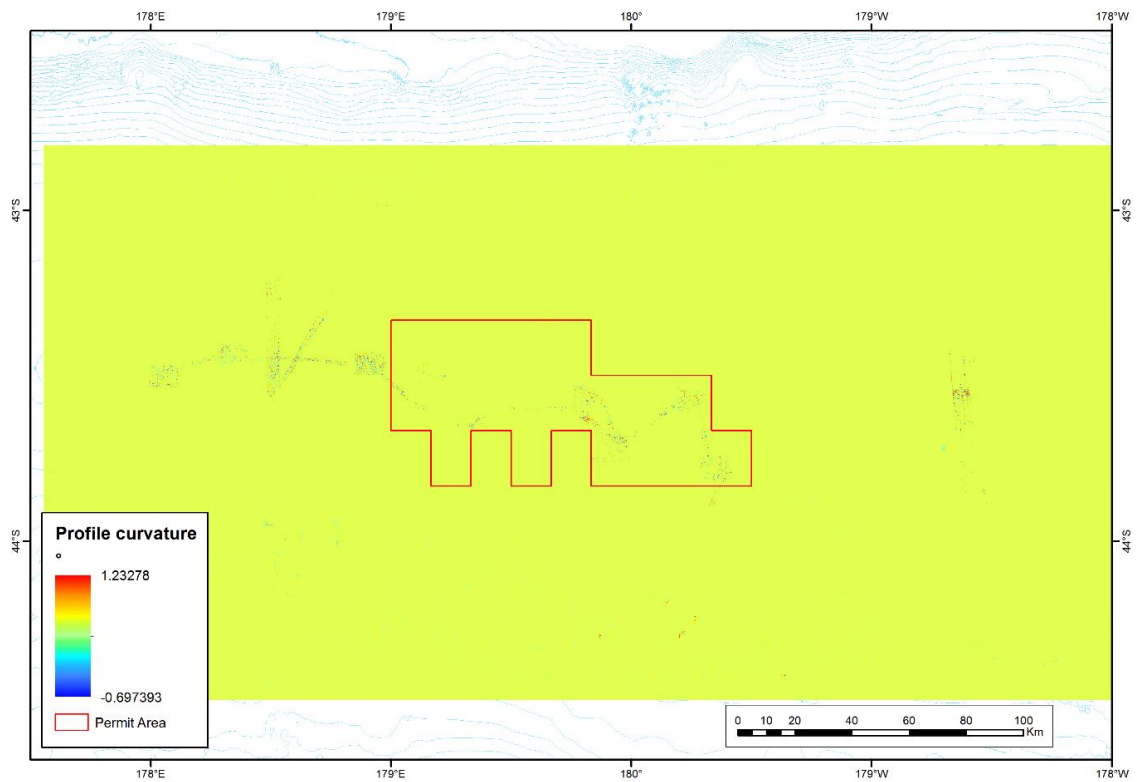


Figure C-6: Seafloor curvature





**Figure C-7: Seafloor plan curvature**



**Figure C-8: Seafloor profile curvature**

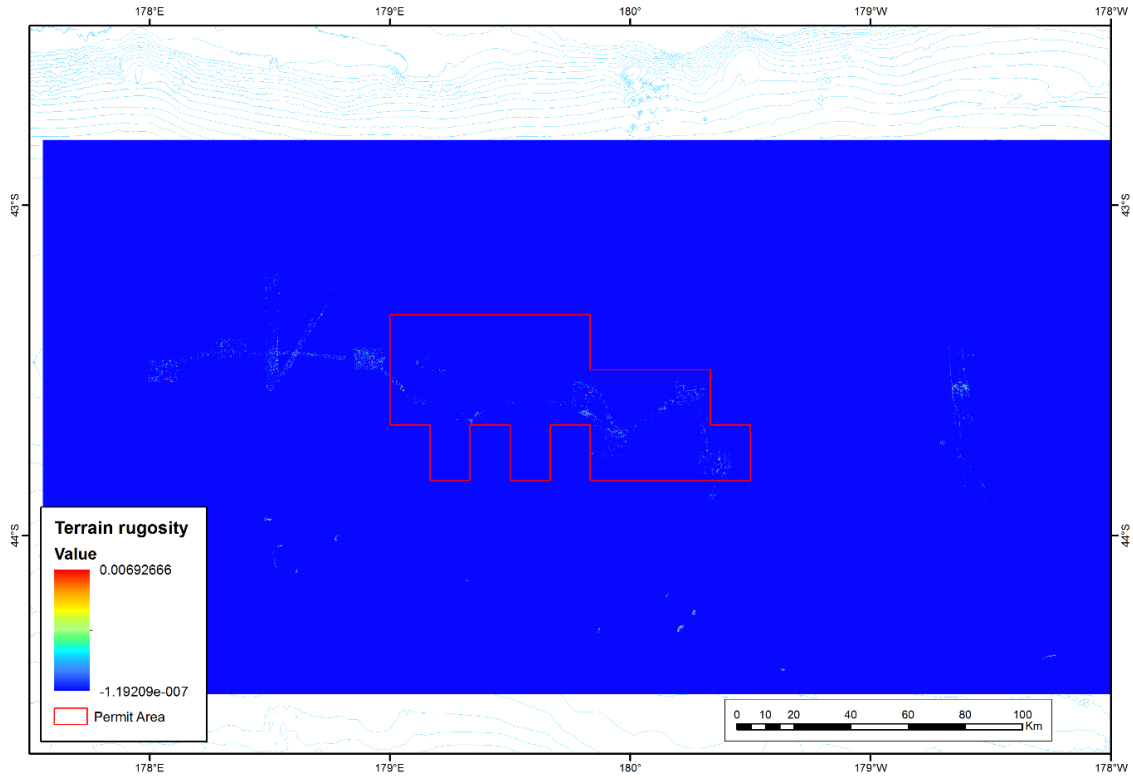


Figure C-9: Seafloor rugosity

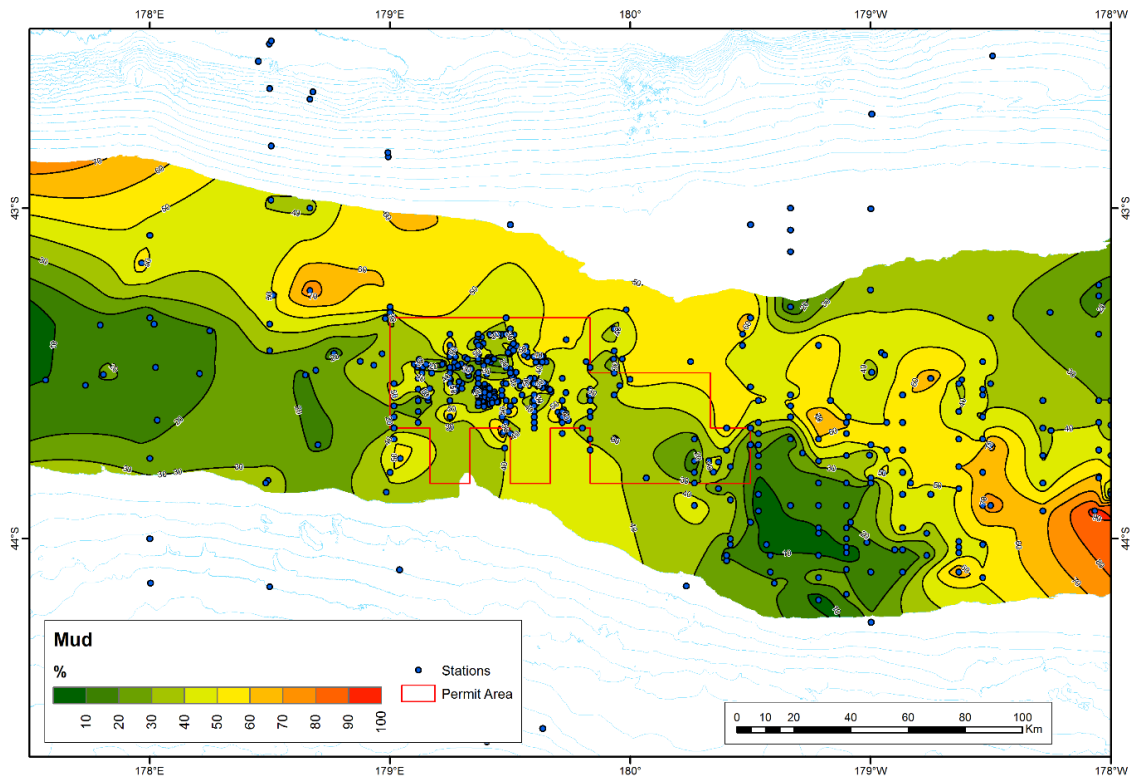


Figure C-10: Mud content of seafloor substratum

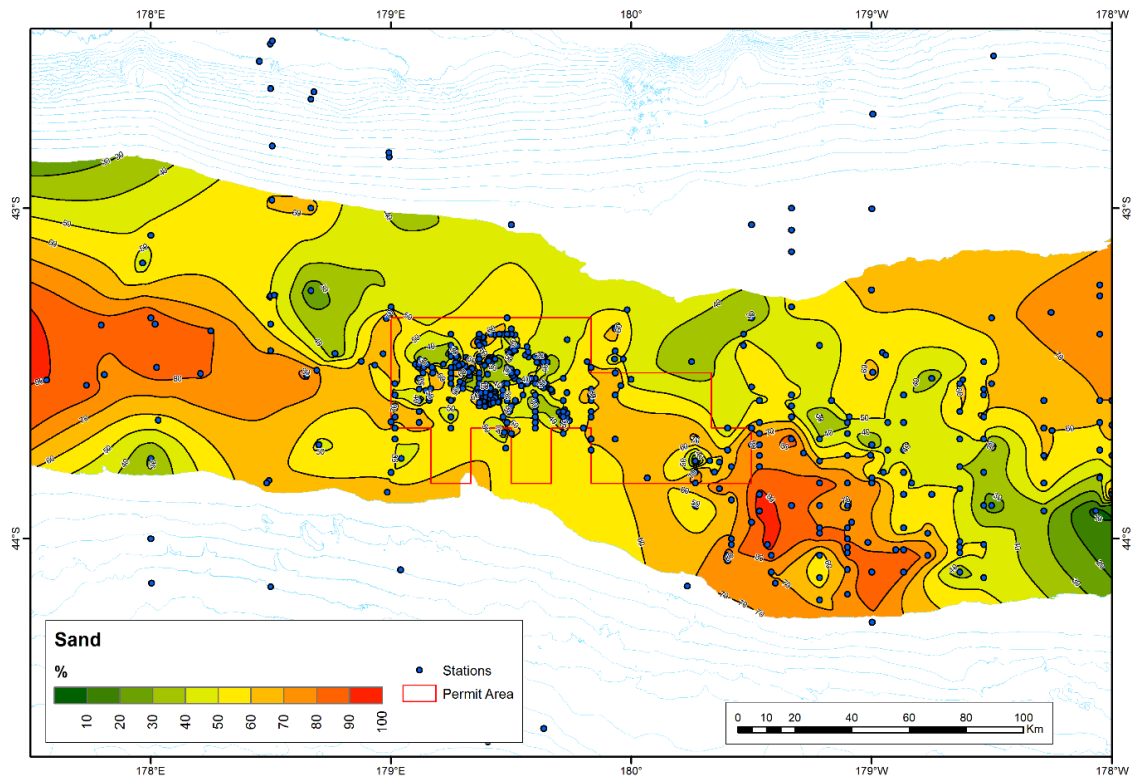


Figure C-11: Sand content of seafloor substratum

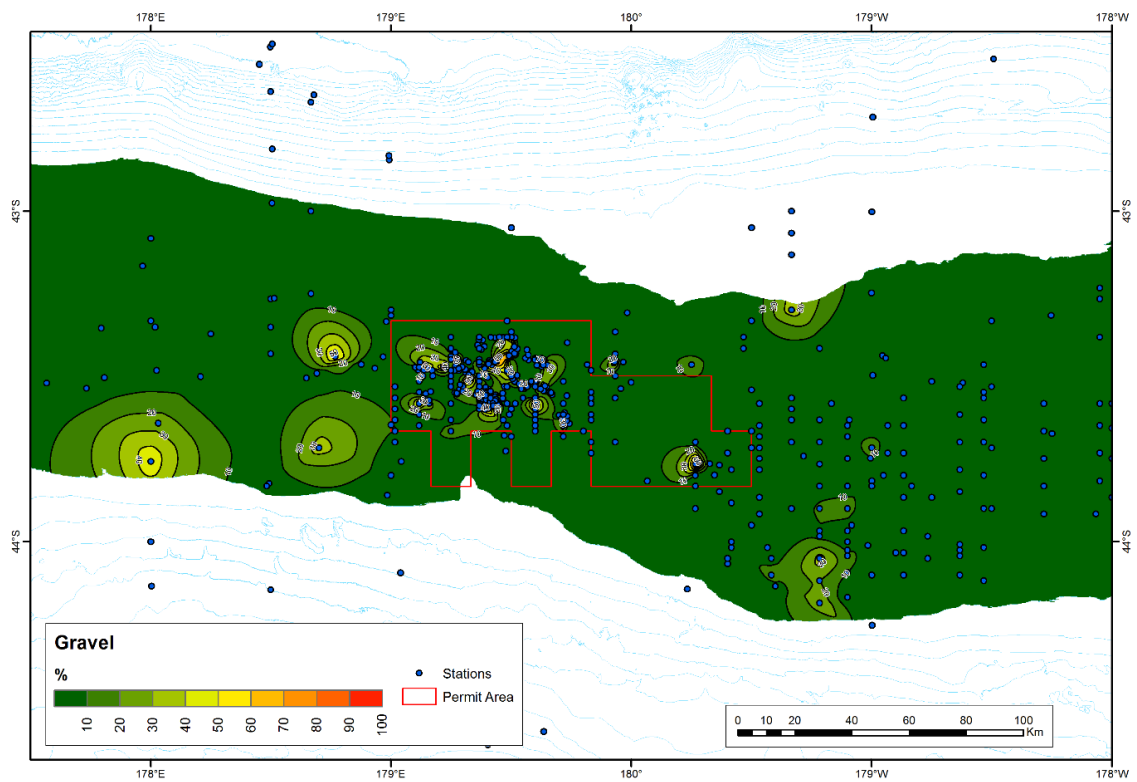
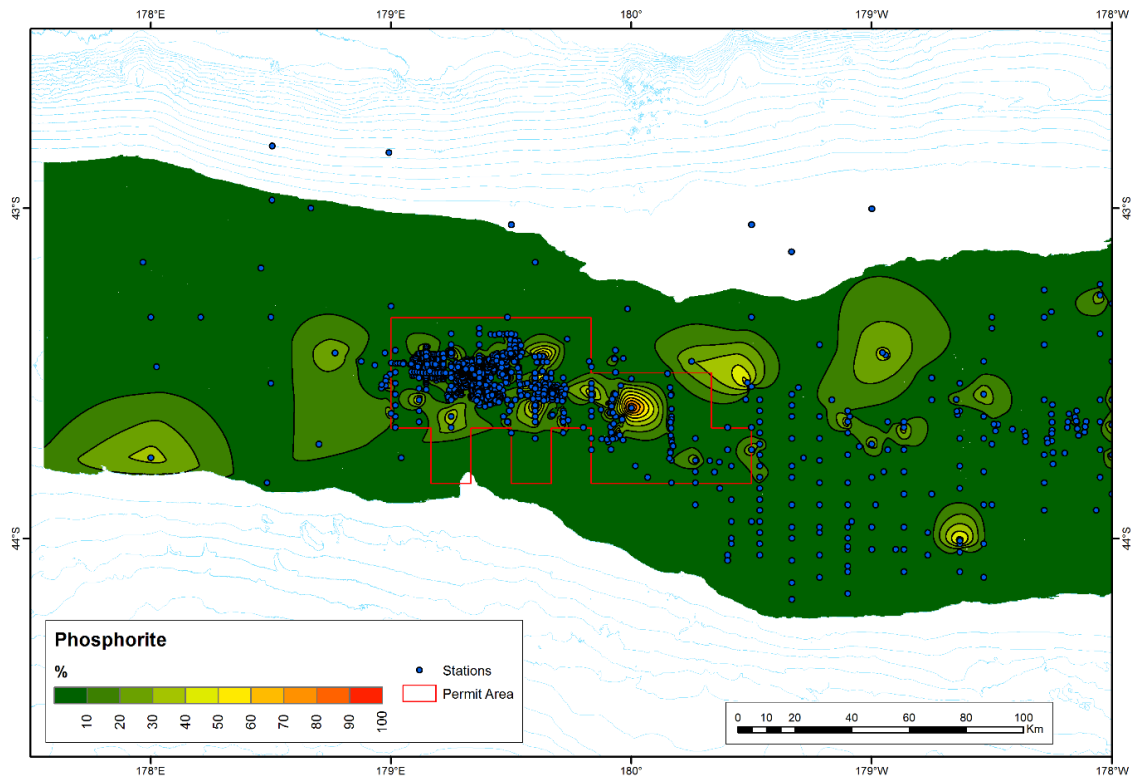
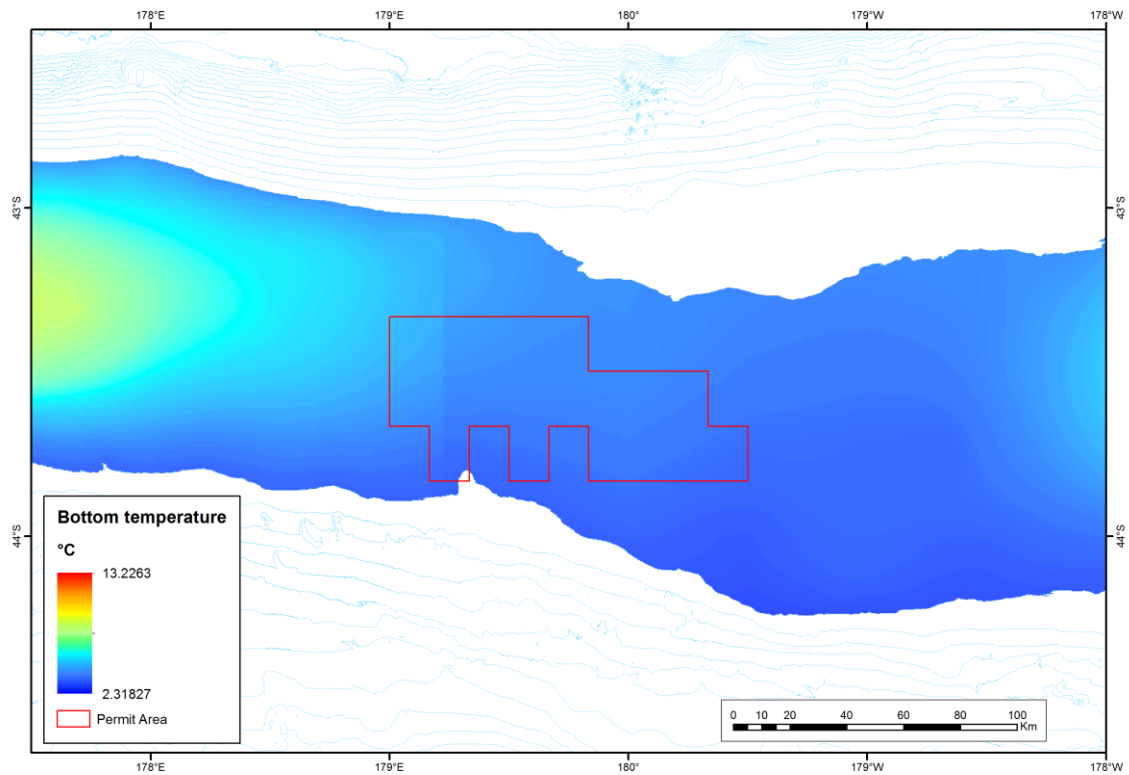


Figure C-12: Gravel content of the seafloor substratum



**Figure C-13: Phosphorite nodule content of the seafloor substratum**



**Figure C-14: Bottom temperature**

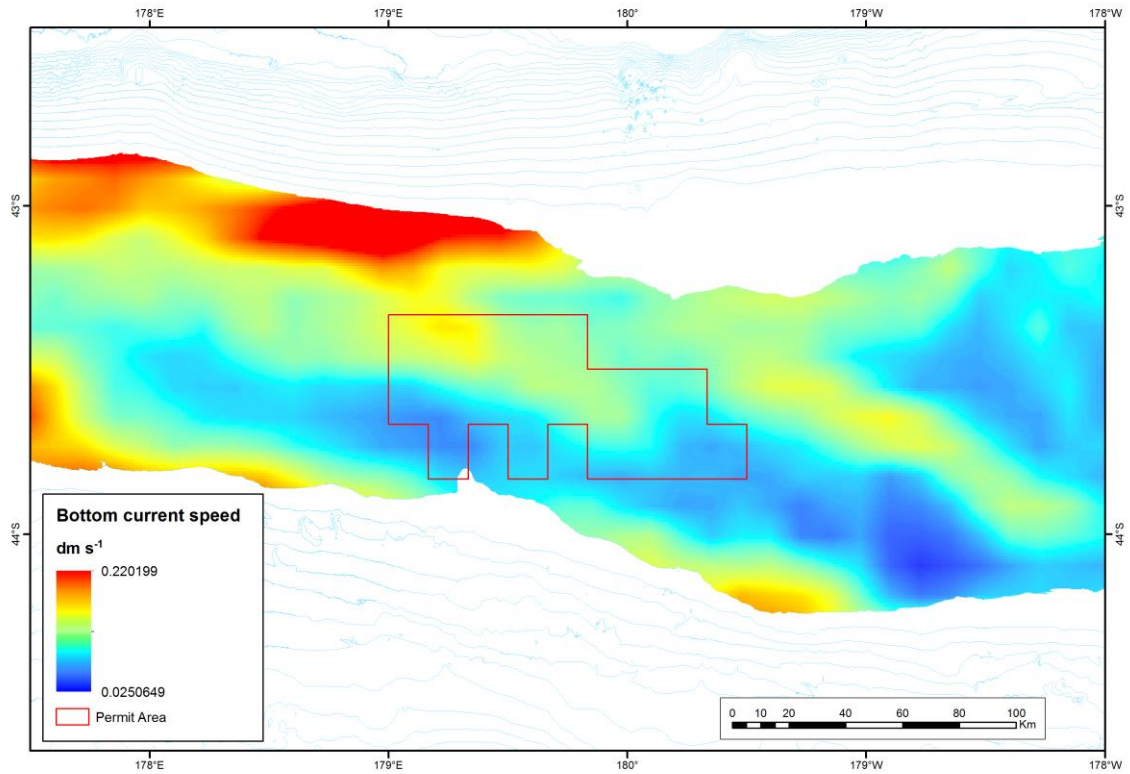


**Figure C-15: Bottom current speed**

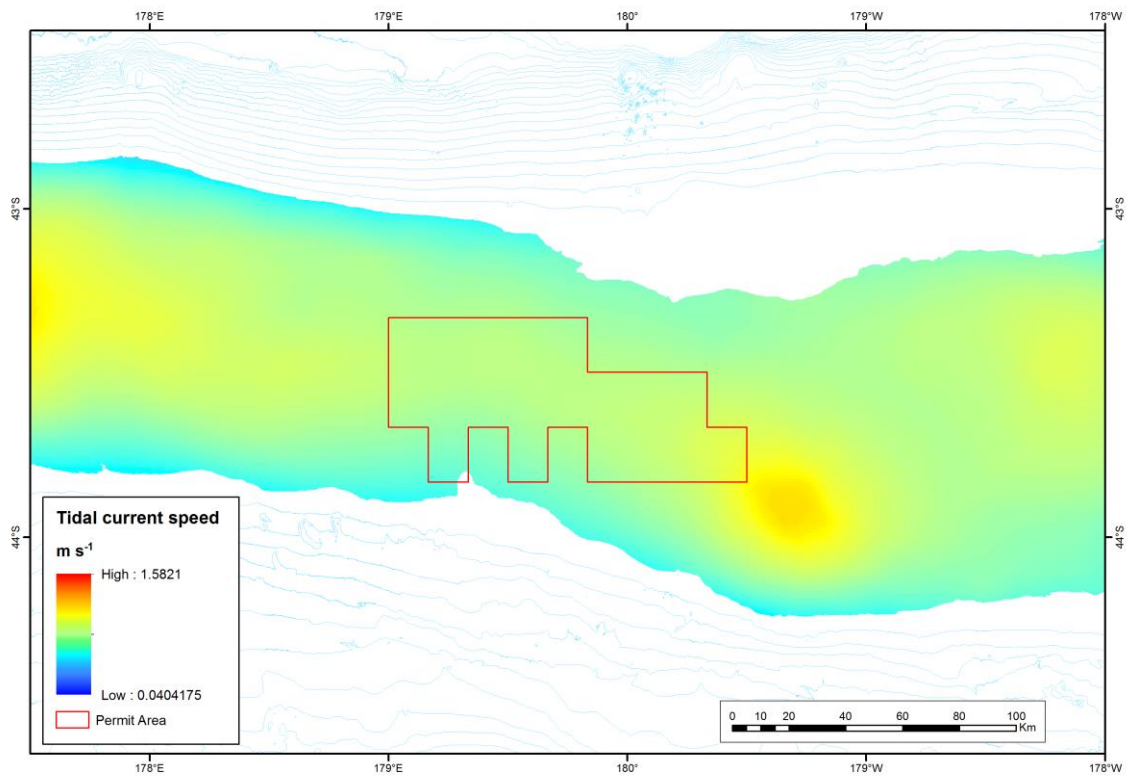


**Figure C-16: Tidal current speed**



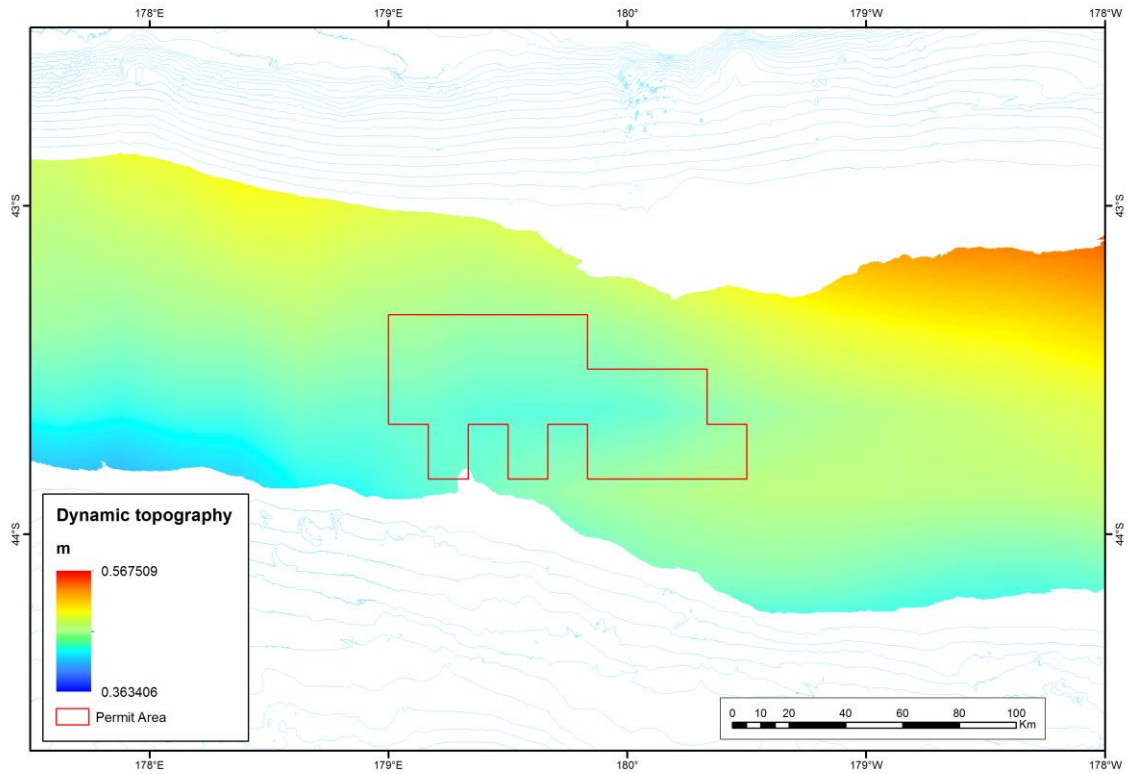


Figure C-17: Dynamic topography

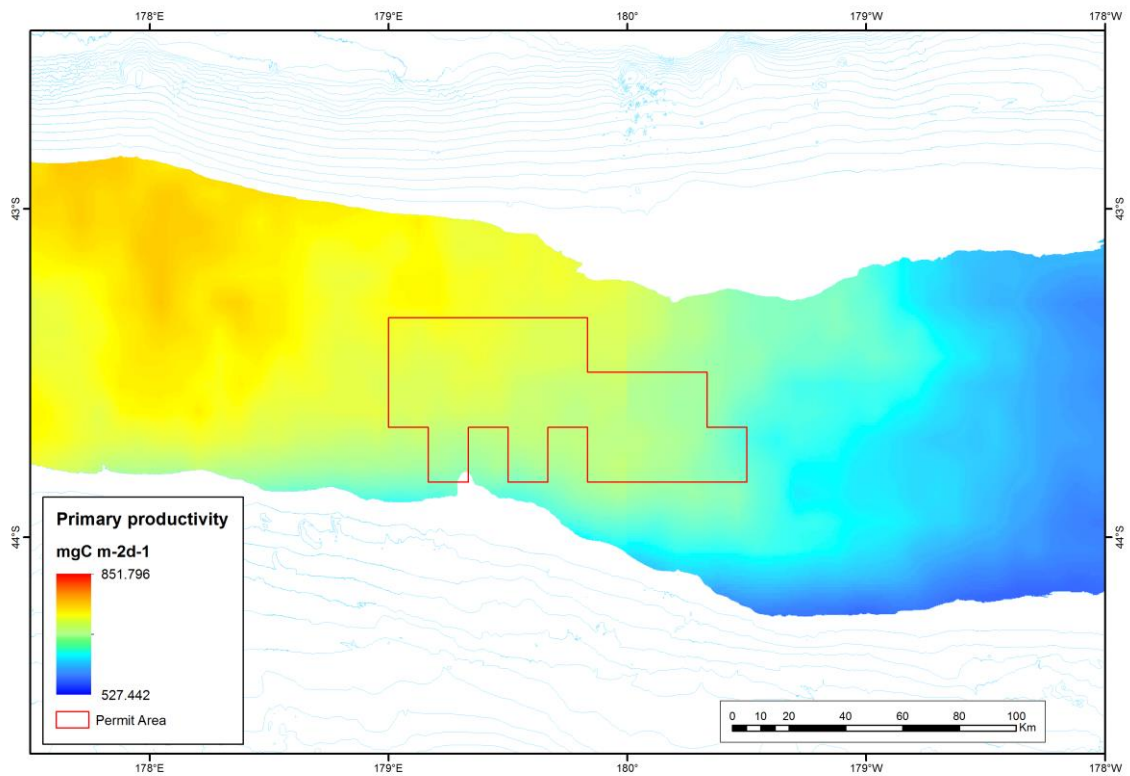
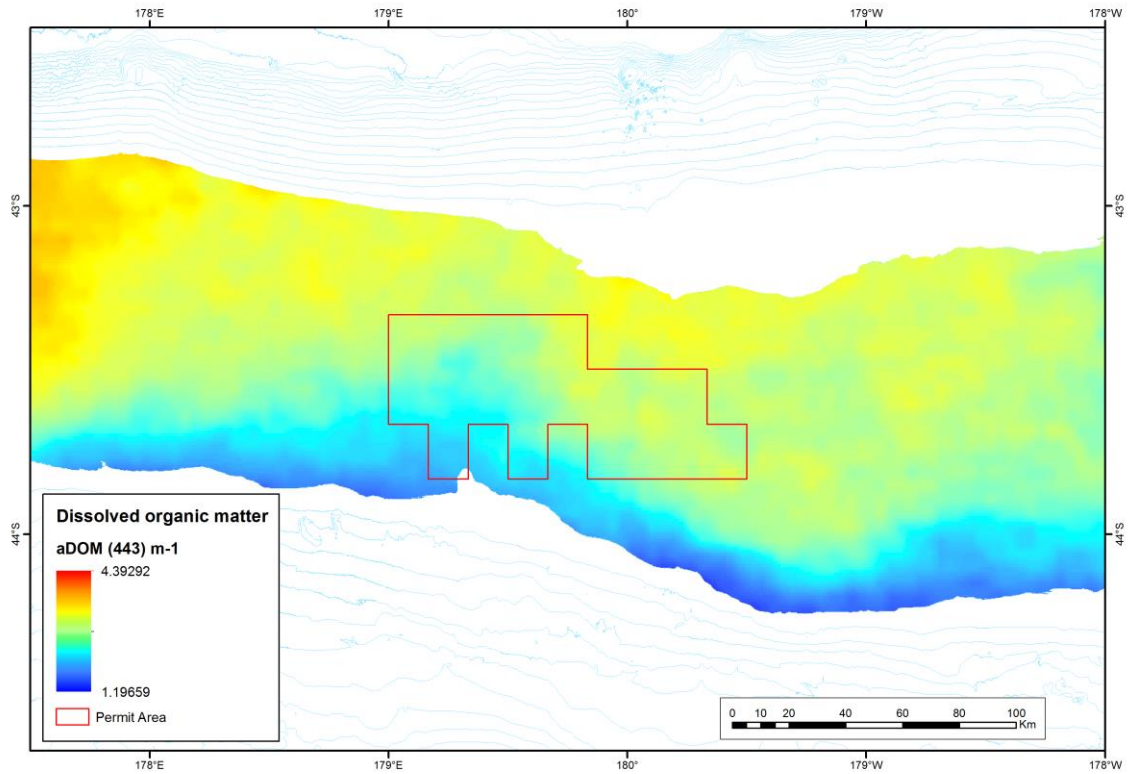
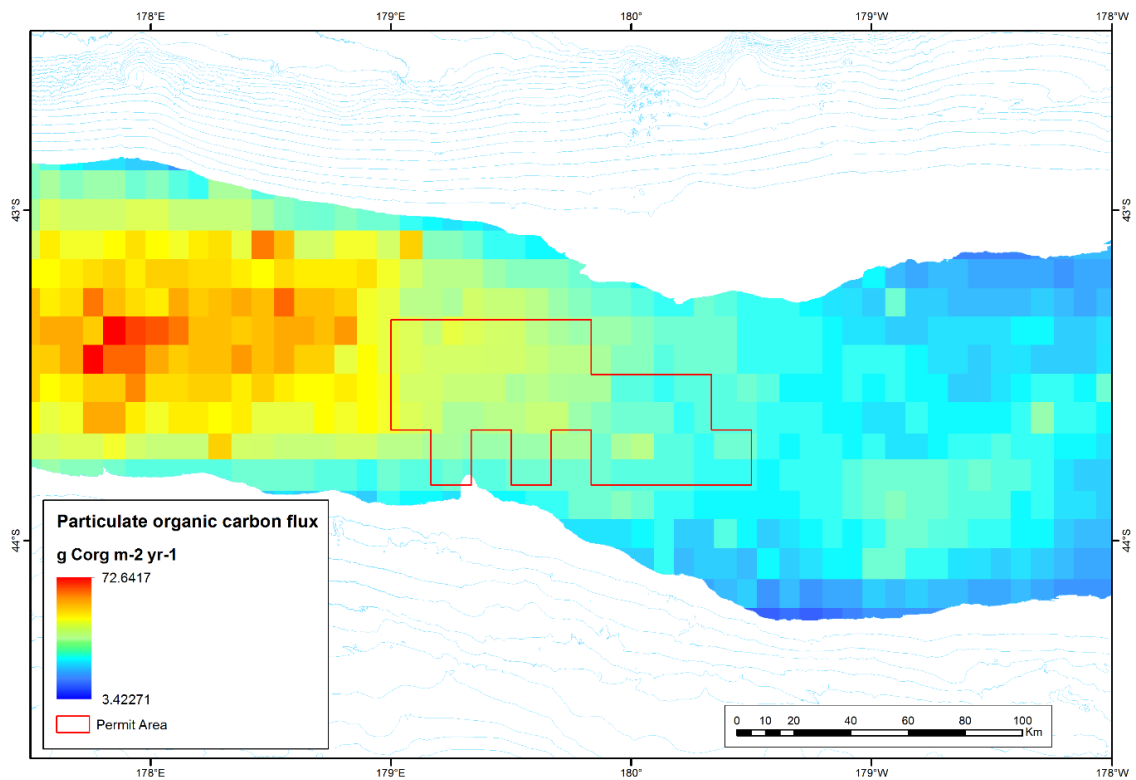


Figure C-18: Primary productivity



**Figure C-19: Dissolved organic matter**



**Figure C-20: Particulate organic carbon flux**

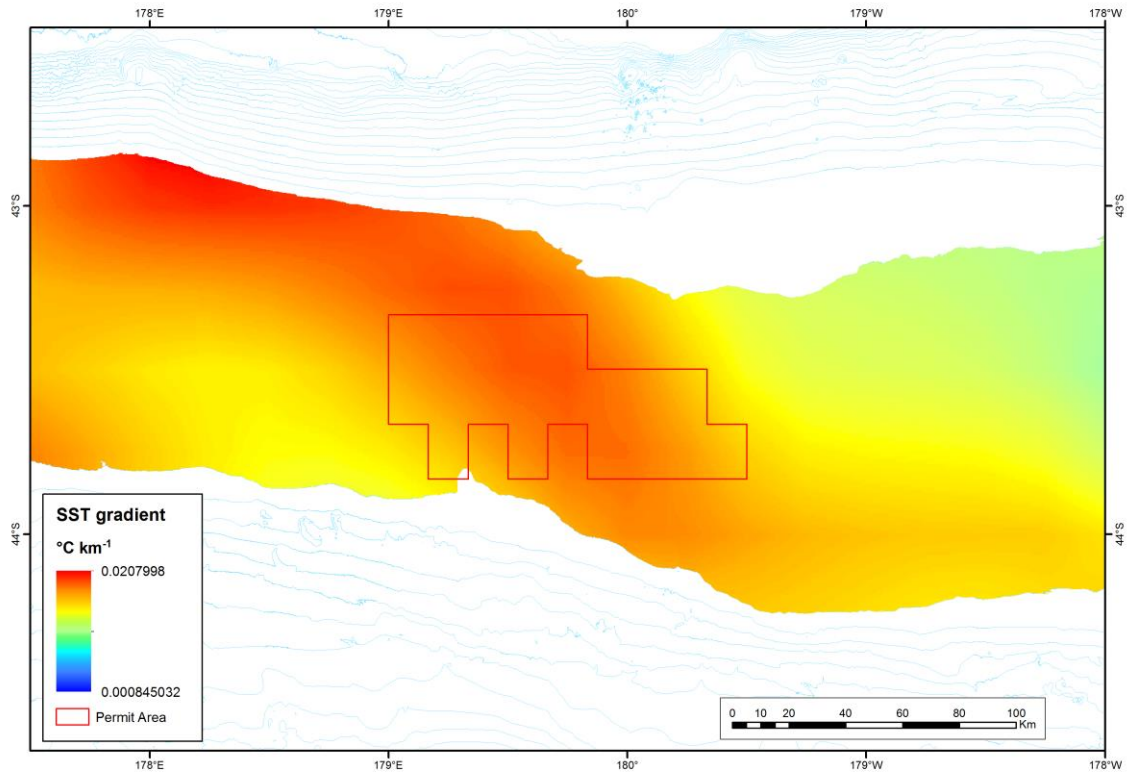


**Figure C-21: Sea surface temperature gradient**



# Appendix D Maps of survey areas showing distribution of epifauna communities (image-level) on ROV/DTIS transects

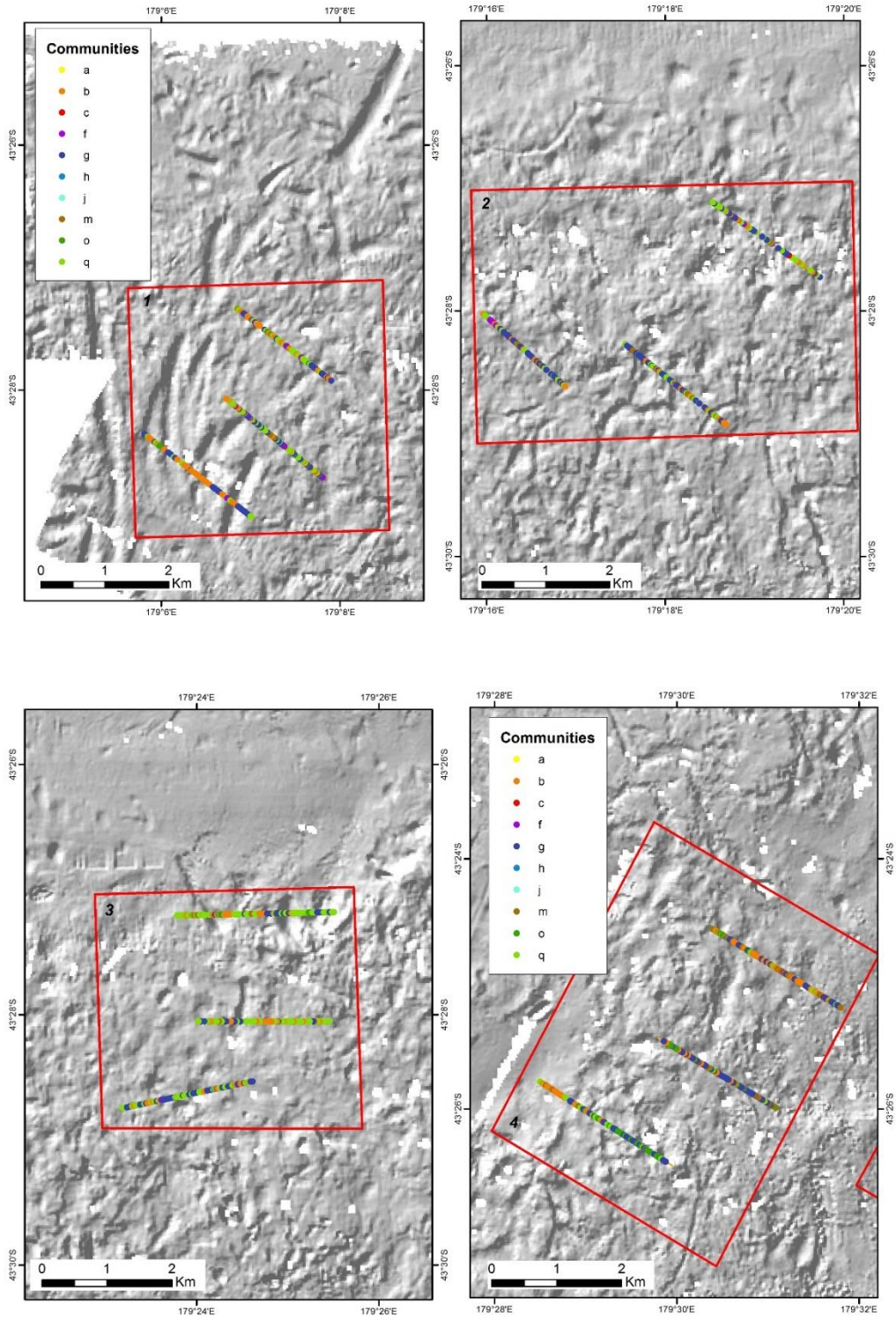


Figure D-1: Epifauna communities (image level) for CRP Environmental Survey areas 1- 4.

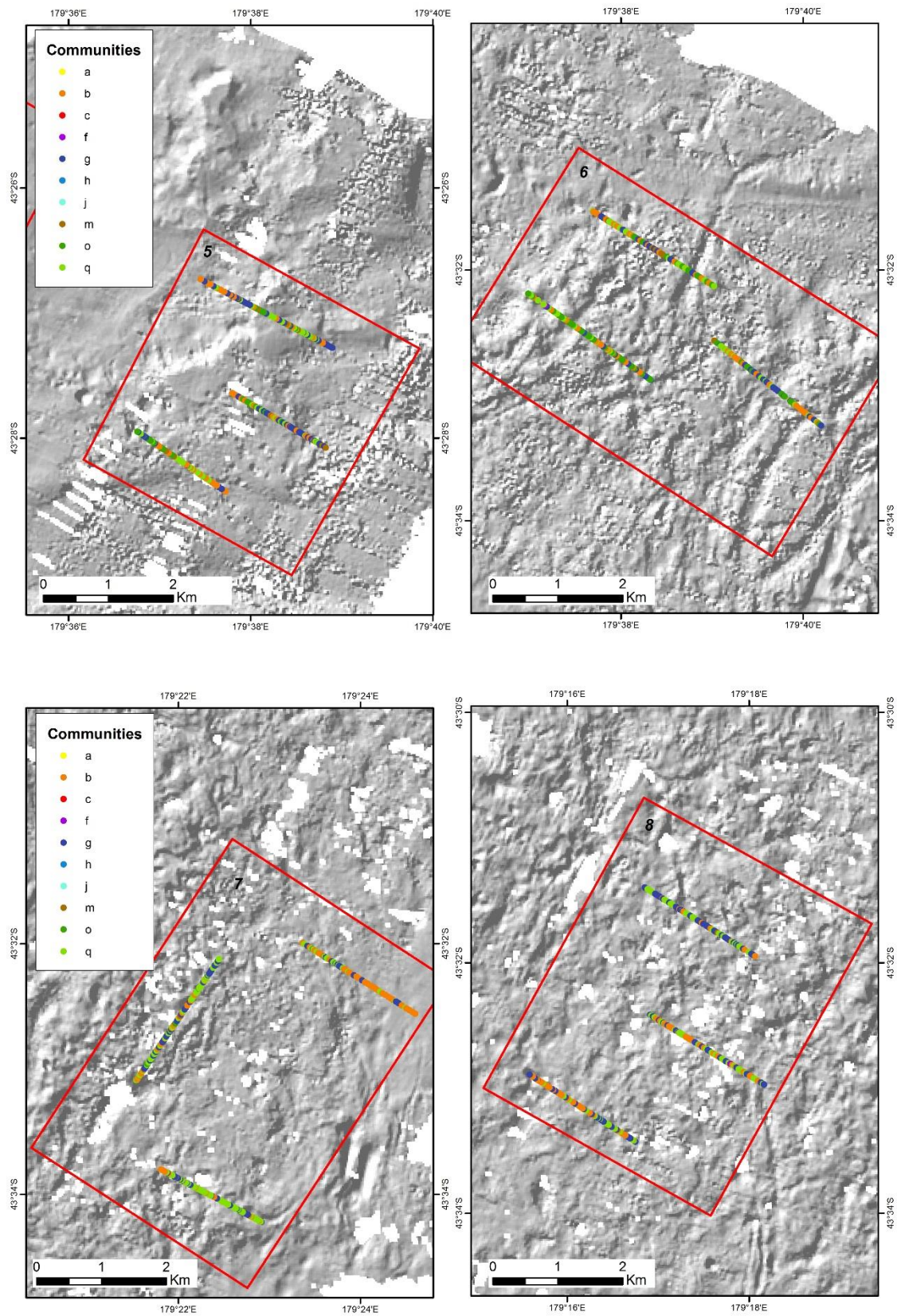
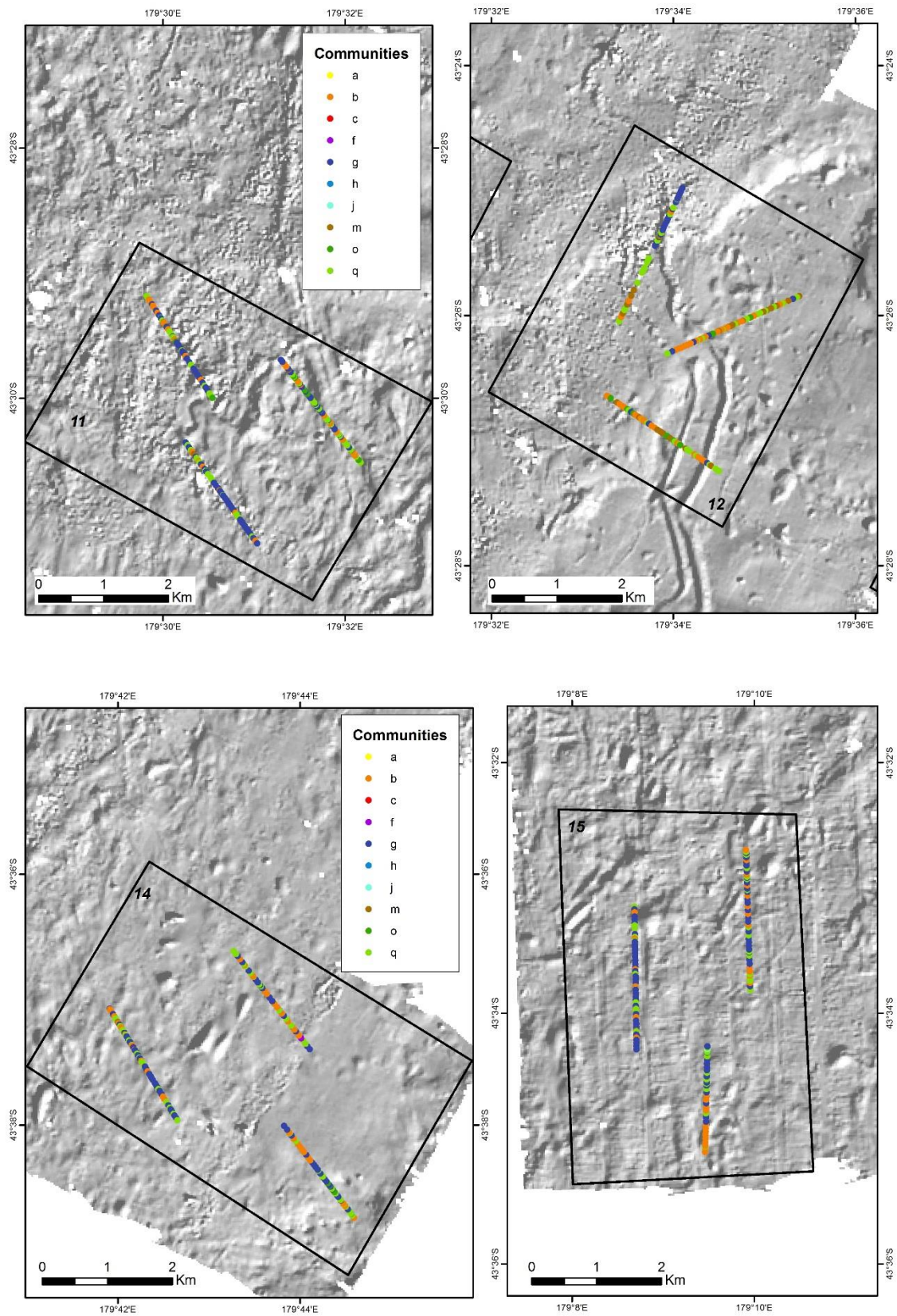
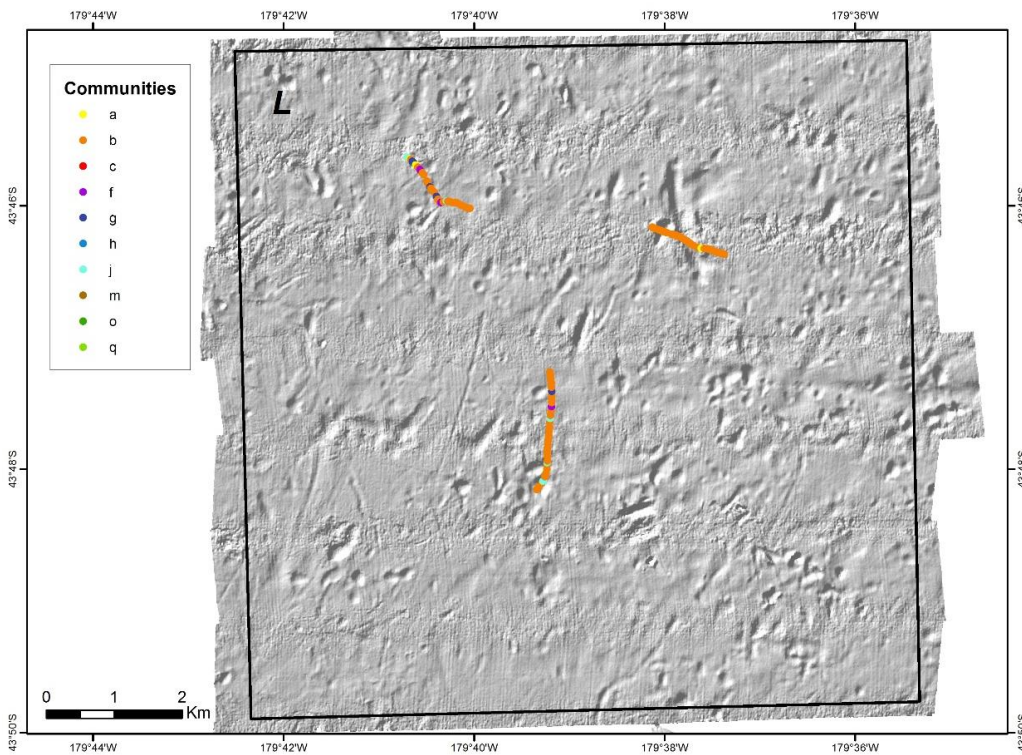
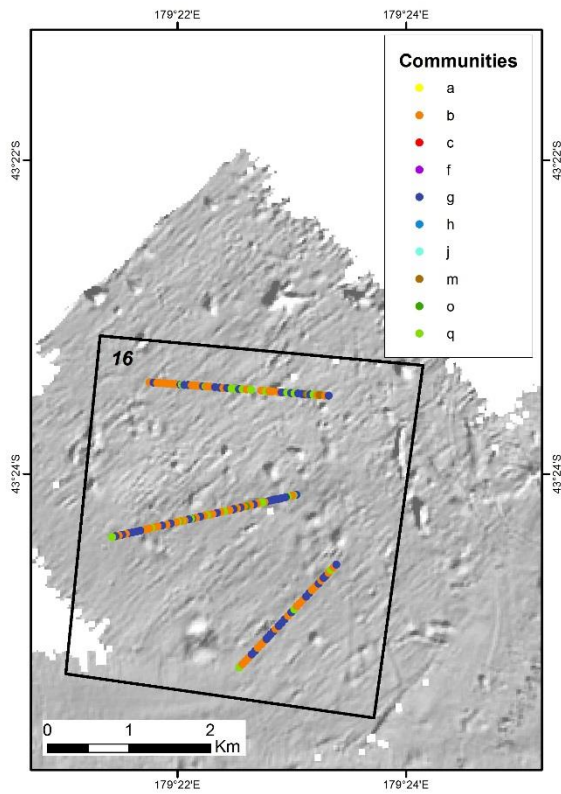


Figure D-2: Epifauna communities (image level) for CRP Environmental Survey areas 5- 8.



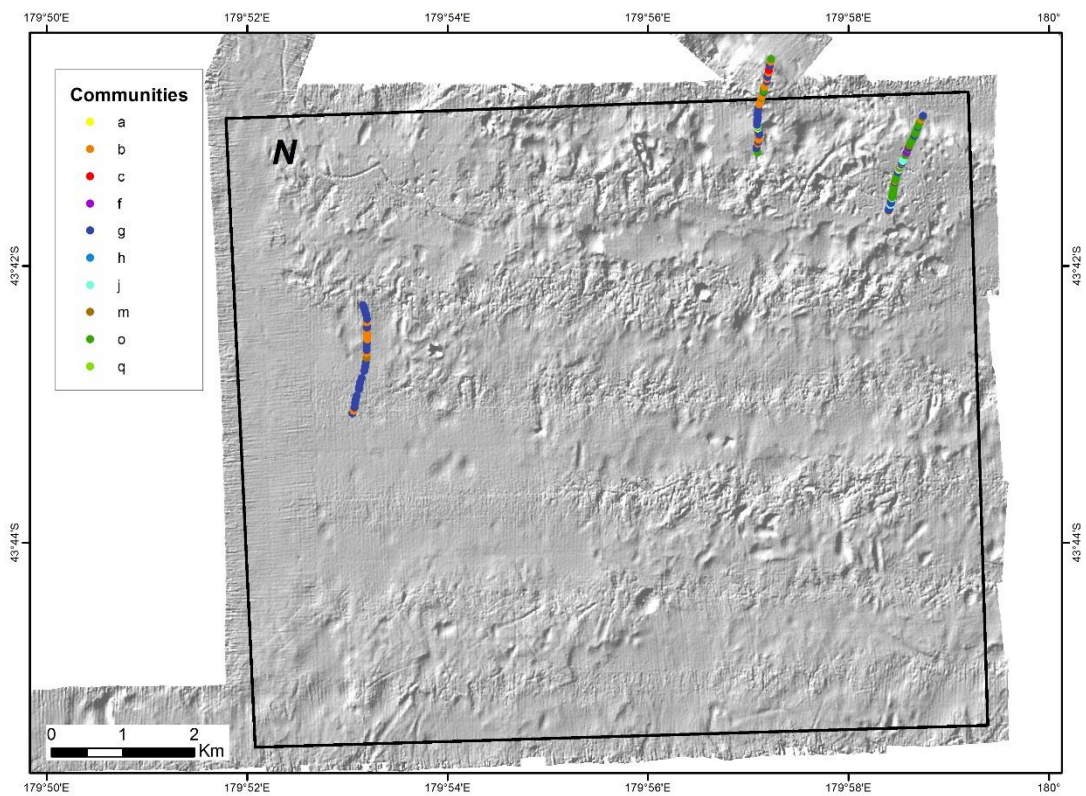
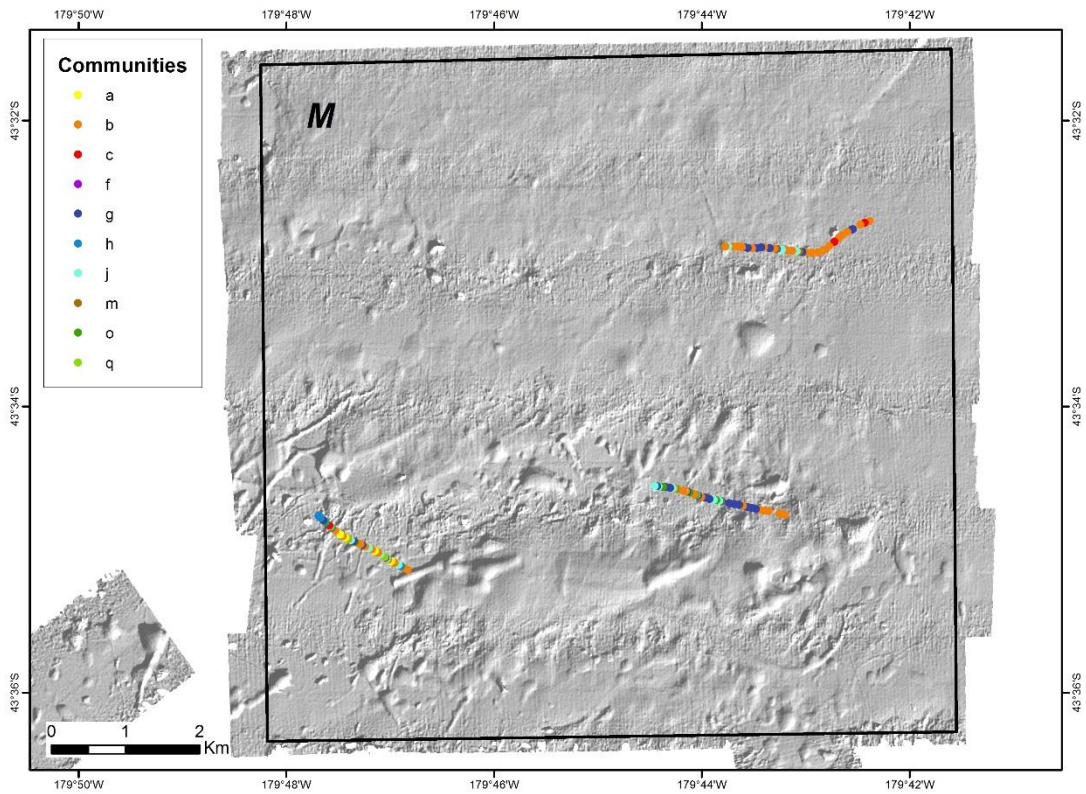


**Figure D-3: Epifauna communities (image level) for CRP Environmental Survey areas 11, 12, 14, 15.**

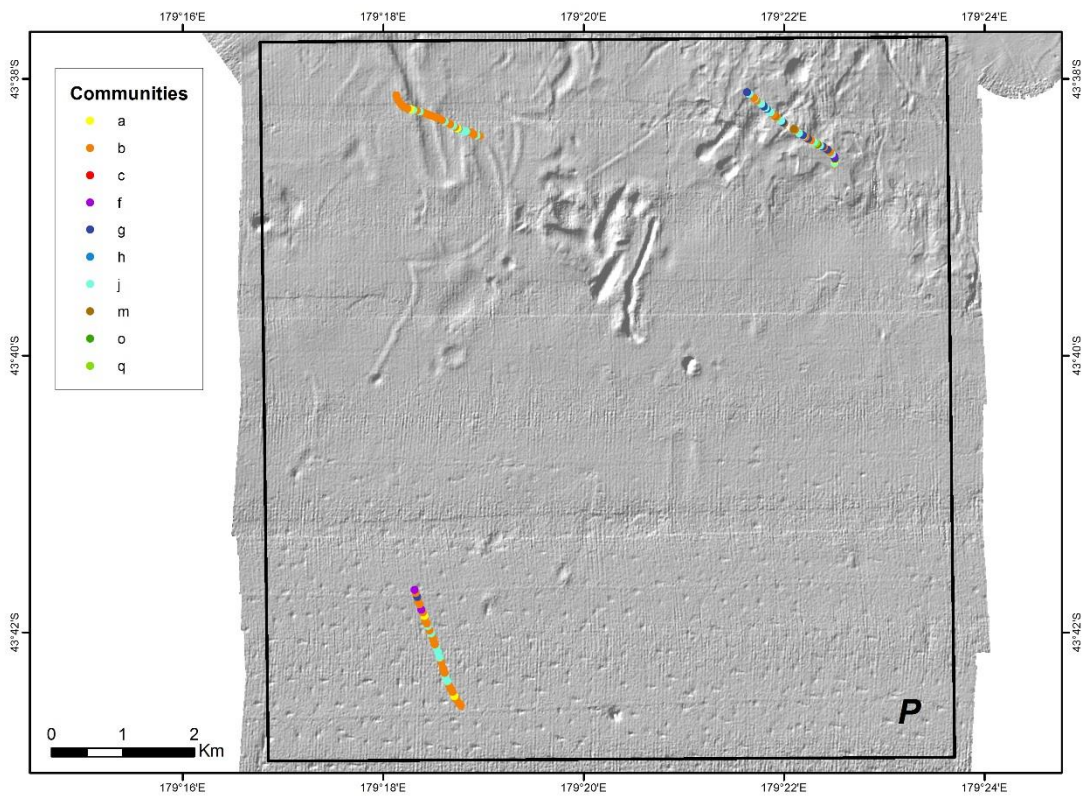
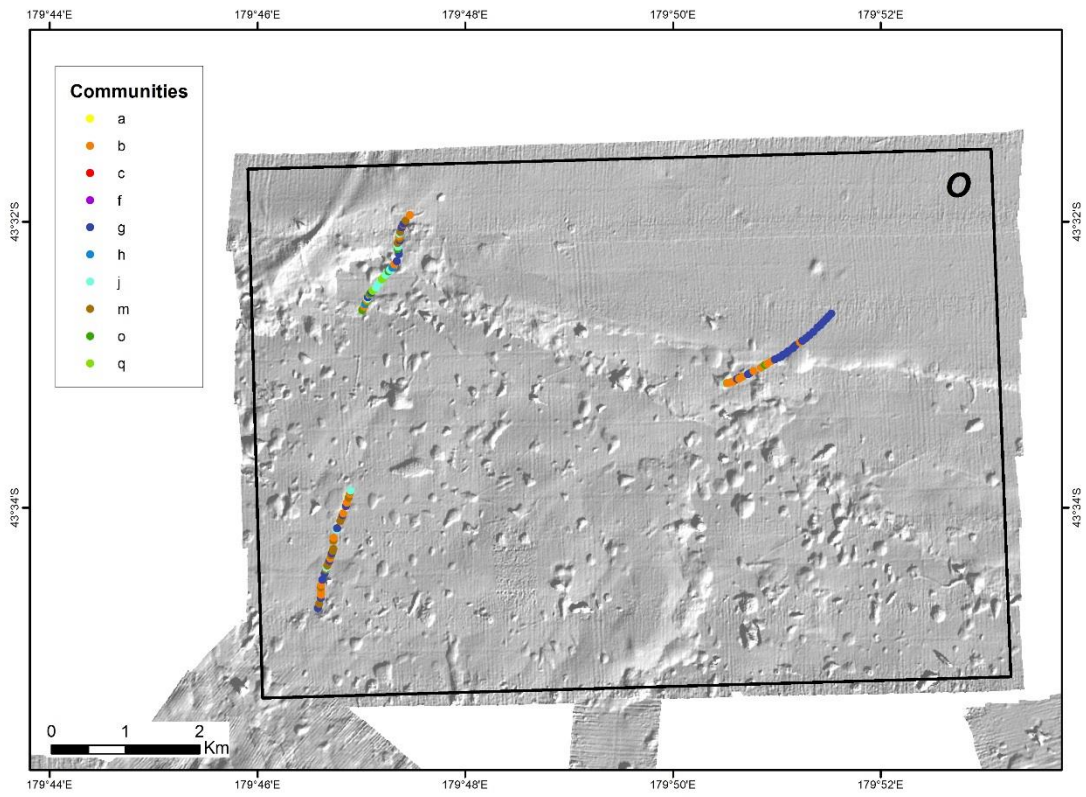


**Figure D-4: Epifauna communities (image level) for CRP Environmental Survey area 16 and Chatham Rise Benthos (OS20/20) Survey area L.**



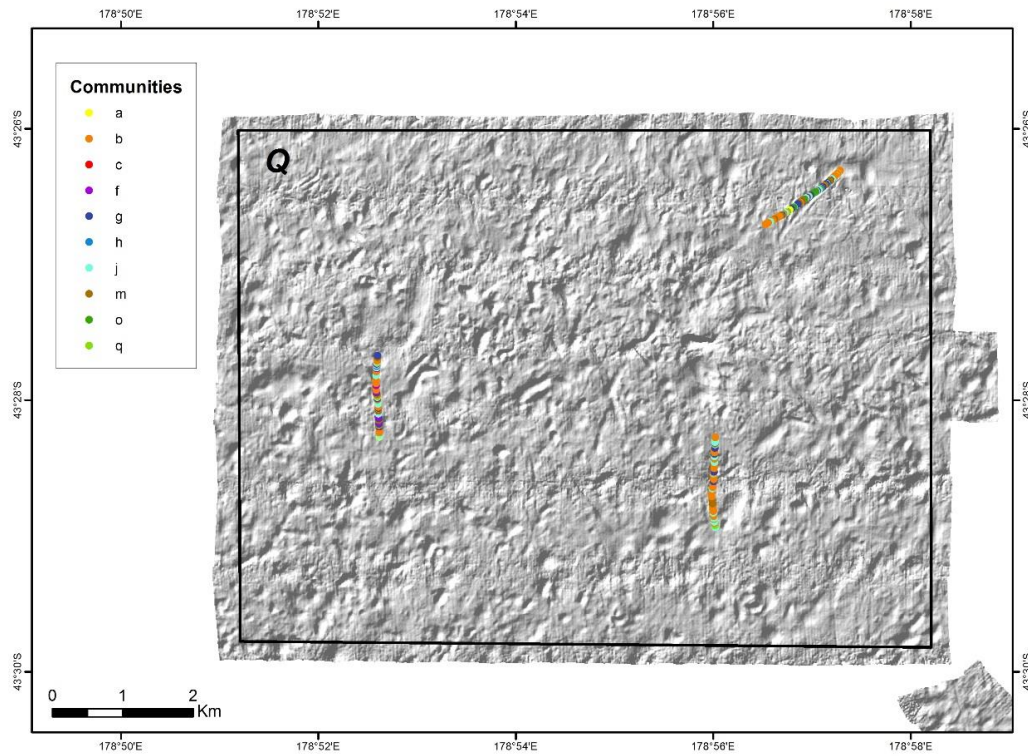


**Figure D-5: Epifauna communities (image level) for Chatham Rise Benthos (OS20/20) Survey areas M and N.**

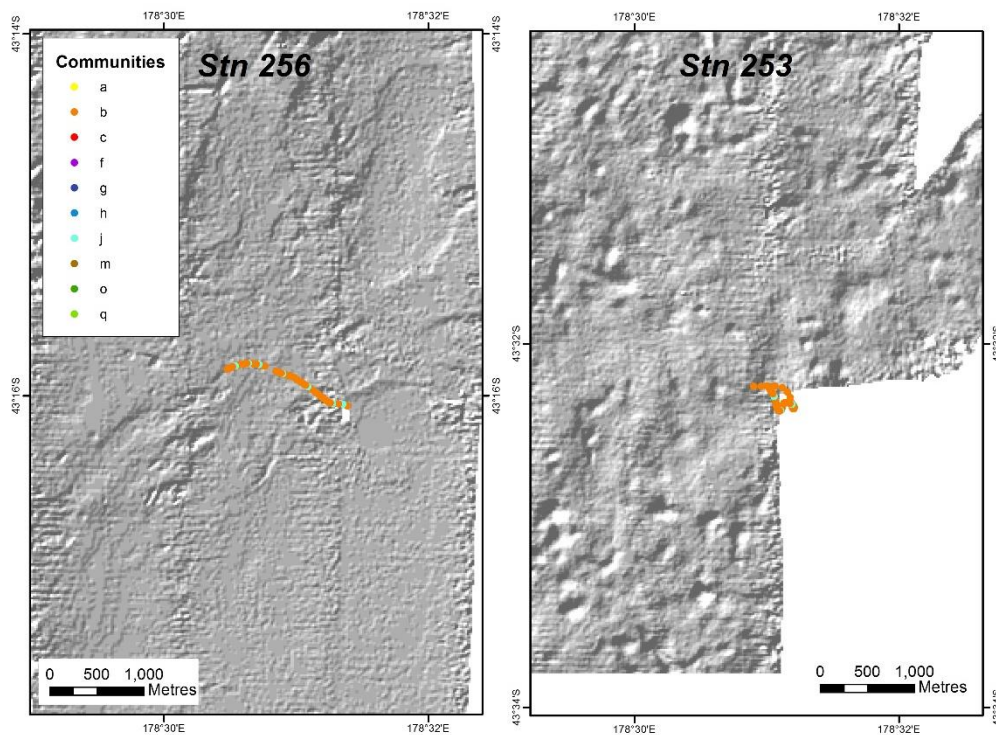


**Figure D-6: Epifauna communities (image level) for Chatham Rise Benthos (OS20/20) Survey areas O and P.**



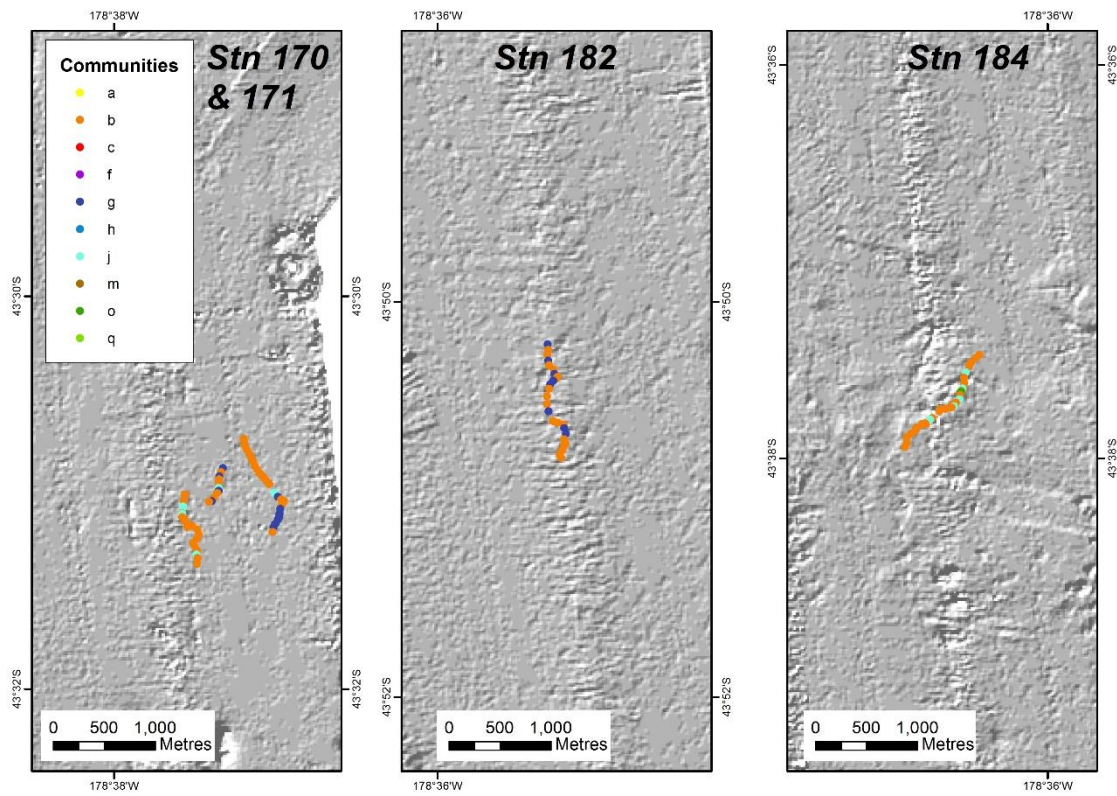


**Figure D-6: Epifauna communities (image level) for Chatham Rise Benthos (OS20/20) Survey area Q.**



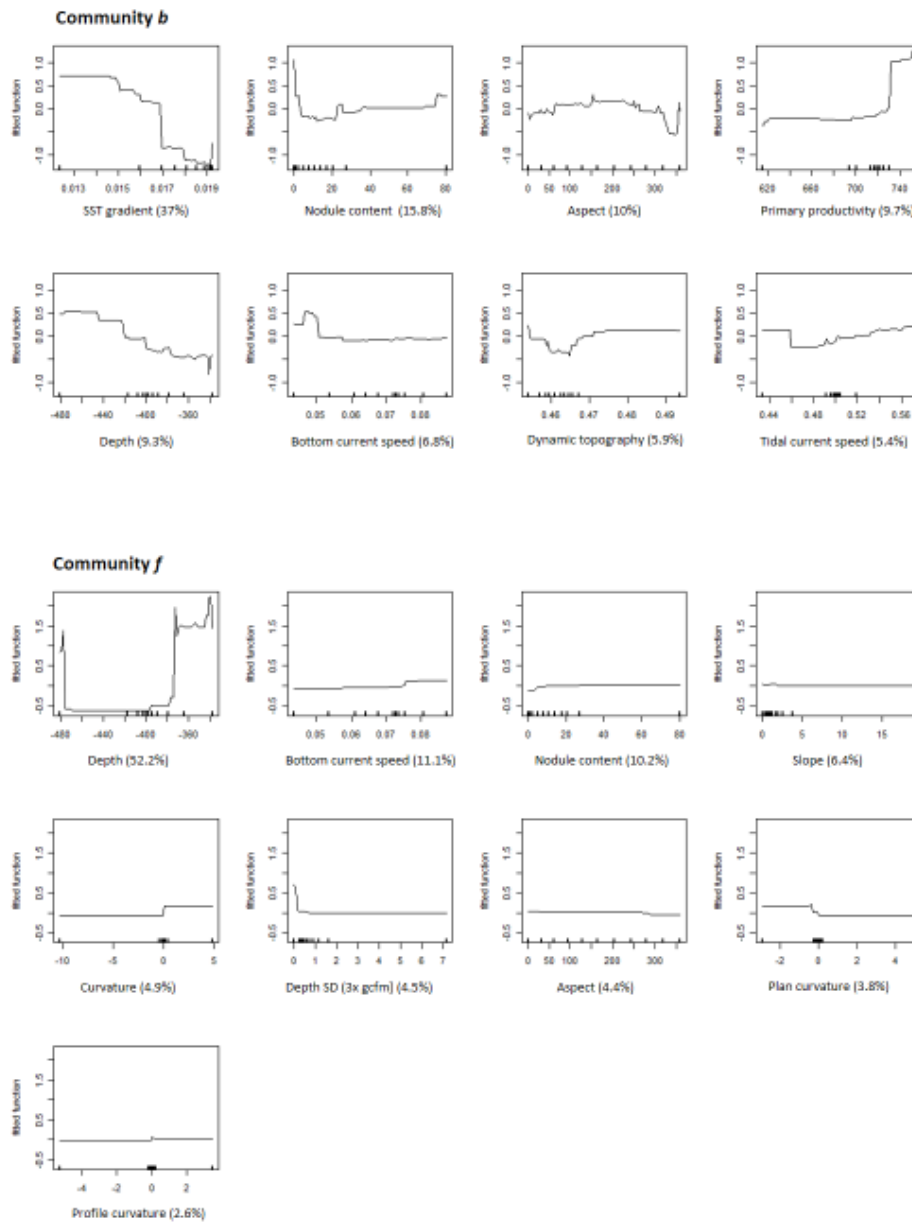
**Figure D-7: Epifauna communities (image level) for Chatham-Challenger (OS20/20) Survey transect stations 256 and 253.**

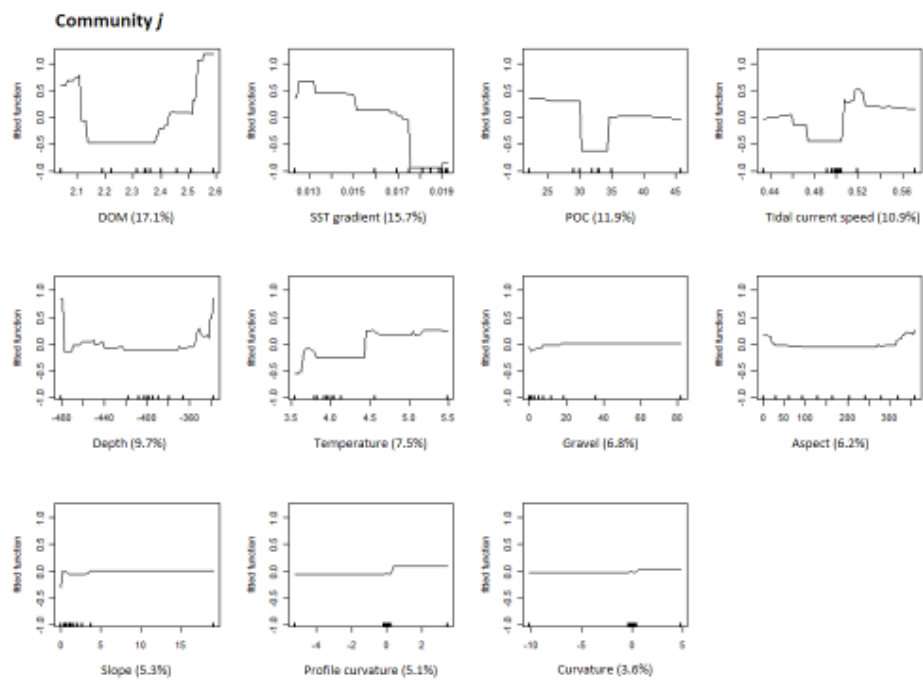
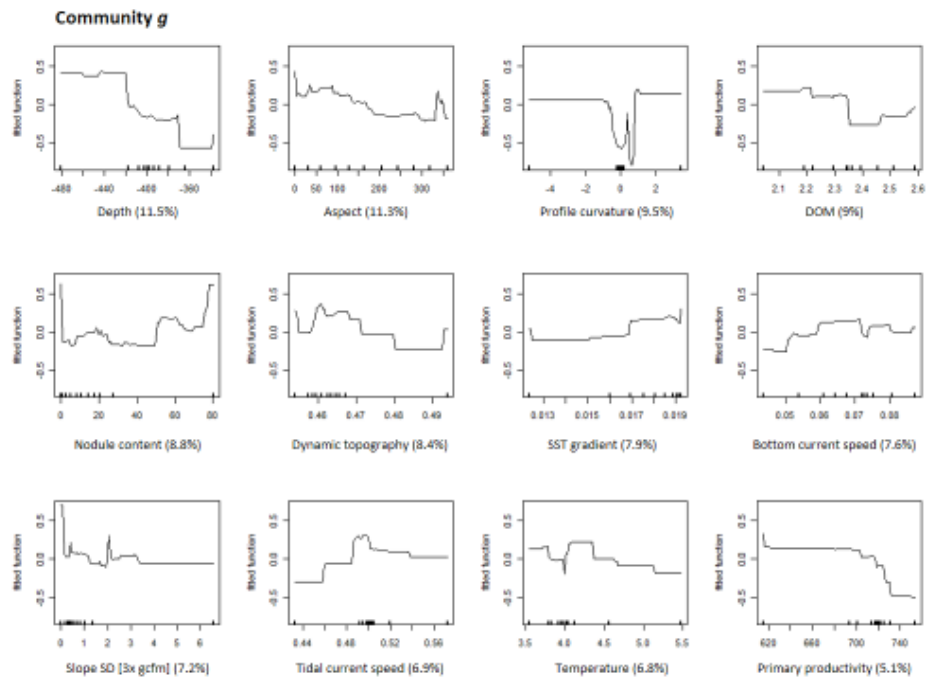


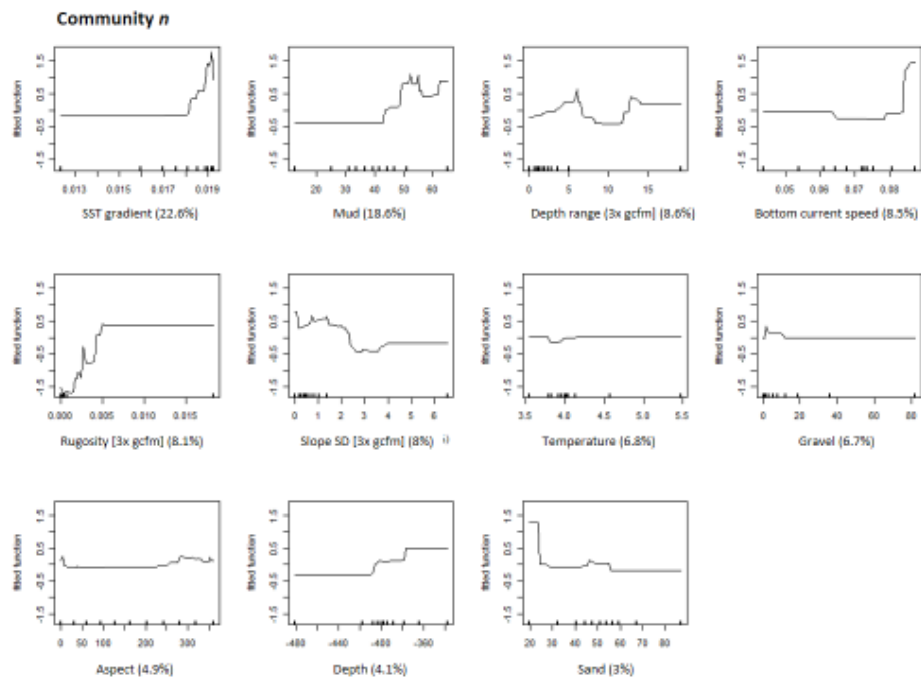
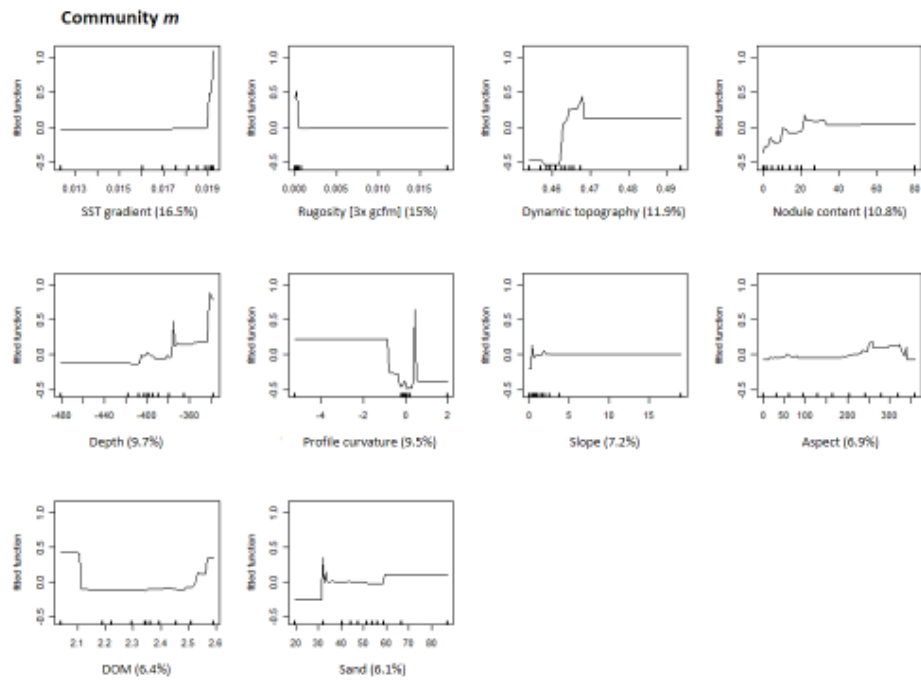


**Figure D-8: Epifauna communities (image level) for Chatham-Challenger (OS20/20) Survey transect stations 170, 171, 182 and 184.**

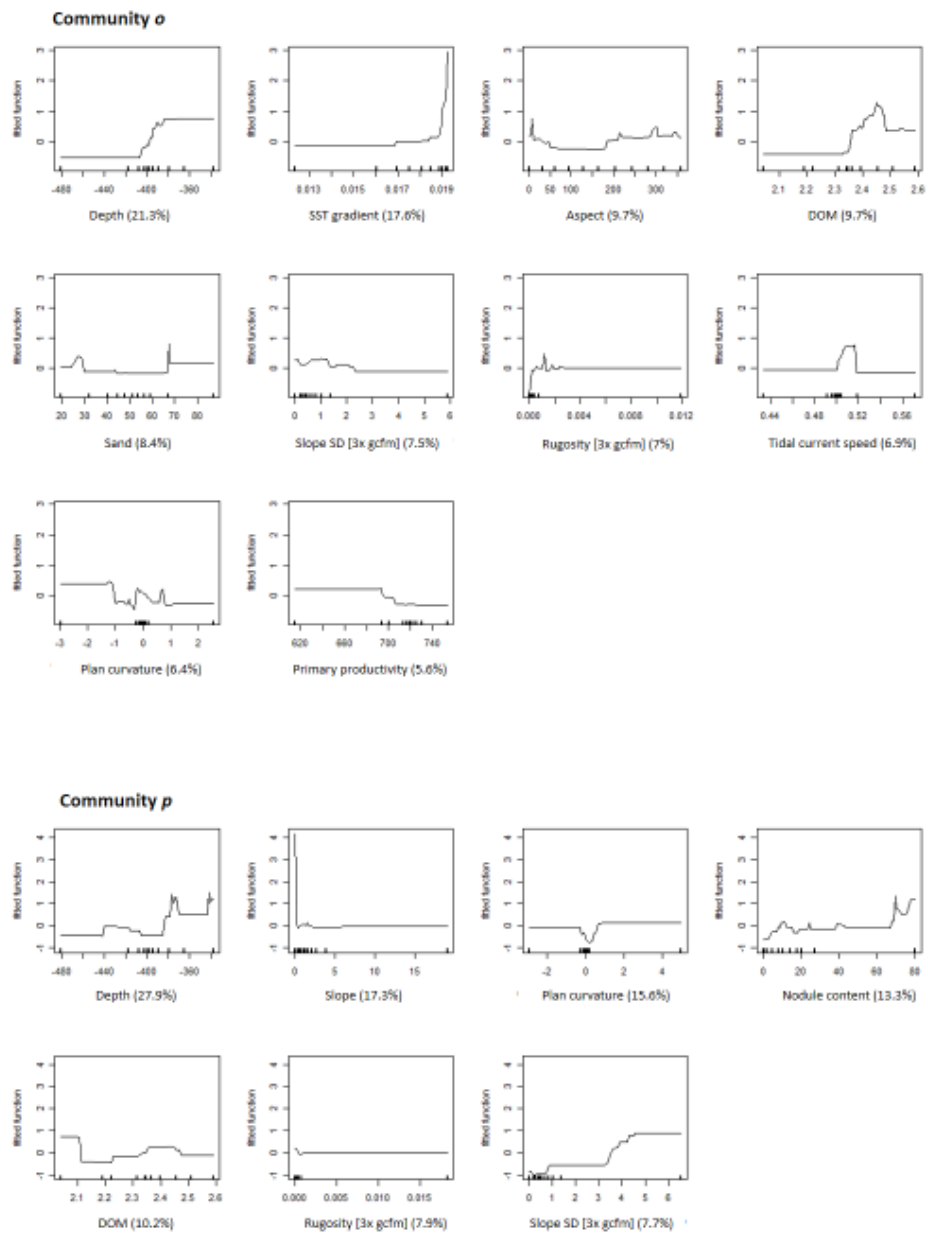
## Appendix E Fitted functions for BRT models of epifauna community (image-level) habitat suitability

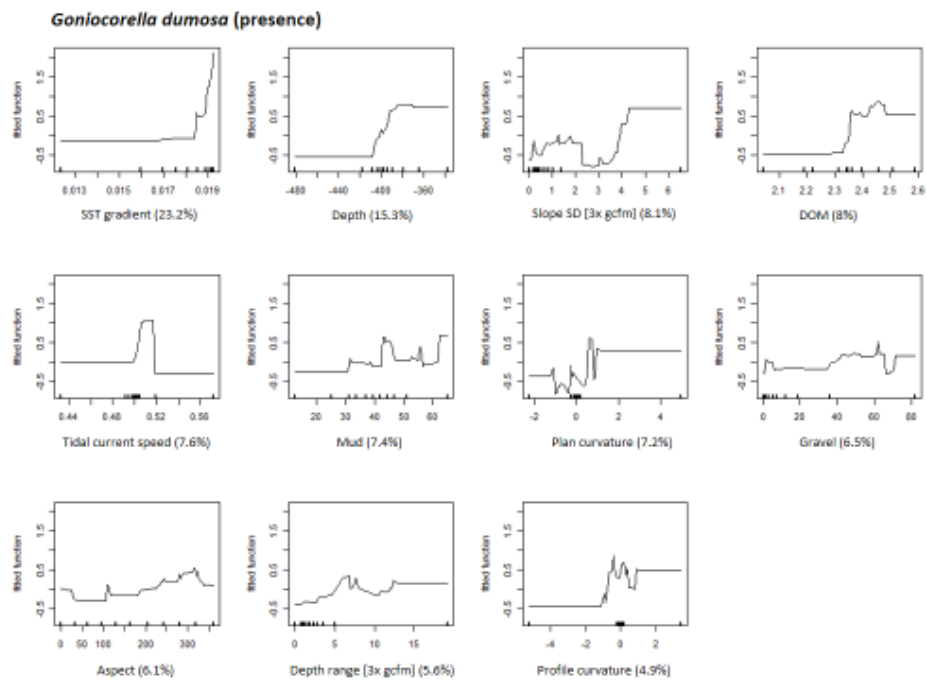
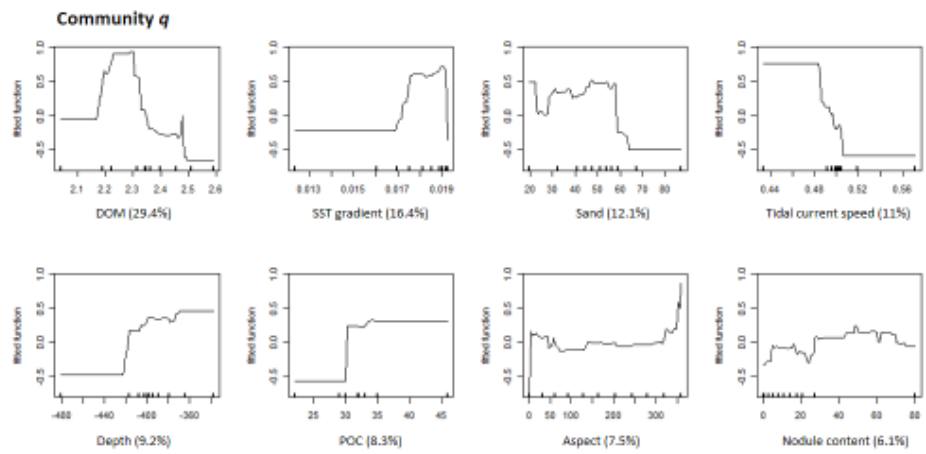








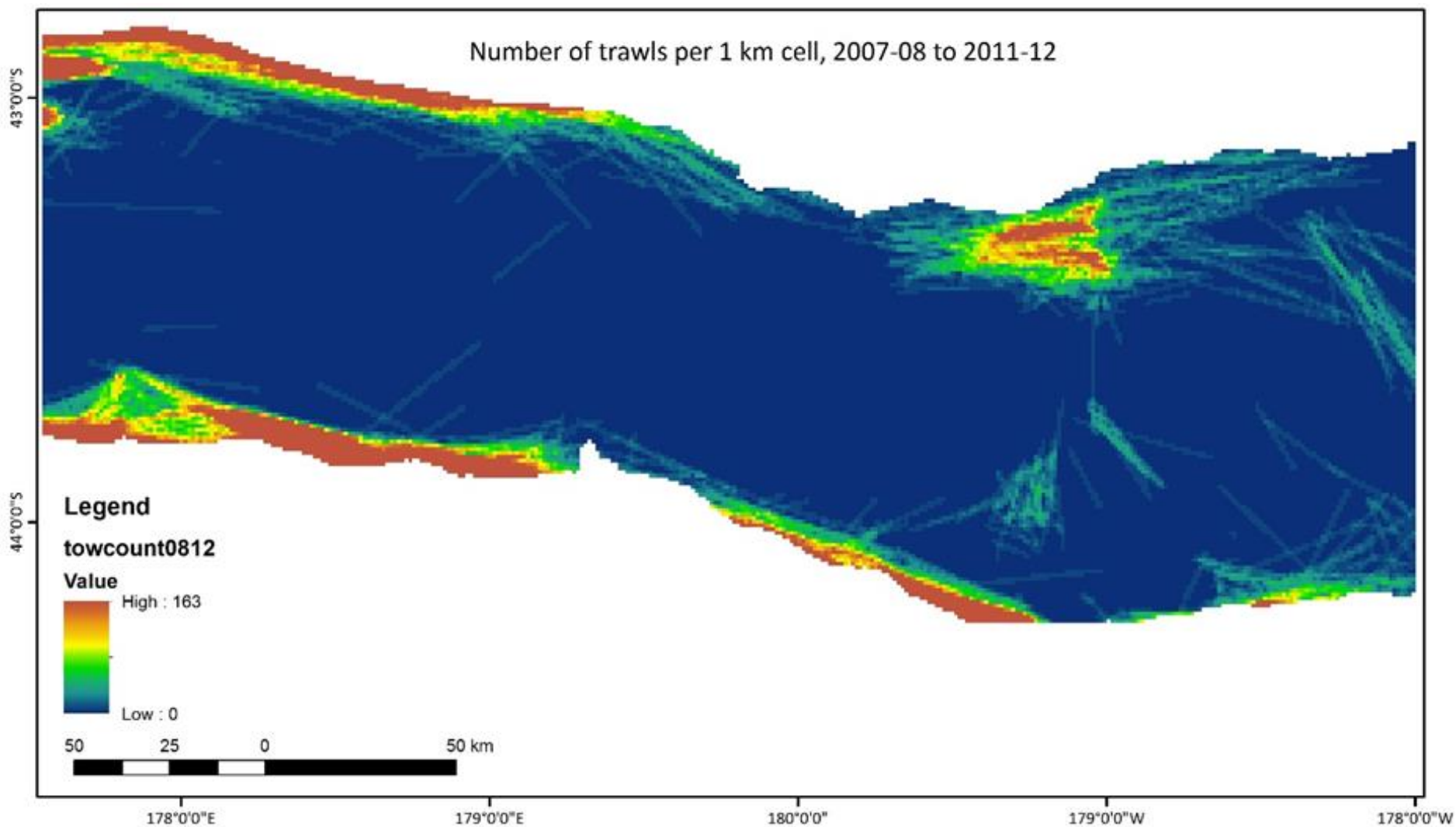




## Appendix F Bottom trawl footprint

Suitable habitat for *Goniocorella dumosa* and the two epifauna communities dominated by this stony coral, Communities *n* and *o*, is predicted to occur in relatively large patches that wholly or partly occur in the mining permit area, but also in a large area in the northwest part of the study area (Figure 3-12, Figure 3-13 and Figure 3-16). The predictive habitat suitability maps for the coral and the coral-dominated communities can be used to design measures to mitigate the effects of the proposed mining on the protected coral and the 'sensitive environments' that *Goniocorella dumosa* forms. However, confidence in any mitigation measures, such as the selection of non-mining or reserve areas, based upon the habitat suitability maps is dependent upon ground-truthing the habitat suitability models. Ground-truthing is particularly important because the large area of predicted habitat suitability in the northwest of the study area (and from where there are no observations of the seafloor) has been subject to bottom fishing (Figure F-1). Analysis indicates that ~70% of 1 km grid cells in the study area with a predicted habitat suitability of >50% (i.e., the habitat is more likely than less likely to be suitable) for *Goniocorella dumosa* and Communities *n* and *o* are within the bottom trawl footprint (Figure F-2).

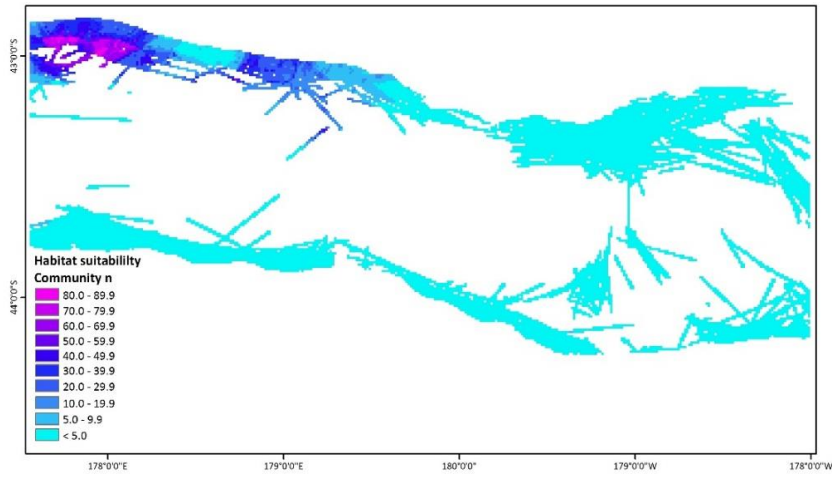
Physical disturbance by bottom trawling may mean the northwest part of the study area does not in effect represent suitable habitat, and *Goniocorella dumosa* and coral-dominated epifauna communities are absent or less extensive than predicted in this region. Knowledge of this kind would necessitate a re-running of the habitat suitability models for the stony coral and associated communities, but would immediately suggest that the mining permit area represents a greater proportion of likely suitable habitat for *Goniocorella dumosa* and Communities *n* and *o* within the study area. Such a finding could influence the selection of no-mining or reserve areas (and their possible extent) within the mining permit area.



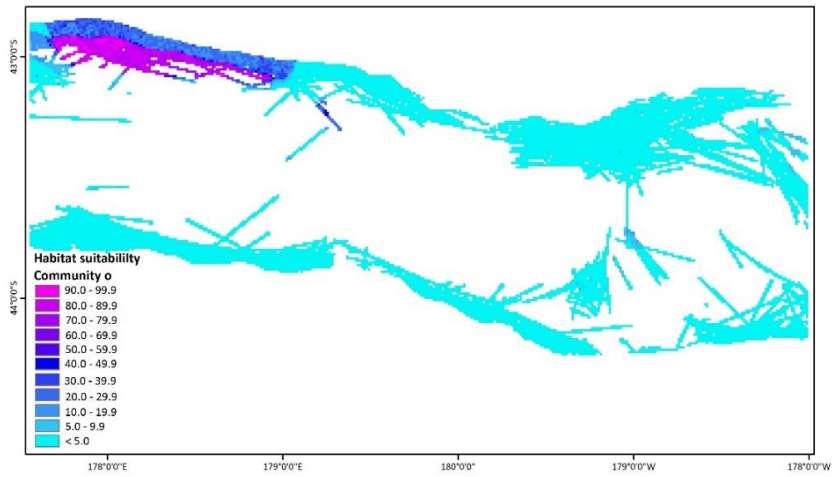
**F-1: Bottom trawl effort in the study area (total number of tows in each 1 km x 1 km cell for fishing years 2007–08 to 2011–12) [data courtesy of Ministry of Primary Industries].**



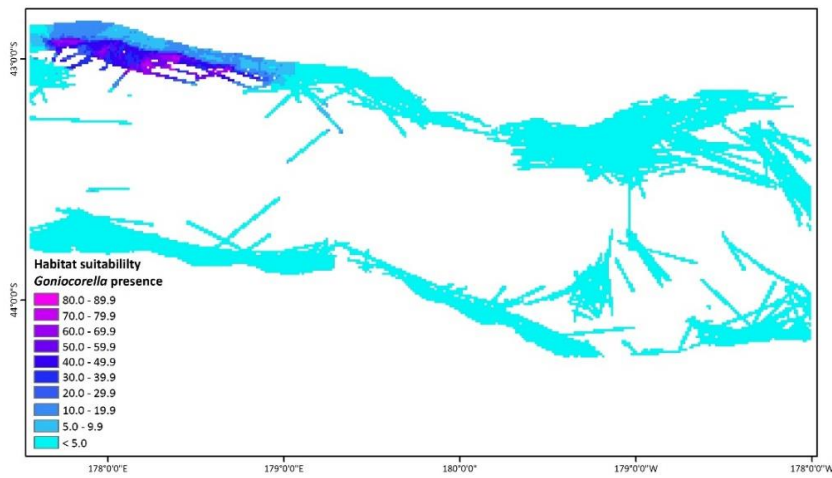
### Community n



### Community o



### *Goniocorella dumosa* (presence)



**F-2: Areas of predicted habitat suitability (%) within the bottom trawl footprint (fishing years 2002-03 to 2011-12) where it overlaps with the modelled domain (white areas within the modelled domain have not been trawled).**